MIT Open Access Articles

Comparing elliptic and toric hypersurface Calabi-Yau threefolds at large Hodge numbers

Massachusetts Institute of Technology

Comparing elliptic and toric hypersurface Calabi-Yau threefolds at large Hodge numbers

Yu-Chien Huang and Washington Taylor

Center for Theoretical Physics, Department of Physics, Massachusetts Institute of Technology, 77 Massachusetts Avenue, Cambridge, MA 02139, U.S.A.

E-mail: yc_huang@mit.edu, wati@mit.edu

Abstract: We compare the sets of Calabi-Yau threefolds with large Hodge numbers that are constructed using toric hypersurface methods with those can be constructed as elliptic fibrations using Weierstrass model techniques motivated by F-theory. There is a close correspondence between the structure of "tops" in the toric polytope construction and Tate form tunings of Weierstrass models for elliptic fibrations. We find that all of the Hodge number pairs $(h^{1,1}, h^{2,1})$ with $h^{1,1}$ or $h^{2,1} \geq 240$ that are associated with threefolds in the Kreuzer-Skarke database can be realized explicitly by generic or tuned Weierstrass/Tate models for elliptic fibrations over complex base surfaces. This includes a relatively small number of somewhat exotic constructions, including elliptic fibrations over non-toric bases, models with new Tate tunings that can give rise to exotic matter in the 6D F-theory picture, tunings of gauge groups over non-toric curves, tunings with very large Hodge number shifts and associated nonabelian gauge groups, and tuned Mordell-Weil sections associated with U(1) factors in the corresponding 6D theory.

Contents

1 Introduction

While Calabi-Yau threefolds have played an important role in string theory since the early days of the subject [1], the set of these geometries is still relatively poorly understood. Following the approach of Batyrev [2], in 2000 Kreuzer and Skarke carried out a complete analysis of all reflexive polytopes in four dimensions, giving a systematic classification of those Calabi-Yau (CY) threefolds that can be realized as hypersurfaces in toric varieties [3]. For many years the resulting database [4] has represented the bulk of the known set of Calabi-Yau threefolds, particularly at large Hodge numbers. More recently, the study of F-theory [5–7] has motivated an alternative method for the systematic construction of Calabi-Yau threefolds that have the structure of an elliptic fibration (with section). By systematically classifying all bases that support an elliptically fibered CY [8–11] and then systematically considering all possible Weierstrass tunings [12, 13] over each such base, it is possible in principle to construct all elliptically fibered Calabi-Yau threefolds. While there are some technical issues that must still be resolved for a complete classification from this approach, at large Hodge numbers this method gives a reasonably complete picture of the set of possibilities. One perhaps surprising result that has recently become apparent both from this work and from other perspectives [14–19] is that a very large fraction of the set of Calabi-Yau threefolds that can be constructed by *any* known mechanism are actually elliptically fibered, particularly at large Hodge numbers.

The goal of this paper is to carry out a direct comparison of the set of elliptically fibered Calabi-Yau threefolds that can be constructed using Weierstrass/Tate F-theory based methods with those that arise through reflexive polytope constructions. While the general methods for construction of elliptic Calabi-Yau threefolds can include non-toric bases [10, 11], and even over toric bases there are non-toric Weierstrass tunings [12, 13], we focus here on the subset of constructions that have the potential for a toric description through a reflexive polytope. In section 2, we review some of the basics of F-theory and the systematic construction of elliptic Calabi-Yau threefolds through the geometry of the base and the tuning of Weierstrass or Tate models from the generic structure over each base. In section 3, we review the Batyrev construction and reflexive polytopes, and the structure of elliptic fibrations in this context. In particular, in section 3.4 we describe the precise correspondence between a particular fibration structure for a reflexive polytope and Tate form Weierstrass models. In section 4, we restrict attention to toric base surfaces B_2 and identify the set of tuned Weierstrass/Tate models over such bases that naturally correspond to a reflexive polytope in the Batyrev construction. This gives us a systematic way of constructing from the point of view of elliptic fibrations over a chosen base a large set of elliptic Calabi-Yau threefolds that are expected to be seen in the Kreuzer-Skarke database with a specific ($\mathbb{P}^{2,3,1}$) fiber type. At large Hodge numbers, for reasons discussed further in section 4.8, we expect that this should give most or all elliptic fibrations that arise in the KS database; we find that this is in fact the case.

The main results of the paper are in section 5 and section 6, where we describe an algorithm to systematically run through all tuned Tate models over toric bases and we compare the results of running this algorithm to the Kreuzer-Skarke database. The initial result, described in section 5, is that these simply constructed sets match almost perfectly in the large Hodge number regimes that we study: both at large $h^{2,1}$ and at large $h^{1,1}$ all the models constructed by an appropriate set of Tate tunings over toric bases appear in the KS database, and virtually all the Hodge numbers in the database are reproduced by elliptic Calabi-Yau threefolds produced using this approach. There is a small set of large Hodge numbers (18 out of 1,827) associated with toric hypersurface Calabi-Yaus, however, that are not reproduced by our initial scan. By examining these individual cases, as described in section 6, we find that all these exceptions also correspond to elliptic fibrations though with more exotic structure, such as non-flat fibrations resolved through extra blow-ups in the base that take the base outside the toric class, and/or force Mordell-Weil sections on the elliptic fiber. The upshot is that when these more exotic constructions are included, *all* Hodge number pairs with either $h^{1,1}$ or $h^{2,1}$ at least 240 are reproduced by an elliptic Calabi-Yau over some explicitly determined base surface. We conclude in section 7 with a summary of the results and some related open questions.

Note that in this paper the focus is on understanding in some detail the connection between elliptic fibration geometry and polytope geometry for these different approaches to construction of elliptic Calabi-Yau threefolds. In a companion paper [20] we will describe a more direct analysis of the polytopes in the KS database that also shows explicitly that there is a toric fiber associated with an elliptic fibration for every polytope in the database at large Hodge numbers. The principal class of Tate tunings that we consider in this paper

have a complementary description in the language of "tops" [21]. The construction of many polytopes in the KS database through combining K3 tops and "bottoms" was accomplished in [14], and a systematic approach to constructing toric hypersurface Calabi-Yau threefold with a given base and gauge group using the language of tops is developed in [23], with particular application to models with gauge group SU(5) as also studied in e.g. [24, 25]. One of the main results of this paper is the systematic relationship of such constructions with certain classes of Tate tunings. This leads in some cases to the identification of new Tate tunings from observed polytope structures, and the observation that some polytopes in the KS database have a more complex structure that does not admit a direct description in terms of standard tops. On the other hand, new structures of tops are also found through the construction of polytopes via the correspondence with Tate tunings.

2 F-theory physics and elliptic Calabi-Yau threefold geometry

We briefly summarize here how the massless spectrum of a six-dimensional effective theory from F-theory compactification is related to the geometric data of the internal manifold, which is an elliptically fibered Calabi-Yau threefold (CY3) over a two-dimensional base B_2 (complex dimensions). F-theory models can then be systematically studied by first choosing a base B_2 and then specifying an elliptic fibration in Weierstrass form over that base. Further background on F-theory can be found in for example [5–7, 26, 27].

F-theory compactified on a (possibly singular) elliptically fibered Calabi-Yau threefold X gives a 6D effective supergravity theory. Such a compactification of F-theory is equivalent to M-theory on the resolved Calabi-Yau $\tilde{X}$ in the decompactification limit of M-theory, where in the F-theory picture the resolved components of the elliptic fiber are shrunk to zero size. F-theory can also be thought of as a nonperturbative formulation of type IIB string theory. In this picture the type IIB theory is compactified on the base B_2. In this F-theory description, spacetime filling 7-branes sit at the codimension-one loci in the base where the fibration degenerates. The non-abelian gauge symmetries of the 6D effective theory arise from the seven-branes and can be inferred from the singularity types of the elliptic fibers along the codimension-one loci in the base, according to the Kodaira classification (table 2). At the intersections of seven-branes there are localized matter fields that are hypermultiplets in the 6D theory; the representations of the matter fields can be determined from the detailed form of the singularities over the codimension-two points in the base (see e.g. [28–30]). Therefore the physics data can be extracted by studying the singular fibers by means of the Weierstrass models (short form) or the Tate models (long form) of X that we review in sections 2.2 and 2.3.[1] There can also be abelian gauge

---

[1]The short form Weierstrass model is the most general form for an elliptic Calabi-Yau threefold. The cases discussed in this paper are elliptically fibered Calabi-Yau threefolds that always have a section and therefore in principle admit a short form Weierstrass form realization. There can also be genus one fibered Calabi-Yau threefolds (lacking a global section), which can be related to Weierstrass models of elliptic Calabi-Yau threefolds through the Jacobian construction (described from the physics perspective in [31, 34]). The physics of these threefolds is more subtle, involving discrete gauge groups [32, 33, 35–37]. In a few cases we find it useful to use the Jacobian construction even for cases with a section, giving an explicit transformation to the short Weierstrass form.

symmetries, which arise from additional rational sections of the elliptic fibration [6, 7]. The study of $\mathfrak{u}(1)$ symmetries is more subtle in that it relates to the global structure of the fibration, as opposed to non-abelian symmetries where we can just study singular fibers locally. We will see cases with abelian factors in section 6, with a detailed example worked out in appendix C. In section 2.4, we review the Zariski decomposition, which allows us to determine the order of vanishing and consequent gauge group of a Weierstrass or Tate form description of an elliptic fibration, and in section 2.5 we describe how this method can be applied systematically in the context of Tate tunings. In section 2.6, we review the 6D anomaly cancellation conditions and their connection to the matter content of a 6D theory and the Hodge numbers of the corresponding Calabi-Yau threefold. In section 2.7 we review the constraints imposed by global symmetry groups on the set of gauge groups that can be supported on curves intersecting a given curve, and we conclude the overview of F-theory in section 2.8 with a summary of the systematic classification of complex surfaces that can support elliptic Calabi-Yau threefolds and can be used for F-theory compactification.

2.1 Hodge numbers and the 6D massless spectrum

By going to the 5D Coulomb branch after reduction on a circle, the F-/M-theory correspondence can be used to relate the geometry of $\tilde{X}$ to the associated 6D supergravity theory [7, 38]. In particular, the Hodge numbers, $h^{1,1}$ and $h^{2,1}$, of $\tilde{X}$ can be related to the (massless) matter content of the 6D theory:

$$h^{1,1}(\tilde{X}) = r + T + 2, \tag{2.1}$$

where T is the number of tensor multiplets, which is determined already by the choice of base B_2,

$$T = h^{1,1}(B_2) - 1, \tag{2.2}$$

and $r = r_{\text{abelian}} + \sum_i r_i$ is the total rank of the gauge group,

$$G = \mathrm{U}(1)^{r_{\text{abelian}}} \times \prod_{\text{non-abelian factors } i} G_i, \tag{2.3}$$

of the 6D effective theory. We also have

$$h^{2,1}(\tilde{X}) = H_{\text{neutral}} - 1, \tag{2.4}$$

where H_{neutral} is the number of hypermultiplets that are neutral under the Cartan subalgebra[2] of the gauge group G of the 6D F-theory.

The spectra of 6D theories are constrained by consistency conditions associated with the absence of anomalies, which we describe in further detail in section 2.6. The gravitational anomaly cancellation condition (2.33) gives $H - V = 273 - 29T$, where V is the

---

[2]In other words, this counts fields that are neutral matter fields in the 5D M-theory sense but may transform under the unhiggsed non-abelian factors of the 6D F-theory. Often, matter charged under the non-abelian factors is still charged under the Cartan subalgebra, but for certain representations of some non-abelian groups there can be charged matter that is neutral under the Cartan subalgebra.

Rank r	Algebras
2	$\mathfrak{su}(3), \mathfrak{g}_2$
3	$\mathfrak{su}(4), \mathfrak{so}(7)$
4	$\mathfrak{so}(8), \mathfrak{so}(9), \mathfrak{f}_4$
$r \geq 5$	$\mathfrak{so}(r), \mathfrak{so}(r+1)$

Table 1. Rank preserving tunings: tunings of these four classes of gauge algebras do not change $h^{1,1}$ or $h^{2,1}$.

dimension of the gauge group G, and $H = H_{\text{charged}} + H_{\text{neutral}}$ is the total number of hypermultiplets (separated into neutral and charged matter under the Cartan of the gauge group G). So we have another expression

$$h^{2,1}(\tilde{X}) = 272 + V - 29T - H_{\text{charged}}. \tag{2.5}$$

This is more useful for some of our purposes than equation (2.4). In particular, as we discuss in further detail in the following section, we are interested in studying various specializations (tunings) of a generic elliptically fibered CY3 over a given base B_2. The number of tensors T is fixed for a given base. Thus, if we start with known Hodge numbers $h^{1,1}$ and $h^{2,1}$ for the generic elliptic fibration over a given (e.g. toric [9, 39]) base, and specialize/tune to a model with a larger gauge group and increased matter content, then the Hodge numbers of the tuned model can be simply calculated by adding to those of the generic models respectively the shifts

$$\Delta h^{1,1} = \Delta r, \tag{2.6}$$
$$\Delta h^{2,1} = \Delta V - \Delta H_{\text{charged}}. \tag{2.7}$$

Such a specialization/tuning amounts physically to undoing a Higgsing transition, and the second of these relations simply expresses the physical expectation that the number of matter degrees of freedom that are lost ("eaten") in a Higgsing transition is equal to the number of gauge bosons lost to symmetry breaking. Note that the data on the right hand sides are associated in general with tuned non-abelian gauge symmetries but also in some special cases involve abelian factors. Note also that the right-hand sides of (2.6) and (2.7) are always non-negative and non-positive respectively for any tuning. In most cases, the gauge group increases in rank and some of the $h^{2,1}$ moduli are used to implement the tuning. In *rank-preserving* tunings, however, the Hodge numbers do not change (see table 1) — $h^{1,1}$ of course does not change in a rank-preserving enhancement; $h^{2,1}$ does not change either in these tunings, as one can check by considering carefully the matter charged under the Cartan subalgebra (cf. footnote 2.)

2.2 Generic and tuned Weierstrass models for elliptic Calabi-Yau manifolds

An elliptic fibration with a section over a base B can be described by the Weierstrass model

$$y^2 = x^3 + fxz^4 + gz^6. \tag{2.8}$$

The Calabi-Yau condition on the total space X requires that f, g are sections of $\mathcal{O}(-4K_B)$, $\mathcal{O}(-6K_B)$, where K_B is the canonical class of the base. More abstractly, we take the weighted projective bundle

$$\pi : P = \mathbb{P}_{\mathbb{P}^{2,3,1}}[\mathcal{L}^2 \oplus \mathcal{L}^3 \oplus \mathcal{O}_B] \to B, \tag{2.9}$$

where $\mathcal{L} = \mathcal{O}(-K_B)$ is required by the Calabi-Yau condition and $x \in \mathcal{O}_P(2) \otimes \pi^* \mathcal{L}^2, y \in \mathcal{O}_P(3) \otimes \pi^* \mathcal{L}^3, z \in \mathcal{O}_P(1)$ and $[x : y : z]$ can be viewed as weighted projective coordinates of the $\mathbb{P}^{2,3,1}$, while f and g are sections of, to be more precise, $\pi^* \mathcal{L}^4$ and $\pi^* \mathcal{L}^6$ respectively.

Consider an elliptic Calabi-Yau threefold over a complex two-dimensional base B_2, so the divisors in the base are curves. The elliptic fiber becomes singular over the codimension-one loci in the base where the discriminant

$$\Delta = 4f^3 + 27g^2 \tag{2.10}$$

vanishes. The type of singular fiber at a generic point along an irreducible component $\{\sigma = 0\}$ of the discriminant locus $\{\Delta = 0\}$ is characterized by the Kodaira singularity type, which is determined by the orders of vanishing of f, g, and Δ in an expansion in σ (see table 2). The physics interpretation is that there are seven-branes on which open strings (and junctions) end located at the discriminant locus, and the resulting gauge symmetries can be determined (up to *monodromies*) by the type of the singular fiber. The gauge algebras that are further determined by monodromy conditions [29, 44] are those of types $I_n, I_0^*, I_n^*, IV, IV^*$, where some factorizability conditions are imposed on the terms of f, g, Δ of lowest degrees of vanishing order along $\{\sigma = 0\}$. We summarize these conditions in table 3, in terms of the first non-vanishing sections $f_i(\zeta), g_j(\zeta), \Delta_k(\zeta)$ in the local expansions

$$f(\sigma, \zeta) = f_0(\zeta) + f_1(\zeta)\sigma + \cdots, \tag{2.11}$$

$$g(\sigma, \zeta) = g_0(\zeta) + g_1(\zeta)\sigma + \cdots, \tag{2.12}$$

$$\Delta(\sigma, \zeta) = \Delta_0(\zeta) + \Delta_1(\zeta)\sigma + \cdots, \tag{2.13}$$

where $\{\zeta = 0\}$ defines a divisor that intersects $\{\sigma = 0\}$ transversely so that σ, ζ together serve as local coordinates on an open patch of base.

A generic Weierstrass model (i.e. with coefficients at a generic point in the moduli space) for an elliptically fibered CY3 over a given base B_2 corresponds physically to a maximally Higgsed phase. In the maximally Higgsed phase over many bases the gauge group and matter content are still nontrivial. The minimal gauge algebras and matter configuration associated with a given base B_2 are carried by *non-Higgsable clusters* (NHCs) [8], which are isolated rational curves of self-intersection m, $-12 \le m \le -3$, and clusters of multiple rational curves of self-intersection ≤ -2: $\{-2, -3\}, \{-2, -2, -3\}$, and $\{-2, -3, -2\}$. The sections f, g, Δ automatically vanish to higher orders along these curves in any Weierstrass model over the given base. This can be understood geometrically as an effect in which the curvature over the negative self-intersection curves must be cancelled by 7-branes to maintain the Calabi-Yau structure of the elliptic fibration. The orders of vanishing and the corresponding minimal gauge groups on these NHCs are listed in table 11 in section 4.4.

– 6 –

Type	ord (f)	ord (g)	ord (Δ)	singularity	nonabelian symmetry algebra
I_0	≥ 0	≥ 0	0	none	none
I_n	0	0	$n \geq 2$	A_{n-1}	$\mathfrak{su}(n)$ or $\mathfrak{sp}(\lfloor n/2 \rfloor)$
II	≥ 1	1	2	none	none
III	1	≥ 2	3	A_1	$\mathfrak{su}(2)$
IV	≥ 2	2	4	A_2	$\mathfrak{su}(3)$ or $\mathfrak{su}(2)$
I_0^*	≥ 2	≥ 3	6	D_4	$\mathfrak{so}(8)$ or $\mathfrak{so}(7)$ or $\mathfrak{g}_2$
I_n^*	2	3	$n \geq 7$	D_{n-2}	$\mathfrak{so}(2n-4)$ or $\mathfrak{so}(2n-5)$
IV^*	≥ 3	4	8	E_6	$\mathfrak{e}_6$ or $\mathfrak{f}_4$
III^*	3	≥ 5	9	E_7	$\mathfrak{e}_7$
II^*	≥ 4	5	10	E_8	$\mathfrak{e}_8$
non-min	≥ 4	≥ 6	≥ 12	does not occur in F-theory	

Table 2. Kodaira classification of singularities in the elliptic fiber along codimension one loci in the base in terms of orders of vanishing of the parameters f, g in the Weierstrass model (2.8) and the discriminant locus Δ.

	ord(f)	ord(g)	ord(Δ)	algebra	monodromy condition
I_n	0	0	n	$\mathfrak{su}(n)$	since $\Delta_0 = 0$, locally $f_0(\zeta) = -\frac{1}{3}u_0^2$ and $g_0(\zeta) = \frac{2}{27}u_0^3$ for some $u_0(\zeta)$, which is a perfect square
				$\mathfrak{sp}(\lfloor n/2 \rfloor)$	otherwise
IV	≥ 2	2	4	$\mathfrak{su}(3)$	$g_2(\zeta)$ is a perfect square
				$\mathfrak{su}(2)$	otherwise
I_0^*	≥ 2	≥ 3	6	$\mathfrak{so}(8)$	$x^3 + f_2(\zeta)x + g_3(\zeta)$ $= (x-a)(x-b)(x+a+b)$ for some $a(\zeta), b(\zeta)$
				$\mathfrak{so}(7)$	$x^3 + f_2(\zeta)x + g_3(\zeta)$ $= (x-a)(x^2+ax+b)$ for some $a(\zeta), b(\zeta)$ (but not $\mathfrak{so}(8)$ condition)
				$\mathfrak{g}_2$	otherwise
I_n^*	2	3	$n \geq 7$	$\mathfrak{so}(2n-4)$	since $\Delta_6 = 0$, locally $f_2(\zeta) = -\frac{1}{3}u_1^2$ and $g_3(\zeta) = \frac{2}{27}u_1^3$ for some $u_1(\zeta)$; $\frac{\Delta_n(\zeta)}{u_1^3}$ is a perfect square for odd n $\frac{\Delta_n(\zeta)}{u_1^2}$ is a perfect square for even n
				$\mathfrak{so}(2n-5)$	otherwise
IV^*	≥ 3	4	8	$\mathfrak{e}_6$	$g_4(\zeta)$ is a perfect square
				$\mathfrak{f}_4$	otherwise

Table 3. Monodromy conditions for certain algebras to satisfy in additional to the desired orders of vanishing of f, g, Δ: $f_i(\zeta), g_j(\zeta), \Delta_k(\zeta)$ are coefficients of the expansions in equations (2.11)–(2.13).

Starting from the generic model over a given base B, we can systematically tune the Weierstrass model coefficients f and g to increase the order of vanishing over various curves beyond what is imposed by the NHCs, producing additional or enhanced gauge groups on some curves in the base. Many aspects of such tunings are described in a systematic fashion in [13]. While over some bases there is a great deal of freedom to tune many different gauge group factors on various curves in the Weierstrass model, there are also limitations imposed by the constraint that there be no codimension one loci over which f, g vanish to orders $(4, 6)$. In this paper we also avoid cases with codimension two $(4, 6)$ loci by blowing up such points on the base as part of the resolution process. Such singularities can be related to 6D superconformal field theories; in the geometric picture such singularities are associated with non-flat fibers[3] and a resolution of the singularity can generally be found by first blowing up the $(4, 6)$ point in the base, which modifies the geometry of the base B, increasing $h^{1,1}(B)$ by one. While in many cases the extent to which enhanced gauge groups can be tuned in the Weierstrass model over any given base can be determined by considerations such as the low-energy anomaly consistency conditions, the precise set of possible tunings is most clearly described in terms of an explicit description of the Weierstrass coefficients. In the case of toric bases, the complete set of monomials in f, g has a simple description (see e.g. [9, 13]) and we have very strong control over the parameters of the Weierstrass model.

2.3 Tate form and the Tate algorithm

The Tate algorithm is a systematic procedure for determining the Kodaira singularity type of an elliptic fibration, and provides a convenient way to study Kodaira singularities in the context of F-theory [29, 44]. The associated "Tate forms" for the different singularities match up neatly with the toric construction that we focus on in this paper. We start with an equation for an elliptic curve in the general form

$$y^2 + a_1 xyz + a_3 yz^3 = x^3 + a_2 x^2 z^2 + a_4 x z^4 + a_6 z^6, \tag{2.14}$$

where for an elliptic fibration a_n are sections of line bundles $\mathcal{O}(-nK_B)$. The general form (2.14) can be related to the standard Weierstrass form (2.8) by completing the square in y and shifting x, which gives the relations

$$b_2 = a_1^2 + 4a_2, \tag{2.15}$$

$$b_4 = a_1 a_3 + 2a_4, \tag{2.16}$$

$$b_6 = a_3^2 + 4a_6, \tag{2.17}$$

$$b_8 = b_2 a_6 - a_1 a_3 a_4 + a_2 a_3^2 - a_4^2, \tag{2.18}$$

$$f = -\frac{1}{48}(b_2^2 - 24b_4), \tag{2.19}$$

$$g = -\frac{1}{864}(-b_2^3 + 36b_2 b_4 - 216b_6), \tag{2.20}$$

$$\Delta = -b_2^2 b_8 - 8b_4^3 - 27b_6^2 + 9b_2 b_4 b_6. \tag{2.21}$$

---

[3]Resolution of non-flat fibers in related cases of tuned Weierstrass models has recently been considered for example in [40, 41]; the explicit connection between resolutions giving non-flat fibrations and flat fibrations over a resolved base through sequences of flops are described explicitly in the papers [42, 43] that appeared after the initial appearance of this preprint.

type	group	a_1	a_2	a_3	a_4	a_6	Δ
I_0	—	0	0	0	0	0	0
I_1	—	0	0	1	1	1	1
I_2	SU(2)	0	0	1	1	2	2
I_3^{ns}	Sp(1)	0	0	2	2	3	3
I_3^{s}	SU(3)	0	1	1	2	3	3
I_{2n}^{ns}	Sp(n)	0	0	n	n	$2n$	$2n$
I_{2n}^{s}	SU(2n)	0	1	n	n	$2n$	$2n$
I_{2n}^{s} (2nd version)	SU(2n)°	0	2	$n-1$	$n+1$	$2n$	$2n$
I_{2n+1}^{ns}	Sp(n)	0	0	$n+1$	$n+1$	$2n+1$	$2n+1$
I_{2n+1}^{s}	SU(2n+1)	0	1	n	$n+1$	$2n+1$	$2n+1$
II	—	1	1	1	1	1	2
III	SU(2)	1	1	1	1	2	3
IV^{ns}	Sp(1)	1	1	1	2	2	4
IV^{s}	SU(3)	1	1	1	2	3 $(2)^\star$	4
$I_0^{*\,ns}$	G_2	1	1	2	2	3	6
$I_0^{*\,ss}$	SO(7)	1	1	2	2	4	6
$I_0^{*\,s}$	SO(8)	1	1	2	2	$(4,3)^\star$	6
$I_{2n-3}^{*\,ns}$	SO(4n+1)	1	1	n	$n+1$	$2n$	$2n+3$
$I_{2n-3}^{*\,s}$	SO(4n+2)	1	1	n	$n+1$	$2n+1$ $(2n)^\star$	$2n+3$
$I_{2n-2}^{*\,ns}$	SO(4n+3)	1	1	$n+1$	$n+1$	$2n+1$	$2n+4$
$I_{2n-2}^{*\,s}$	SO(4n+4)	1	1	$n+1$	$n+1$	$2n+2$ $(2n+1)^\star$	$2n+4$
$IV^{*\,ns}$	F_4	1	2	2	3	4	8
$IV^{*\,s}$	E_6	1	2	2	3	5 $(4)^\star$	8
III^*	E_7	1	2	3	3	5	9
II^*	E_8	1	2	3	4	5	10
non-min	—	1	2	3	4	6	12

Table 4. Tate forms: extends earlier versions of table by including alternative SU(2n) and SO(2k) tunings that can be realized purely by orders of vanishing without additional monodromy constraints. In particular, alternate tuning (°) of SU(6) gives alternate exotic matter content; see text for further details. Groups and tunings marked with * require additional monodromy conditions.

An advantage of the general form (2.14) is that by requiring specific vanishing orders of the a_n's according to table 4, specific desired vanishing orders of (f, g, Δ) can be arranged to implement any of the possible gauge algebras. Moreover, the monodromy conditions in table 3 imposed by some gauge algebras on f, g, or Δ are also satisfied automatically by these "Tate form" models. For example, for tunings of fiber types I_m or I_m^* where Δ is required to vanish to a certain order while $\mathrm{ord}(f)$ and $\mathrm{ord}(g)$ are kept fixed, the vanishing

order of a_n's prescribed by the Tate algorithm immediately give the desired ord(Δ). This makes the Tate form much more convenient for constructing these singular fibers by only requiring the order of vanishing of the a_n's to be specified, in contrast to the Weierstrass form (2.8) where it is necessary to carefully tune the coefficients of f and g to arrange for a vanishing of Δ to higher order. The Tate forms described in table 4 are also connected very directly to the geometry of reflexive polytopes. As we discuss in the subsequent sections, tuning a Tate form can be described by simply removing certain monomials from the general form (2.14), which corresponds geometrically to removing certain points from a lattice in the toric construction. We refer to tunings of this type as "Tate tunings" in contrast to tunings of the coefficients of f and g; when applied to the polytope toric construction, we refer to Tate tunings as "polytope tunings".

Note that table 4 has incorporated some results of the present study into the Tate table originally described in the F-theory context in [29] and later modified in [44]. The most significant new feature is an alternate Tate form for the algebras $\mathfrak{su}(2n)$, with a_2 vanishing to order 2. For $n = 3$, in particular, this Tate form gives a tuning with exotic 3-index antisymmetric SU(6) matter. An example of a polytope that realizes this tuning is described in section 6.1.1. For higher n, in cases where a_1 is a constant — i.e. on curves of self-intersection -2 — this simply gives an alternate Tate tuning of SU($2n$). On any other kind of curve, at the codimension two loci where $a_1 = 0$ there is a codimension two $(4, 6)$ singularity when $n > 3$. This can immediately be seen from the fact that at the locus $a_1 = 0$, each a_k vanishes to order k so that (2.15)–(2.21) give a vanishing of (f, g, Δ) to orders $(4, 6, 12)$. Resolving this singularity generally involves blowing up a point on the base, so that the resulting elliptic fibration is naturally thought of as living on a base with larger $h^{1,1}$, but this kind of Tate model for SU(8) and higher would be relevant in a complete analysis of all reflexive polytopes.

We have also identified Tate tunings of $\mathfrak{so}(4n+4)$, like those of $\mathfrak{so}(4n+2)$ that do not require an extra monodromy condition and only require the vanishing order of a_i's; this arises naturally in the context of the geometric constructions of polytopes. We discuss briefly how these two types of Tate tunings are relevant in the constructions of this paper. For $\mathfrak{so}(4n+4)$, if a_6 is of order $2n+1$, then the necessary monodromy condition is that [44, 45] $(a_4^2 - 4a_2a_6)/z^{2n+2}|_{z=0}$ is a perfect square. This condition is clearly automatically satisfied if a_6 is actually of order $2n+2$, so can be guaranteed simply by setting certain monomials in the Tate coefficients to vanish (in a local coordinate system, which can become global in the toric context used in the later sections of the paper). On the other hand, if the leading terms in a_2, a_4, a_6 are each constrained to be powers of a single monomial m, m^{n+1}, m^{2n+1}, then the monodromy condition will be automatically satisfied with a_6 of order $2n+1$ without specifying any particular coefficients for these monomials. We encounter both kinds of situation in this paper. For $\mathfrak{so}(8)$, the monodromy condition when a_6 is of order 4 is that $(a_2^2 - 4a_4)/z^2|_{z=0}$ is a perfect square [44].[4] This can be satisfied if a_2, a_4 contain only

---

[4]To relate this to the condition stated in table 3, note that the leading term in the discriminant when that condition is satisfied becomes $-(a - b)^2(2a + b)^2(2b + a)^2$, so that condition implies the perfect square condition. Going the other way, when the perfect square condition is satisfied we can determine a, b by noting that $a_2/3$ is one of the roots $a, b, -a - b$ of the cubic $x^3 + f_2x + g_3$, so without loss of generality we have $a = a_2/3$, and solving for b gives $b = -a_2/6 + (a_2^2 - 4a_4)^{1/2}/2$.

a single monomial each m, m^2 at leading order, but cannot be imposed by simply setting the orders of vanishing of each a_i. The situation is similar when a_6 is of order 3, though the monodromy condition is more complicated when a_2, a_4, a_6 are not single monomials m, m^2, m^3. This is the only gauge algebra with no monodromy-independent Tate tuning except through this kind of single monomial condition. Finally, for $\mathfrak{so}(4n+2)$, with a_6 of order $2n$, the monodromy condition is that $(a_3^2 + 4a_6)/z^{2n}|_{z=0}$ is a perfect square, satisfied in particular if a_6 is actually of order $2n+1$ or if the leading terms in a_3, a_6 are each a single monomial proportional to m, m^2. We explore further, for example, in section 4.6 for $\mathfrak{so}(12)$ the subtleties in using the Tate tuning $\{1, 1, 3, 3, 5\}$ described in [29], which requires an additional monodromy condition, vs. our alternative tuning $\{1, 1, 3, 3, 6\}$; in fact, analogous situations occur in tuning all gauge algebras with monodromies.

2.4 The Zariski decomposition

A central feature of the geometry of an F-theory base surface is the structure of the intersection form on curves (divisors) in B_2. The intersection form on $H_2(B, \mathbb{Z})$ has signature $(1, T)$. Curves of negative self-intersection $C \cdot C < 0$ are rigid. A simple but useful algebraic geometry identity, which follows from the Riemann-Roch theorem, is that

$$C \cdot (C + K_B) = 2g - 2, \qquad (2.22)$$

for any curve C of genus g. We are primarily interested in rational (genus 0) curves, for which therefore $C \cdot C = -K_B \cdot C - 2$. All toric curves on a toric base B_2 are rational, and the intersection product of toric curves has a simple structure that we review in the following section.

To study the orders of vanishing of f, g and Δ along some irreducible divisors in the base, aside from looking explicitly at the sets of monomials of f, g and Δ, it is convenient to consider the more abstract "Zariski decomposition", in which an effective divisor A is decomposed into (minimal) multiples of irreducible effective divisors C_i of negative self-intersection and a residual part Y

$$A = \sum_i q_i C_i + Y, \quad q_i \in \mathbb{Q}, \qquad (2.23)$$

where Y is effective and satisfies

$$Y \cdot C_i = 0, \quad \forall i. \qquad (2.24)$$

Then the order of vanishing along the curve C_i of a section of the line bundle corresponding to the divisor A must be at least $c_i = \lceil q_i \rceil$. Mathematically, the Zariski decomposition is normally considered over the rationals, so $q_i \in \mathbb{Q}$. Here, however, we are simply interested in the smallest integer coefficient of C_i compatible with the decomposition over the ring of integers. For example, consider the decomposition

$$-nK_B = \sum_i c_i C_i + Y \qquad (2.25)$$

The goal is to find the minimal set of integer values c_i such that the conditions $Y \cdot C_i \geq 0$ are satisfied. Taking the intersection product on both sides with C_j, the conditions can be

rewritten as the set of inequalities

$$v_{j,n} - \sum_i M_{ji} c_i \geq 0 , \ \forall j, \tag{2.26}$$

where $M_{ji} \equiv C_j \cdot C_i$ are pairwise intersection numbers (non-negative for $i \neq j$) and self-intersection numbers $M_{jj} = C_j \cdot C_j \equiv m_j$, and $v_{j,n} \equiv -nK_B \cdot C_j$.

The Zariski decomposition of $-4K_B$ and $-6K_B$ was used in [8] to analyze the non-Higgsable clusters that can arise in 6D theories. More generally, we can use the same approach to analyze models where we tune a given gauge factor on a specific divisor beyond the minimal content specified by the non-Higgsable cluster structure. In such a situation, we would choose by hand to take some values of c_i in (2.25) to be larger than the minimal possible values; this may in turn force other coefficients c_j to increase. As a simple example, consider a pair of -2 curves (i.e. curves of self-intersection -2) C, D that intersect at a point ($C \cdot D = 1$). The Zariski decomposition of the discriminant locus gives simply $-12K_B = Y$, since $K_B \cdot C = K_B \cdot D = 0$ from (2.22), so the discriminant need not vanish on C or D. If, however, we tune for example an $\mathfrak{su}(4)$ gauge algebra on D so that Δ vanishes to order 4 on D then we have the Zariski decomposition $-12K_B - 4D = 2C + Y'$, since $-4D \cdot C = -4$, implying that Δ must also vanish to order 2 on C, so that C must therefore also carry at least an $\mathfrak{su}(2)$ gauge algebra.

2.5 Zariski decomposition of a Tate tuning

A particular application of the Zariski decomposition that we use here extensively is in the context of a Tate tuning. In particular, assume that we have an elliptic fibration in the Tate form (2.14) over a complex surface base B, and we have a set of curves C_j in the base that includes all curves of negative self-intersection. The parameter space of the elliptic fibration is given by the five sections $a_n \in \mathcal{O}(-nK), n = 1, 2, 3, 4, 6$. We denote by $c_{j,n}$ the order of vanishing of a_n on C_j. The minimal necessary order of vanishing of each a_n on each curve C_j can be determined by applying the Zariski decomposition for $-nK$. This gives rise to a set of vanishing orders $c_{j,n}$ associated with each non-Higgsable cluster, which we list in table 5. These are the minimal values $c_{j,n} = c_{j,n}^{\mathrm{NHC}}$ that satisfy the inequalities (2.26) for each value of $n \in \{1, 2, 3, 4, 6\}$. In doing a Tate tuning, we impose the additional condition that over certain curves C_j, the vanishing order is at least some specified value that is higher than the minimum imposed by the NHCs, $c_{j,n} \geq c_{j,n}^{\mathrm{tuned}} \geq c_{j,n}^{\mathrm{NHC}}$. We can then use the Zariski decomposition to determine the minimum values of the $c_{j,n}$ compatible with this lower bound that also satisfy the inequalities (2.26).

More concretely, to determine the unique minimum set of values $c_{j,n}$ that satisfy the inequalities (2.26), we proceed iteratively, following an algorithm described in appendix A of [8]. For each n, we begin with an initial assignment of vanishing orders

$$c_{j,n}^{(0)} = c_{j,n}^{\mathrm{tuned}} \tag{2.27}$$

when we are imposing a given tuning. When we are computing the minimal values from NHC's without tuning we simply use the minimal order of vanishing from the Zariski

decomposition on each isolated curve of self-intersection $m_j = M_{jj}$,

$$c_{j,n}^{(0)} = \begin{cases} \left\lceil \frac{n(2+m_j)}{m_j} \right\rceil, & m_j \le -3, \\ 0, & m_j > -3. \end{cases} \tag{2.28}$$

We can then use the inequalities (2.26) to determine the minimal correction that is needed to each vanishing order (label n dropped for clarity of the notation),

$$\Delta c_j^{(1)} = \text{Max}\left(0, \left\lceil \frac{v_j - \sum_i M_{ji}\,(c_i^{(0)})}{m_j} \right\rceil\right). \tag{2.29}$$

The second corrections are obtained similarly, replacing $c^{(0)}$ on the r.h.s. with $c^{(1)} = c^{(0)} + \Delta c_j^{(1)}$. We continue to repeat this procedure until the corrections in the f-th step all become zero, $\Delta c_j^{(f)} = 0$ for all j. The final solutions $\{c_j\}$ are obtained iteratively this way by adding the non-negative correction values $\{\Delta c_j^{(k)}\}$:

$$c_j = c_j^{(0)} + \Delta c_j^{(1)} + \Delta c_j^{(2)} + \cdots + 0,$$
$$\text{where} \quad \Delta c_j^{(l+1)} = \text{Max}\left(0, \left\lceil \frac{v_j - \sum_i M_{ji}\,(c_i^{(0)} + \sum_{k=1}^{l} \Delta c_i^{(k)})}{m_j} \right\rceil\right). \tag{2.30}$$

At each step this algorithm clearly increases the orders of vanishing in a minimal way, so when the algorithm terminates the solution is clearly a minimal solution of the inequalities (2.26). Note that in some cases, the algorithm leads to a runaway behavior when there is no acceptable solution without (4, 6) loci. When this occurs, or when one of the factors of the gauge algebra exceeds that desired by the tuning, we terminate the algorithm and do not consider this tuning as a viable possibility.

As an example, consider the set of curves $\{C_j\}$ to be the NHC $\{-3, -2\}$, so $M_{ji} = \{\{-3, 1\}, \{1, -2\}\}$, and

$$\{\{v_1, v_2\}|n = 1, 2, 3, 4, 6\} = \{\{-1, 0\}, \{-2, 0\}, \{-3, 0\}, \{-4, 0\}, \{-6, 0\}\},$$
$$\{\{c_{1,n}^{(0)}, c_{2,n}^{(0)}\}|n\} = \{\{1, 0\}, \{1, 0\}, \{1, 0\}, \{2, 0\}, \{2, 0\}\}.$$

Then the vanishing orders calculated from (2.30) are $\{c_{1,n}\} = \{1, 1, 2, 2, 3\}$ and $\{c_{2,n}\} = \{1, 1, 1, 1, 2\}$, as shown in table 5.

Note that a tuning beyond that shown in table 5 does not necessarily increase the gauge group on any of the curves. In particular, for some gauge groups there are multiple possible Tate tunings. Both for the generic gauge group associated with the generic elliptic fibration over a given base and for constructions with gauge groups that are enhanced through a Tate tuning, this means that there may be distinct Tate tunings with the same physical properties. As we will see later, these distinct Tate tunings can correspond through distinct polytopes to different Calabi-Yau threefold constructions. Note also that for the toric bases we are studying here, an essentially equivalent analysis could be carried out by explicitly working with the various monomials in the sections a_n, which in the toric context are simply points in a dual lattice, as we discuss in the next section. We use the Zariski procedure because it is more efficient and more general; the results of this analysis should, however, match an explicit toric computation in each case.

NHC	$\{c_{j,n}^{\text{NHC}}\}$
$\{-3\}$	$\{\{1, 1, 1, 2, 2\}\}$
$\{-4\}$	$\{\{1, 1, 2, 2, 3\}\}$
$\{-5\}$	$\{\{1, 2, 2, 3, 4\}\}$
$\{-6\}$	$\{\{1, 2, 2, 3, 4\}\}$
$\{-7\}$	$\{\{1, 2, 3, 3, 5\}\}$
$\{-8\}$	$\{\{1, 2, 3, 3, 5\}\}$
$\{-12\}$	$\{\{1, 2, 3, 4, 5\}\}$
$\{-3, -2\}$	$\{\{1, 1, 2, 2, 3\}, \{1, 1, 1, 1, 2\}\}$
$\{-3, -2, -2\}$	$\{\{1, 1, 2, 2, 3\}, \{1, 1, 2, 2, 2\}, \{1, 1, 1, 1, 1\}\}$
$\{-2, -3, -2\}$	$\{\{1, 1, 1, 1, 2\}, \{1, 2, 2, 2, 4\}, \{1, 1, 1, 1, 2\}\}$

Table 5. The minimal vanishing orders of sections $a_{1,2,3,4,6}$ over NHCs.

2.6 Matter content from anomaly constraints in F-theory

Six-dimensional $\mathcal{N} = (1, 0)$ supergravity theories potentially suffer from gravitational, gauge, and mixed gauge-gravitational anomalies. We focus here primarily on nonabelian gauge anomalies, though similar considerations hold for abelian gauge factors. On the one hand, the anomaly information can be encoded in an 8-form I_8, which is built from the 2-forms characterizing the non-abelian field strength F and the Riemann tensor R, and which has coefficients that can be computed in terms of T, V, H, and the explicit numbers of chiral matter fields in different representations. On the other hand, the anomalies can be cancelled through a generalized Green-Schwarz term if I_8 factorizes for some constant coefficients a^α, b_i^β in the vector space $\mathbb{R}^{1,T}$ associated with self-dual and anti self-dual two-forms $B_{\mu\nu}$ in the gravity and tensor multiplets,

$$I_8 = \frac{1}{2}\Omega_{\alpha\beta}X_4^\alpha X_4^\beta, \tag{2.31}$$

where

$$X_4^\alpha = \frac{1}{2}a^\alpha \text{tr} R^2 + \sum_i b_i^\alpha \frac{2}{\lambda_i}\text{tr}F_i^2. \tag{2.32}$$

Here $\Omega_{\alpha\beta}$ is a signature $(1, T)$ inner product on the vector space, and λ_i are normalization constants for the non-abelian gauge group factors G_i. Then, using the notation and conventions of [46], the conditions for anomaly cancellation are obtained by equating the

coefficients of each term from the two polynomials

$$R^4 : \quad H - V = 273 - 29T, \tag{2.33}$$

$$F^4 : \quad 0 = B^i_{Adj} - \sum_R x^i_R B^i_R, \tag{2.34}$$

$$(R^2)^2 : \quad a \cdot a = 9 - T, \tag{2.35}$$

$$F^2 R^2 : \quad a \cdot b_i = \frac{1}{6} \lambda_i \left(A^i_{Adj} - \sum_R x^i_R A^i_R \right), \tag{2.36}$$

$$(F^2)^2 : \quad b_i \cdot b_i = \frac{1}{3} \lambda_i^2 \left(\sum_R x^i_R C^i_R - C^i_{Adj} \right), \tag{2.37}$$

$$F_i^2 F_j^2 : \quad b_i \cdot b_j = 2 \sum_{R,S} x^{ij}_{RS} A^i_R A^j_S, \ \ i \neq j, \tag{2.38}$$

where A_R, B_R, C_R are group theory coefficients[5] defined by

$$\text{tr}_R F^2 = A_R \text{tr}_{\text{fund.}} F^2, \tag{2.39}$$

$$\text{tr}_R F^4 = B_R \text{tr}_{\text{fund.}} F^4 + C_R (\text{tr}_{\text{fund.}} F^2)^2, \tag{2.40}$$

x^i_R is the number of matter fields[6] in the representation R of the non-abelian factor G_i, and x^{ij}_{RS} is the number of matter fields in the (R, S)-representation of $G_i \otimes G_j$.

For 6D theories coming from an F-theory compactification, the vectors a, b^i are related to homology classes in the base B_2 through the relations

$$a \leftrightarrow K_B, \tag{2.41}$$

$$b_i \leftrightarrow C_i, \tag{2.42}$$

where, again, K_B is the canonical class of B_2, and $C_i \in H_2(B_2, \mathbb{Z})$ are irreducible curves in the base supporting the singular fibers associated with the non-abelian gauge group factors G_i. With this identification, the Dirac inner products between vectors in $\mathbb{R}^{1,T}$ are related to intersection products between divisors in the base.

In principle, the matter content of a 6D theory can be determined by a careful analysis of the codimension two singularities in the geometry. In many situations, however, the generic matter content of a low-energy theory is uniquely determined by the gauge group content and anomaly cancellation simply from the values of the vectors a, b^i. For example, a theory with an SU(N) gauge factor associated with a vector b generically has g adjoint matter fields, $(8-N)n + 16(1-g)$ fundamental matter fields, and $(n+2-2g)$ two-index antisymmetric matter fields, where $n = b \cdot b$ and $g = 1 + (a \cdot b + n)/2$ (see e.g. [13]); this simplifies

---

[5]A summary of A_R, B_R, C_R in different representations and λ_i for different non-abelian gauge groups can be found in appendix B in [13].

[6]For each representation the matter content contains one complex scalar field and a corresponding field in the conjugate representation. For special representations like the **2** of SU(2), the representation is pseudoreal, so that the conjugate need not be included; such a field is generally referred to as a "half-hypermultiplet".

in the $g = 0$ case of primary interest to us here to a spectrum of $n+2$ two-index antisymmetric matter fields and $16 + (8 - N)n$ fundamental fields. For most of the theories we consider here the matter content follows uniquely in this way from the values of a, b^i. In some situations, however, more exotic matter representations can arise; we encounter some cases of this later in this paper, such as the three-index antisymmetric representation of SU(6).

In general, the anomaly constraints on 6D theories provide a powerful set of consistency conditions that we use in many places in this paper to analyze and check various models that arise through tunings; in particular, using the anomaly conditions to determine the matter spectrum gives a direct and simple way in many cases to compute the Hodge numbers of the associated elliptic Calabi-Yau manifold that can be matched to the Hodge numbers of a toric hypersurface construction.

2.7 Global symmetry constraints in F-theory

In many cases, the anomaly cancellation conditions impose constraints not only on the matter content of the theory but also on what gauge groups may be combined on intersecting curves, corresponding to vectors b^i with non-vanishing inner products in the low-energy theory. For example, two gauge factors of $\mathfrak{g}_2$ or larger in the Kodaira classification cannot be associated with vectors b, b' having $b \cdot b' > 0$; in the low-energy supergravity theory this is ruled out by the anomaly conditions while in the F-theory picture this would correspond to a configuration with a codimension two (4, 6) point at the intersection between the corresponding curves. In addition to these types of constraints, another set of constraints on what combination of gauge groups can be tuned on specific negative self-intersection curves in a base B_2 can be derived from the low-energy theory by considering the maximum global symmetry of an SCFT that arises by shrinking a curve C of self-intersection $n < 0$ that supports a given gauge factor G_i [47]. While in most cases these global symmetry conditions simply match with the expectation from anomaly cancellation, in some circumstances the global symmetry condition imposes stronger constraints. For example the "E_8 rule" [48] states that the maximal global symmetry on a -1 curve that does not carry a nontrivial gauge algebra is $\mathfrak{e}_8$; i.e., the direct sum of the gauge algebras carried by the curves intersecting the -1 curve should be a subalgebra of $\mathfrak{e}_8$. While the global symmetry constraints are completely consistent with F-theory geometry, they may not be a complete and sufficient set of constraints; for example a similar constraint appears to hold in F-theory for the algebras on a set of curves intersecting a 0 curve [13], though the low-energy explanation for this is not understood in terms of global constraints from SCFT's.

The maximal global symmetry groups realized in 6D F-theory for each possible algebra on a curve of self-intersection $m \leq -1$ are worked out in [47]. We use their results in our algorithm to constrain possible gauge algebra tunings. More explicitly, given a gauge algebra on a curve, the maximal global symmetry on the curve is determined, so the direct sum of the algebras on the curves intersecting it should be a subalgebra of the maximal global symmetry algebra. For instance, consider a linear chain of three curves $\{C_1, C_2, C_3\}$ carrying gauge algebras $\{\mathfrak{g}_1, \mathfrak{g}_2, \mathfrak{g}_3\}$. These can be either minimal or enhanced algebras, but they have to satisfy $\mathfrak{g}_3 \oplus \mathfrak{g}_1 \subset \mathfrak{g}_2^{(\mathrm{glob})}$, where $\mathfrak{g}_2^{(\mathrm{glob})}$ is the maximal global symmetry algebra given $\mathfrak{g}_2$ on the curve C_2, as enumerated in the tables in [47]. This will be useful

for us to constrain the possible tunings on a curve when the gauge symmetries on its neighboring curves are known, making our search over possible tunings more efficient. This is also convenient sometimes for us to determine the gauge algebras that have monodromy conditions without having to figure out the monodromy directly; the trick to doing this is described in section 4.6. We also include the "E_8 rule" in our algorithm in section 5.1, corresponding to the case where $m = -1$ and $\mathfrak{g}_2$ is trivial.

2.8 Base surfaces for 6D F-theory models

There is a finite set of complex base surfaces that support elliptic Calabi-Yau threefolds. It was shown by Grassi [49] that all such bases can be realized by blowing up a finite set of points on the minimal bases $\mathbb{P}^2, \mathbb{F}_m$ with $0 \leq m \leq 12$, and the Enriques surface. This leads to a systematic constructive approach to classifying the set of allowed F-theory bases. The structure of non-Higgsable clusters limits the configurations of negative self-intersection curves that can arise on any given base, so we can in principle construct all allowed bases by blowing up points in all possible ways and truncating the set of possibilities when a disallowed configuration such as a curve of self-intersection -13 or below arises. This was used in [9] to classify the full set of toric bases B_2 that can support elliptic Calabi-Yau threefolds (toric geometry is described in more detail in the following section). While further progress has been made [10, 11] in classifying non-toric bases, we focus here primarily on toric base surfaces, as these are the primary bases that arise in the toric hypersurface construction of Calabi-Yau threefolds. Note, however, that as we discuss later in the paper, particularly in e.g. section 4.7, section 6.1.3, there are cases in the Kreuzer-Skarke database where a toric polytope corresponds to an elliptic fibration over a non-toric base. The primary context in which this distinction is relevant involves curves of self-intersection $-9, -10$, and -11. As discussed in [8], the Weierstrass model over such curves automatically has 1, 2, or 3 points on the curve where f, g vanish to degrees $(4, 6)$. Such points on the base can be blown up for a smooth Calabi-Yau resolution, so that the actual base supporting the elliptic fibration is generally a non-toric complex surface.[7] In the simplest cases, such as $\mathbb{F}_{11}$ and $\mathbb{F}_{10}$, the blown up base still has a toric description; in other simple cases, such as $\mathbb{F}_9$, the resulting surface is a "semi-toric" surface admitting only a single $\mathbb{C}^*$ action [10], but on surfaces with, for example, multiple curves of self-intersection $-9, -10, -11$, the blow-up of all $(4, 6)$ points in the base gives generally a non-toric base that is neither toric nor admits a single $\mathbb{C}^*$ action. Despite this complication, this blow-up and resolution process is automatically handled in a natural way in the framework of the toric hypersurface construction, so that (non-flat) elliptic fibrations over bases with these types of curves arise naturally in the Kreuzer-Skarke database. Thus, we include toric bases with curves of self-intersection $-9, -10, -11$ in the set of bases we consider for Tate/Weierstrass constructions. The complete set of such bases was enumerated in [9], where it was shown that there are 61,539 toric bases that support elliptic CY3's. Generic elliptic Calabi-Yau threefolds over these bases give rise to a range of Hodge number pairs

---

[7]More precisely, as described in [31] and section 2.2, and discussed in more detail in section 4.7, the original base supports an elliptic fibration that is "non-flat," meaning that the fiber becomes two dimensional at some points, while the elliptic fibration over the blown up base is a flat elliptic fibration.

that fill out the range of known Calabi-Yau Hodge numbers, in a "shield" shape with peaks at $(11, 491)$, $(251, 251)$, and $(491, 11)$ [39]. As we see in section 6, in some cases the base needed for a tuned Weierstrass model to match a toric hypersurface construction is even more exotic than those arising from blowing up points on curves of self-intersection $-9, -10, -11$. In these more complicated cases as well, however, the general story is the same. The polytope construction gives rise to a non-flat elliptic fibration with codimension two $(4, 6)$ points on the toric base. Blowing these curves up gives rise to another, generically non-toric, base with multiple additional curves. After these blow-ups, there is a tuned Weierstrass model giving a (flat) elliptic fibration over the new base. While the toric base is what arises most clearly from the polytope construction, the structure of the blown up base admitting the flat elliptic fibration is relevant when considering F-theory models and anomaly cancellation.

In section 4 we consider Tate tunings over the toric bases and compare to the toric hypersurface construction of elliptic Calabi-Yau threefolds, which we now describe in more detail.

3 Elliptic fibrations in the toric reflexive polytope construction

3.1 Brief review of toric varieties

Following [50, 51], we review some basic features of toric geometry. An n-dimensional toric variety X_Σ can be constructed by defining the *fan* of the toric variety. A fan Σ is a collection of cones[8] in $N_{\mathbb{R}} = N \otimes \mathbb{R}$, each with the apex at the origin, and where N is a rank n lattice, satisfying the conditions that

- Each face of a cone in Σ is also a cone in Σ.

- The intersection of two cones in Σ is a face of each.

Then X_Σ can be described by the homogeneous coordinates z_i corresponding to the one-dimensional cones v_i (also called rays) of Σ; X_Σ may be constructed as the quotient of an open subset in $\mathbb{C}^k$ (k is the number of rays), by a group G,

$$X_\Sigma = \frac{\mathbb{C}^k - Z(\Sigma)}{G}, \tag{3.1}$$

where

- $Z(\Sigma) \subset \mathbb{C}^k$ is the union of the zero sets of the polynomial sets $\mathcal{S} = \{z_i\}$ associated with the sets of rays $\{v_i\}$ that do not span a cone of Σ.

- $G \subset (\mathbb{C}^*)^k$ is the kernel of the map

$$\phi : (\mathbb{C}^*)^k \to (\mathbb{C}^*)^n, (z_1, \ldots, z_k) \mapsto \left(\prod_{j=1}^k z_j^{v_{j,1}}, \ldots, \prod_{j=1}^k z_j^{v_{j,n}} \right),$$

where $v_{j,l}$ specifies the lth component of the ray v_j in the coordinate representation in $\mathbb{C}^n$.

---

[8]More rigorously, these are *strongly convex cones*, which are generated by a finite number of vectors in N and which contain no line through the origin.

Toric divisors D_i are given by the sets $D_i \equiv \{z_i = 0\}$ associated to all the rays v_i. The anti-canonical class $-K$ of a toric variety is given by the sum of toric divisors

$$-K = \sum_i D_i. \qquad (3.2)$$

Smooth two-dimensional toric varieties are particularly simple. The irreducible effective toric divisors are rational curves with one intersecting another forming a closed linear chain. This is easily seen from the 2D toric fan description, where each ray of the 2D fan corresponds to an irreducible effective toric divisor. The intersection products are also easy to read off from the fan diagram, where (including divisors cyclically by setting $D_{k+1} \equiv D_1$, etc.)

$$D_i \cdot D_{i+1} = 1, \qquad (3.3)$$

and the self-intersection of each curve is

$$D_i \cdot D_i = m_i, \qquad (3.4)$$

where m_i is such that

$$-m_i v_i = v_{i-1} + v_{i+1}, \qquad (3.5)$$

and zero otherwise. We will generally denote the data defining a smooth 2D toric base by the sequence of self-intersection numbers. (The 2D fan can be recovered given the intersections, up to lattice automorphisms.)

In the context of this paper, toric varieties play two distinct but related roles. On the one hand, we can use toric geometry to describe many of the bases that support elliptically fibered Calabi-Yau threefolds. On the other hand, toric geometry can be used to describe ambient fourfolds in which CY threefolds can be embedded as hypersurfaces, as we describe in the next section.

3.2 Batyrev's construction of Calabi-Yau manifolds from reflexive polytopes

Given a *lattice polytope*, which is the convex hull of a finite set of lattice points (in particular, the vertices are lattice points), we may define a *face fan* by taking rays to be the vertices of the lattice polytope, and the top-dimensional (n-dimensional) cones to correspond to the facets of the polytope. By including more lattice points in addition to vertices of the polytope as rays, and thus subdividing ("triangulating") the facets of the polytope into multiple smaller top-dimensional cones, we can refine the fan to impose further properties such as simpliciality or smoothness.[9] In this way, a lattice polytope can be associated with a toric variety. In general, a given lattice polytope can lead to many different varieties, depending upon the refinement of the face fan. Even for a given set of additional rays added, there can be many different triangulations of the fan.

---

[9]A fan is simplicial if all its cones are simplicial. A cone is simplicial if its generators are linearly independent over $\mathbb{R}$. A fan is smooth if the fan is simplicial and for each top-dimensional cone its generators generate the lattice N.

We will be interested in particular in the fans from *reflexive polytopes,* which are defined as follows. Let N be a rank n lattice, $N_{\mathbb{R}} \equiv N \otimes \mathbb{R}$. A lattice polytope $\nabla \subset N$ containing the origin is reflexive if its *dual polytope* is also a lattice polytope. The dual of a polytope ∇ in N is defined to be

$$\nabla^* = \{u \in M_{\mathbb{R}} = M \otimes \mathbb{R} : \langle u, v \rangle \geq -1, \forall v \in \nabla\}, \tag{3.6}$$

where $M = N^* = \mathrm{Hom}(N, \mathbb{Z})$ is the dual lattice. If ∇ is reflexive, its dual polytope $\Delta = \nabla^*$ is also reflexive as $(\nabla^*)^* = \nabla$. We call the pair of reflexive polytopes a mirror pair. Both of them contain the origin as the only interior lattice point. Calabi-Yau manifolds in Batyrev's construction [52] are built out of reflexive polytopes. Given a mirror pair $\nabla \subset N$ and $\Delta \subset M$, the (possibly refined) face fan of ∇ describes a toric ambient variety, in which a Calabi-Yau hypersurface is embedded using the anti-canonical class of the ambient toric variety, so that the hypersurface itself has trivial canonical class. Explicitly, a section of the anti-canonical bundle is given by

$$p = \sum_{i}^{\# \text{ lattice points in } \Delta} c_i m_i, \tag{3.7}$$

where c_i are generic coefficients taking values in $\mathbb{C}$ and each monomial m_i is given by an associated lattice point w_i in Δ

$$m_i = \prod_j z_j^{\langle w_i, v_j \rangle + 1}, \tag{3.8}$$

where z_j is the homogeneous coordinate associated with the ray v_j in the fan associated to ∇. The well-definedness of each m_i in terms of the homogeneous coordinates z_j is guaranteed by the linear equivalence relations among the divisors associated to v_j's, and holomorphicity in the z_js by the reflexivity of ∇. We can check that equation (3.7) indeed defines a section of the anti-canonical class, so that a CY hypersurface is cut out by $p = 0$. We can determine the class by looking at any one of the monomials; we pick the origin since we know it is always an interior point. Its associated monomial by equation (3.8) is simply the product of all homogeneous coordinates associated to all toric divisors $\prod_{j=1}^{\# \text{ rays}} z_j$, which immediately we see by equation (3.2) is a section in the anti-canonical class. For the smoothness of the Calabi-Yau, as mentioned previously, there exists a refinement[10] of the face fan of ∇ such that the fan is simplicial so the ambient toric variety will have at most orbifold singularities. In the case of $n \leq 4$, with the anti-canonical embedding, a hypersurface will generically avoid these singularities and therefore is generically smooth.

M. Kreuzer and H. Skarke have classified all 473,800,776 four-dimensional reflexive polytopes for the Batyrev Calabi-Yau construction [4, 53]. A pair of reflexive polytopes in the KS database are described in the format:

M:# lattice points, # vertices (of Δ) N:# lattice points, # vertices (of ∇) H: $h^{1,1}$, $h^{2,1}$.

---

[10]Appropriate subdivisions of the face fan of the toric ambient variety by additional lattice points in the facets of the polytope give the resolved description of the embedded Calabi-Yau, where extra coordinates in equation (3.8) define the exceptional divisors in the resolution of the ambient space. The added lattice points that do not lie in the interior of the facets also correspond to exceptional divisors in the resolution of the Calabi-Yau. (Generic hypersurface CYs do not meet the divisors that correspond to interior points of facets.)

We will refer to ∇ as the (fa)N polytope and Δ as the M(onomial) polytope to remind ourselves that ∇ gives the fan of the ambient toric variety for the CY anti-canonical embedding and Δ determines the monomials of the anti-canonical hypersurface. In many cases, it is sufficient to specify polytopes with the information given in the format above, but sometimes there can be distinct polytopes with identical information of this type, in which case we will either give further the vertices of the N polytope to specify the polytope more precisely, or indicate its numerical order as it appears among those with identical data in the KS database website () with a superscript, e.g., M:165 11 N:18 9 H:9,129[1] or M:165 11 N:18 9 H:9,129[2].

Note that conversely, we can start from Δ and associate it with the polytope that defines the fan of the ambient space, and calculate monomials associated with lattice points in ∇. Then the hypersurface CY is mirror to the previous one. The Hodge numbers of mirror pairs are related by $h^{p,q}(CY_\nabla) = h^{d-p,q}(CY_\Delta)$, where $d = n - 1$ is the complex dimension of the CY; in particular, we will look at 4 dimensional reflexive polytopes for CY threefolds, where the only non-trivial Hodge numbers are $h^{1,1}$ and $h^{2,1}$, and mirror CY hypersurfaces have exchanged values for $h^{1,1}$ and $h^{2,1}$. As ∇ and Δ are a pair of 4D reflexive polytopes, there is a one-to-one correspondence between l-dimensional faces θ of Δ and $(4 - l)$-dimensional faces $\tilde{\theta}$ of ∇ related by the dual operation

$$\theta^* = \{y \in \nabla, \langle y, pt \rangle = -1| \text{ for all } pt \text{ that are vertices of } \theta\}. \tag{3.9}$$

For the CY associated with ∇, the Hodge numbers are given by

$$h^{2,1} = \text{pts}(\Delta) - \sum_{\theta \in F_3^\Delta} \text{int}(\theta) + \sum_{\theta \in F_2^\Delta} \text{int}(\theta)\text{int}(\theta^*) - 5, \tag{3.10}$$

$$h^{1,1} = \text{pts}(\nabla) - \sum_{\tilde{\theta} \in F_3^\nabla} \text{int}(\tilde{\theta}) + \sum_{\tilde{\theta} \in F_2^\nabla} \text{int}(\tilde{\theta})\text{int}(\tilde{\theta}^*) - 5, \tag{3.11}$$

where θ are faces of Δ, $\tilde{\theta}$ are faces of ∇, $F_l^{\nabla/\Delta}$ denotes the set of l-dimensional faces of ∇ or Δ ($l < n$), and $\text{pts}(\nabla/\Delta) :=$ number of lattice points of ∇ or Δ, $\text{int}(\theta/\tilde{\theta}) :=$ number of lattice points interior to θ or $\tilde{\theta}$. The correspondence (3.9) makes the duality between the Hodge number formulae manifest. Note that the Hodge numbers depend only on the polytope and not on the detailed refinement of the fan.

3.3 Fibered polytopes in the KS database

For the purpose of studying (often singular) elliptically fibered Calabi-Yau threefolds that arise in the KS database, we will be interested in 4D reflexive *fibered polytopes* [31, 54–56]. A fibered polytope ∇ is a polytope in the N lattice that contains a lower-dimensional subpolytope, $\nabla_2 \subset N_2 = \mathbb{Z}^2$, which passes through the origin. We are interested in the case where ∇_2 is itself a reflexive 2D polytope, containing the origin as an interior point. Such a fibered polytope ∇ admits a projection map $\pi : \nabla \to N_B$ such that $\pi^{-1}(0) = \nabla_2$, and $N_B = \mathbb{Z}^2$ is the quotient of the original lattice N by the projection. We can construct a set of rays $v_i^{(B)}$ in N_B that are the primitive rays with the property that an integer multiple of $v_i^{(B)}$ arises as the image $\pi(v_i)$ of a ray in ∇. (A *primitive* ray $v \in N$ is one that

cannot be described as an integer multiple $v = nw$ of another ray $w \in N$, with $n > 1$.) We define the base B_2 to be the 2D toric variety given by the 2D fan Σ_B with $v_i^{(B)}$ taken to be the 1D cones; the 2D cones are uniquely defined for a 2D variety. Note that in higher dimensions, the base of the fibration is not uniquely defined as a toric variety since the cone structure of the base may not be unique.

In the toric geometry language, a *fan morphism* is a projection $\pi : \Sigma \to \Sigma_B$ with the property that for any cone in Σ the image is contained in a cone of Σ_B. Such a fan morphism can be translated to a map between toric varieties $\pi : X_\Sigma \to B_2$. Such a map is a *toric morphism*, which is an equivariant map with respect to the torus action on the toric varieties that maps the maximal torus in X_Σ to the maximal torus in B_2. As far as the authors are aware, it is not known whether in general every fibered polytope admits a triangulation leading to a compatible fan morphism and toric morphism. Note, however, that the elliptic fiber structure of the polytope does not depend upon the existence of a triangulation with respect to which there is a fan morphism $\pi : \Sigma_\nabla \to \Sigma_B$. Thus, to recognize an elliptic Calabi-Yau threefold in the KS database, it is only necessary to find a reflexive subpolytope $\nabla_2 \subset \nabla$. The Calabi-Yau manifold defined by an anti-canonical hypersurface in X_Σ through the Batyrev construction with reflexive polytopes will then be an elliptically fibered Calabi-Yau threefold over the base B_2 [55]. A primary goal of this paper is to relate reflexive polytopes in the Kreuzer-Skarke database that have this form to elliptic fibrations of tuned Weierstrass models as described in section 2.

There are in total 16 2D reflexive polytopes, which give slightly different realizations of an elliptic curve when an anti-canonical hypersurface is taken [23, 31, 57]. The hypersurface equations $p = 0$, with p given in (3.7), of all 16 types of fibered polytopes can be brought into the Weierstrass form (2.8) by the methods described in appendix A in [31]; this gives an equivalent description of the same Calabi-Yau as long as the fibration has a global section. The Kreuzer-Skarke database of reflexive polytopes and associated Calabi-Yau hypersurface constructions contains a wide range of polytopes that include fibered polytopes with many different examples of the 16 fiber types.

For a given base B_2 and a given fiber type, there can be a variety of different polytopes corresponding to configurations with different "twists" of the fibration, associated with different embeddings of the rays v_i defining the base B_2 with respect to the fiber subpolytope ∇_2. For example, the Hirzebruch surfaces $\mathbb{F}_m$ are each associated with fibered polytopes with fiber and base $\mathbb{P}^1$, distinguished by the different twists of the fibration. For a fibered polytope ∇ with a reflexive subpolytope ∇_2, the dual Δ admits a projection to $\Delta_2 = (\nabla_2)^*$.

One of the findings of this paper is that the bulk of KS models with large Hodge numbers appear to have a description in the form of a *standard* $\mathbb{P}^{2,3,1}$-fibered type, with a specific form for the twist of the fiber over the base surface B_2; these models can be connected directly to the Tate form for elliptic fibrations, and in fact can be constructed from that point of view directly. On the one hand, we describe the structure of this type of standard polytope in section 3.4, with the result that the anti-canonical hypersurface equations from (suitably refined) standard $\mathbb{P}^{2,3,1}$-fibered polytopes are in the form of equation (2.14). On the other hand, we describe the direct construction of polytopes by carrying out Tate tunings on the effective curves in the toric bases in section 4, and develop an algorithm
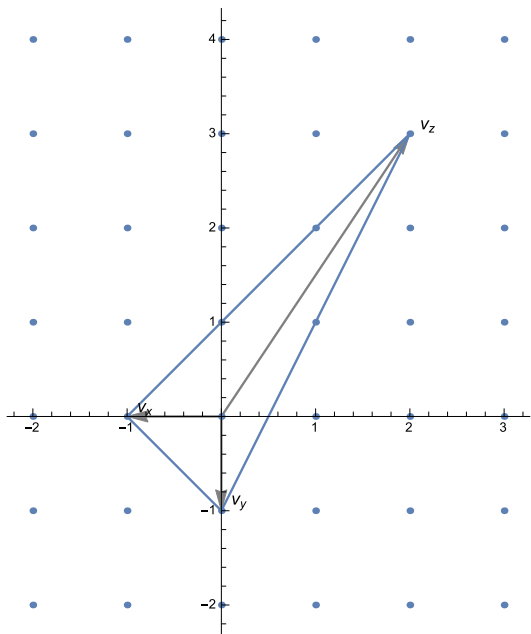
(a) The toric fan for $\mathbb{P}^{2,3,1}$. The convex hull of $\mathbb{P}^{2,3,1}$ plays the role of the reflexive sub-polytope ∇_2 for *standard $\mathbb{P}^{2,3,1}$-fibered polytopes* ∇ in the N lattice. The rays v_x, v_y, v_z are associated with the homogeneous coordinates x, y, z, respectively, in the hypersurface equation.
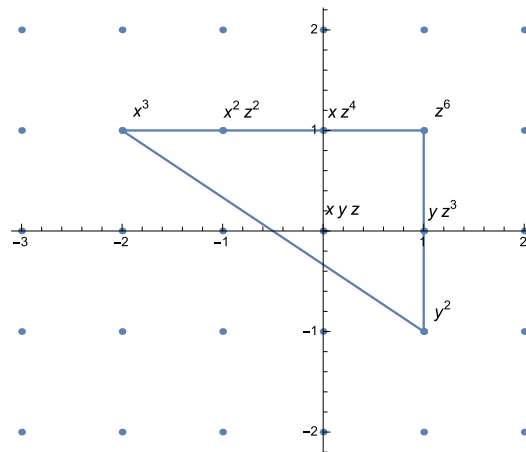
(b) The dual polytope Δ_2 to ∇_2 in the M_2 lattice. Projection onto the M_2 plane projects the lattice points in Δ into seven lattice points in Δ_2. These lattice points correspond to the five sections $a_{1,2,3,4,6}$ in the Tate form of the Weierstrass model, indicated in the figure by $xyz, x^2z^2, yz^3, xz^4, z^6$, respectively, and to the coefficients of the remaining two terms x^3, y^2 in the hypersurface equation.

Figure 1. The reflexive polytope pair for the $\mathbb{P}^{2,3,1}$ ambient toric fiber.

in section 5 to systematically classify models of this type that give polytopes and elliptic Calabi-Yau threefolds with large Hodge numbers; these models are all expected to have a corresponding standard $\mathbb{P}^{2,3,1}$-fibered polytope, and we compare the two constructions in the remainder of section 6. For a given base B_2 there are generally many distinct polytopes that have the standard $\mathbb{P}^{2,3,1}$-fibered structure; as we describe in the following section, these correspond to different Tate tunings over the same base.

3.4 Standard $\mathbb{P}^{2,3,1}$-fibered polytopes and corresponding Tate models

The fiber polytope ∇_2 that provides a natural correspondence with the Tate form models (2.14) is associated with the toric fan giving the weighted projective space $\mathbb{P}^{2,3,1}$; this is a toric variety given by the rays $v_x = (-1,0), v_y = (0,-1), v_z = (2,3)$ (see figure 1a). Given a $\mathbb{P}^{2,3,1}$-fibered polytope ∇ over a toric base B_2, where the fiber is defined by three rays satisfying $2v_x + 3v_y + v_z = 0$, we can always perform a $\mathrm{SL}(2,\mathbb{Z})$ transformation to put the rays in the fiber into the coordinates

$$v_x = (0,0,-1,0), v_y = (0,0,0,-1), v_z = (0,0,2,3). \tag{3.12}$$

We can define a *standard*[11] $\mathbb{P}^{2,3,1}$-fibered polytope over the base B_2 as one where there is a coordinate system after an $\mathrm{SL}(4,\mathbb{Z})$ transformation such that the vectors

$$v_i^{(a)} = (v_{i,1}^{(B)}, v_{i,2}^{(B)}, 2, 3) \tag{3.13}$$

are contained within ∇ for every ray $v_i^{(B)} = (v_{i,1}^{(B)}, v_{i,2}^{(B)})$ in Σ_B. Note that in fact, these lattice points are all on the boundary of ∇ since the only interior point of a reflexive polytope is the origin. This particular choice of fiber and twist geometry represents a very specific class of fibered polytopes that produce elliptically fibered Calabi-Yau threefolds as hypersurfaces. These standard $\mathbb{P}^{2,3,1}$-fibered polytopes play a central role in the analysis of this paper, and are a generalization of the well-studied 3D reflexive polytope for a K3 surface that is an elliptic fibration over a $\mathbb{P}^1$ base [56]. As mentioned above, these polytopes appear to be highly prevalent in the Kreuzer Skarke database at large Hodge numbers. This seems to occur for several reasons. The $\mathbb{P}^{2,3,1}$ fiber is the only one of the 16 reflexive 2D polytopes that is possible in the presence of curves of very negative self intersection in the base (see discussion in section 4.8). And the natural correspondence between tuned Tate models and the particular twist structure defined by (3.13) makes this twist structure particularly compatible with the reflexive polytope Calabi-Yau construction. We do, however, encounter some specific examples of other twists in later sections.

For a standard $\mathbb{P}^{2,3,1}$-fibered polytope, the lattice points of $\Delta \subset M$ in this coordinate system organize into the following sets of points:

$$\{(0,0,1,-1), (0,0,-2,1), (\_,\_,0,0), (\_,\_,-1,1), (\_,\_,1,0), (\_,\_,0,1), (\_,\_,1,1)\}. \tag{3.14}$$

The elliptically fibered CY hypersurface equation $p = 0$ with p from (3.7) then takes precisely the Tate form (2.14). The sets of points in (3.14) are associated with the monomials $y^2, x^3, xy, x^2, y, x, 1$ respectively; y^2 and x^3 have a single overall coefficient, and the monomials in the base associated with the other five sets of points correspond precisely to monomials in the five sections $\{a_1, a_2, a_3, a_4, a_6\}$ (see figure 1). In particular, the condition that Δ is the dual polytope of ∇ precisely imposes the condition that $a_n \in \mathcal{O}(-nK_B)$. For example, for a_6 we have the condition on the monomial associated with the point $(m_1, m_2, 1, 1)$ that $v_1^{(B)} m_1 + v_2^{(B)} m_2 + 2 + 3 \geq -1$ for each ray $v^{(B)} = \pi((v_1^{(B)}, v_2^{(B)}, 2, 3))$ in the fan of the base B_2, so (m_1, m_2) represents a section of $-6K_{B_2}$, in much the same way that the monomials in (3.8) represent sections of $-K$ of the ambient toric variety. A similar computation for each a_n confirms that the corresponding monomials satisfy $v_1^{(B)} m_1 + v_2^{(B)} m_2 \geq -n$, and the degree d in the variable $z^{(B)}$ associated with the ray $v^{(B)}$ of a monomial (m_1, m_2) is given by $v_1^{(B)} m_1 + v_2^{(B)} m_2 = -n + d$. An analogous computation shows that for the points associated with y^2 and x^3 the condition is $v_1^{(B)} m_1 + v_2^{(B)} m_2 \geq 0$; for any compact base this implies that $m_1 = m_2 = 0$, so the first two points in (3.14) are

---

[11]Because the rays of the base are "stacked" in (3.13) over the vertex $(2,3)$ of the fiber, we sometimes refer to constructions of this form as "stacking" fibrations. The "standard stacking" we have defined here, corresponding to the fiber $\mathbb{P}^{2,3,1}$ and the specific point $(2,3)$ in the fiber over which the base is stacked plays a special role in the analysis of this paper. We describe more general polytopes that have the form of a "stacking" with different fibers and/or different specified points in the fiber supporting the stacking, which generalize the specific "standard stacking" used here, in the companion paper [20].

the only points of the form $(m_1, m_2, 1, -1)$ and $(m_1, m_2, -2, 1)$ and are associated with constant functions on the base. This matches with the fact that these are sections of the trivial bundle $\mathcal{O}$ over the base, and the fact that the only global holomorphic functions on any compact base are constants. This proves that for any standard $\mathbb{P}^{2,3,1}$-fibered polytope, the lattice points in Δ are associated precisely with the Tate form of a Weierstrass model over the base, as stated above.

In the simplest cases, all the lattice points of the polytope ∇ are simply given by the vectors (3.12) and the vectors of the form (3.13). This corresponds to the generic elliptic fibration over a toric base B_2 without non-Higgsable clusters. In other cases, however, there are lattice points in ∇ other than those given by (3.12) and (3.13). This corresponds to situations with NHCs or gauge groups tuned over curves in B_2 by removing Tate monomials. The set of monomials in Δ completely span the set of sections of the appropriate line bundles $\mathcal{O}(-nK_B)$ for the generic elliptic fibration over a given base. In the case of NHCs, in particular, the monomials in Δ span the appropriate set of sections, while in the case of gauge group tunings, some of these monomials are set to zero. From the point of view of the Calabi-Yau geometry, the lattice points in ∇ other than those given by (3.12) and (3.13) reflect the singular nature of the resulting Calabi-Yau hypersurface. Up to some monodromy subtleties that we discuss further in section 4, the set of new lattice points introduced together with $v_i^{(a)}$ in $\pi^{-1}(v_i^{(B)})$ is known as a *top* [21, 58, 59], which forms the extended Dynkin diagram of the gauge algebra of the singular fiber over the associated divisor $D_i^{(B)}$, with $v_i^{(a)}$ the affine root (this is the only inverse image when the fiber is smooth). In section 4 we describe in more detail the dictionary between Tate tunings and toric/polytope geometry for specific gauge groups on particular local curve configurations in the base geometry.

3.5 A method for analyzing fibered polytopes: fiber types and 2D toric bases

Our primary approach in this paper is to systematically construct Tate tunings that should have counterparts as reflexive polytopes in the Kreuzer-Skarke database. Thus, we start from the F-theory construction and match the results with the known data in the KS database. This gives us something like a "sieve" that leaves behind a set of special cases of KS data not produced by our algorithm. After implementing this sieve, we have then considered separately those few examples in the KS database in the range of interest that were not found by our F-theory construction. We have found that there are a few polytopes in the KS database that can be described in terms of the standard $\mathbb{P}^{2,3,1}$-fibered type; i.e., have Tate forms, but were nonetheless not found with the initial sieve. This turns out to be because they involve such extensive tunings that the starting bases needed are outside the range we considered. There are also data in the KS database that we did not identify in the original sieve because they are accompanied by more sophisticated constructions involving $\mathfrak{u}(1)$ tunings, novel $\mathfrak{su}(6)$ tunings associated with exotic matter representations, or tunings of generic models over non-toric bases, which we had not considered. Moreover, we encounter a type of novel models that did not arise from our systematic construction because they are involved with tunings on non-toric curves in the base; they turn out

nonetheless to also be described by reflexive polytopes with toric fibers associated with elliptic fibrations.

We had to explicitly study these specific polytopes with Hodge numbers that we did not immediately identify from Weierstrass/Tate tunings to determine whether these polytopes give hypersurfaces that are actually elliptically fibered. We provide here a summary of our algorithm to analyze reflexive polytopes. We can learn from this analysis whether one of the 16 reflexive fiber types is a fiber of the polytope in question; we then define the 2D toric base from the fibered polytope. As we describe later in the paper, we can thereby determine the singularities of the elliptic fiber over the curves in the base, and then we check that the Hodge numbers of the inferred tuned model are consistent with those of the polytope model. Here we briefly summarize the first piece of this analysis: the algorithm to determine if a given reflexive 2D polytope is a fiber of a 4D polytope. There are also software programs like Sage [60] with built in routines to identify the reflexive subpolytopes of a given polytope.

1. We assume that we are interested in a fiber described by the 2D reflexive polytope ∇_2. To increase the efficiency of the algorithm in the case that the number of lattice points in ∇ is large (which is true in the case of large $h^{1,1}$ that we are focusing on), we begin by focusing on only a subset of these lattice points that can possibly play a role as the points in a fiber ∇_2. As mentioned in section 3.3, the presence of a fiber subpolytope $\nabla_2 \subset \nabla$ implies that there is a projection from $\Delta \to \Delta_2$. Let us call the maximum value of the inner product for any pair of vectors in the fiber and its dual

$$M_{\max} = \max v \cdot w, \quad v \in \nabla_2, w \in \Delta_2. \tag{3.15}$$

For example, for $\mathbb{P}^{2,3,1}$, $M_{\max} = 5$, and for $\mathbb{P}^{1,1,2}$, $M_{\max} = 3$. We can then check for each lattice point $v \in \nabla$ whether there exists a vertex w in Δ with $v \cdot w > M_{\max}$. If there is, then v cannot be a ray in a fiber ∇_2. We collect the subset of rays in ∇ that are not ruled out by this condition:

$$S = \{v \in \nabla : v \cdot w \leq M_{\max} \ \forall w \text{ vertex of } \Delta\}. \tag{3.16}$$

2. We then look for a subset of rays of S that satisfy the necessary linear relations to be elements of the fiber ∇_2. For example, for $\mathbb{P}^{2,3,1}$, we want to find rays $\{v_x, v_y, v_z\}$ that satisfy

$$2v_x + 3v_y + v_z = 0. \tag{3.17}$$

In this case we can look at all pairs of rays v, v' in S, and check to see if $2v + 3v'$ is also an element of S. If so, we can then check that the intersection of ∇ with the plane spanned by v, v' precisely contains the 7 points in the polytope ∇_2 shown in figure 1a. If this is the case than ∇ has a fiber ∇_2. The other fiber types can be checked in a similar fashion.

By equations (3.8), (3.15) and the projection $\Delta \to \Delta_2$, the maximum exponent of all monomials in the variables associated with the rays in the fiber should be $M_{\max} + 1$,

and the monomials can be grouped according to the powers of the fiber coordinates into sets that are in one-to-one correspondence with the lattice points in Δ_2. For example, for $\mathbb{P}^{2,3,1}$-fibered polytopes (see figure 1b), we have the maximum exponent in z among all fiber coordinates; $M_{\max} + 1 = 6$, and the lattice points in Δ_2 are in one-to-one correspondence with the sections

$$\{y^2, xyz, yz^3, x^3, x^2z^2, xz^4, z^6\}. \tag{3.18}$$

Note that, following the definition of a standard $\mathbb{P}^{2,3,1}$-fibered polytope from section 3.4, the lattice points in Δ_2 are in one-to-one correspondence with the sections of the line bundles $\mathcal{O}(-nK_B)$, and the monomials x^3 and y^2 are the only two independent of the base coordinates.

Similarly, the sections of the $\mathbb{P}^{1,1,2}$-fibered polytope (see figure 5) are

$$\{y^2, yz^2, xyz, x^2y, z^4, xz^3, x^2z^2, x^3z, x^4\} \tag{3.19}$$

when the associated rays are such that

$$v_x + 2v_y + v_z = 0, \tag{3.20}$$

and $M_{\max} + 1 = 4$. The first step in the algorithm above is only used to speed up the algorithm, but particularly when the number of lattice points in ∇ is large, this speedup is significant. For example, for the polytope associated with the Calabi-Yau with Hodge numbers H:491, 11, the number of lattice points in ∇ is 680, while the number in S is only 9. Since the second step of the algorithm is quadratic in the number of lattice points considered, this represents a speedup by a factor of hundreds or thousands of times in many cases. While in this paper we are only considering a few examples, such a speedup is useful when considering larger datasets. In the companion paper [20] we will describe the systematic application of this algorithm to all elements of the KS database with large Hodge numbers.

Once we have determined the fiber, we can then compute the base B_2 of the fibration. We define the set of rays of the fan describing B_2 to be

$$\left\{ v_i^{(B)} / \text{GCD}\left(v_{i,1}^{(B)}, v_{i,2}^{(B)} \right), \forall v_i \in \nabla \right\}, \tag{3.21}$$

where $v_i^{(B)} \equiv \pi(v_i) = (v_{i,1}^{(B)}, v_{i,2}^{(B)})$ and π is the projection along the fiber subpolytope $(\pi(\nabla_2) = 0)$. The division by $\text{GCD}(v_{i,1}^{(B)}, v_{i,2}^{(B)})$ is done to restrict to primitive rays in the image, as discussed in section 3.3. Given the rays $v_i^{(B)}$, we associate a 2D cone with each pair of adjacent rays, giving a unique toric structure to the base geometry B_2.[12] Note that the base defined this way gives a flat toric fibration, but not necessarily a flat elliptic fibration [31]. We discuss this point in more detail in later sections.

In the regions of the Hodge numbers that we study in this paper, we also encounter polytopes that have no standard $\mathbb{P}^{2,3,1}$ fiber. These polytopes can be described using two different types of models. One of these other types of model that we encounter is very

---

[12]Note that in higher dimensions, the cone structure of the fan is not uniquely determined by the rays.

similar to the standard $\mathbb{P}^{2,3,1}$-fibered polytopes, but has a fiber that is a single blowup of $\mathbb{P}^{2,3,1}$. This $\mathrm{Bl}_{[0,0,1]}\mathbb{P}^{2,3,1}$ fiber, which is one of the other 16 reflexive 2D fiber types, is shown in figure 7. The corresponding fiber subpolytope Δ_2 is identical to that for the $\mathbb{P}^{2,3,1}$ fiber except that it has an additional vertex at $(-1, -1)$, so that the number of lattice points in the plane of the fiber subpolytope is 8 rather than 7. From the Tate point of view, such a fiber occurs when all the monomials in the coefficient a_6 are taken to vanish. This vanishing of a_6 forces a global $\mathfrak{u}(1)$ symmetry that we mentioned earlier [23, 36]. We describe an explicit example of this type of model in appendix C. Models with this fiber can be treated in essentially the same fashion as standard $\mathbb{P}^{2,3,1}$-fibered polytopes.

The other unusual kind of fibration that we encounter in a few models is a fibered polytope with fiber Δ_2 given by the usual $\mathbb{P}^{2,3,1}$ polytope, but with a different "twist" to the $\mathbb{P}^{2,3,1}$ bundle over the base. In other words, while there is a projection of Δ to the dual polytope Δ_2 of the $\mathbb{P}^{2,3,1}$ fiber, the base rays in ∇ do not all lie in a plane that contains the vector v_z; i.e., the base of the polytope defined in (3.21) can not be constituted by a set of rays all in the form (3.13). The consequence of this is that the hypersurface equations (3.7) for these Calabi-Yau threefolds do not take on the Tate form (2.14). In particular, there is generically more than one lattice point projected to the points in Δ_2 associated with y^2 and/or x^3. To determine the Weierstrass form (2.8) for the models of this type that we found and analyze their structure, we found that it was useful to view them as essentially "$\mathbb{P}^{1,1,2}$-fibered polytopes" (or more precisely, $\mathbb{P}^{1,1,2}$ with two more blowups) rather than the standard $\mathbb{P}^{2,3,1}$-fibered polytopes (see figure 5 for comparison). This allows us to follow the method for analyzing $\mathbb{P}^{1,1,2}$-fibered models described in appendix A of [31] to bring them into Weierstrass form. This type of novel model gives rise to an enhancement over non-toric curves as we mentioned earlier. We refer to this type of models as *non-standard* $\mathbb{P}^{2,3,1}$-*fibered* polytopes, and describe their analysis in more detail in section 6.2. The treatment of non-standard $\mathbb{P}^{2,3,1}$ models in terms of models with a blow-up of $\mathbb{P}^{1,1,2}$ as a fiber is closely analogous to the analysis of models with a $\mathrm{Bl}_{[0,0,1]}\mathbb{P}^{2,3,1}$ fiber as special cases of $\mathbb{P}^{2,3,1}$ Weierstrass/Tate models.

4 Tate tunings and the Kreuzer-Skarke database

We want to understand how the set of Calabi-Yau threefolds produced by toric hypersurface constructions through reflexive polytopes in the Kreuzer-Skarke database can be related to the general construction of elliptic Calabi-Yau threefolds through tuned Weierstrass models. The approach we take is to identify a specific subclass of tuned models that match with toric hypersurface constructions. In particular, we begin with the set of toric bases identified in [9] and consider Tate tunings over these bases.

In principle, to find all the elliptically fibered threefolds in the Kreuzer-Skarke database we might want to consider a variety of tunings and singularity structures that correspond to all 16 of the toric fiber types mentioned in section 3.3. To simplify the set of possibilities, however, we focus on a region of Hodge numbers where we expect a single toric fiber type to dominate. A generic Tate-form elliptic fibration over a given toric base can always be constructed starting from the "standard stacking" procedure as we will describe in section 4.1

and section 4.3; this procedure uses the $\mathbb{P}^{2,3,1}$ fiber type. Tuning the resulting generic Tate model by removing monomials in the dual polytope then leads to a set of possible tunings corresponding to further reflexive polytopes that can appear in the database; we describe this process in section 4.3.3 and section 4.5, and give an example in appendix A. Such a construction can be carried out for any base. The gauge symmetries associated with the tunings can be read off from the tops [21, 56, 58, 59] of the polytopes. We review polytope tops in section 4.2, and we address some subtle issues about the multiple tops of a gauge algebra in section 4.4, which are related to the monodromy choices of the Tate tunings of the algebra that we have discussed in section 2.3.

The other 15 fiber types, however, implicitly constrain the Weierstrass model associated with an elliptic fibration. We explain in section 4.8 some constraints on the other 15 fiber types, which are related to the structure of the base. Based on these constraints, we expect that when we confine the range of Hodge numbers to relatively large values, as we do in section 5, the simplest $\mathbb{P}^{2,3,1}$ fiber type will dominate the set of polytopes.[13] By focusing on this simple class of constructions, therefore, we realize almost all the Hodge numbers in the range of interest with a single class of Tate-tuned elliptic fibration models. Although we will not deal with the matching of the multiplicity in KS database of a given Hodge pair with our systematic tuning construction, we will explore a bit more this aspect in sections 4.6 and 4.7.

4.1 Reflexive polytopes from elliptic fibrations without singular fibers

In section 3.4 we defined a standard $\mathbb{P}^{2,3,1}$-fibered polytope, and showed that there is always a corresponding Tate model. Now we are trying to do the converse — given a toric base and a corresponding Tate model, we wish to construct a corresponding reflexive polytope. As alluded to earlier, the recipe for the construction of a 4D standard $\mathbb{P}^{2,3,1}$-fibered polytope for an elliptically fibered threefold is the natural generalization of the 3D reflexive polytope for a K3 surface that is an elliptic fibration over a $\mathbb{P}^1$ base as described in e.g. [56].

To construct a 4D $\mathbb{P}^{2,3,1}$-fibered polytope, we start with the 2D $\mathbb{P}^{2,3,1}$ fiber and a 2D base, and we construct the polytope in a straightforward way to have the desired fibration structure over the base. We denote the toric fan associated with the base B by Σ_B, with the set of rays being $\{v_i^{(B)}\}$. Taking the fan of $\mathbb{P}^{2,3,1}$ to be the ambient space of the elliptic fiber, we can embed this in the 4D coordinates such that the three rays are $\{v_x, v_y, v_z\} = \{(0,0,-1,0),(0,0,0,-1),(0,0,2,3)\}$. Since in the Weierstrass or Tate model framework of equation (2.9) the fiber coordinate z is associated with the trivial bundle over the base, the lattice point associated with the ray $v_z = (0,0,2,3)$ should be in the plane of the base. Thus, we define a polytope $\tilde{\nabla}$ to be the convex hull of the set

$$\left\{\left(v_{i,1}^{(B)}, v_{i,2}^{(B)}, 2, 3\right) | v_i^{(B)} \text{ rays in } \Sigma_B\right\} \cup \{(0,0,-1,0),(0,0,0,-1)\}, \qquad (4.1)$$

where $v_{i,1}^{(B)}, v_{i,2}^{(B)}$ are the first and the second components of the 1D ray $v_i^{(B)}$ in the smooth 2D toric base B. From the definition in the previous section, this is a standard $\mathbb{P}^{2,3,1}$-fibered

---

[13]That this expectation is correctly borne out is also verified explicitly with a systematic analysis of the KS database in the companion paper [20].

Table 6. Non-convexity of NHCs: the rays corresponding to an NHC cannot be a vertices; hence, the vertex contribution from the base can only come from curves of self-intersection ≥ -1 (isolated -2 curves will be on a 1D face, and also cannot be vertices).

polytope; we refer sometimes to this construction as the "standard stacking" approach to construction of a polytope. Note that the 4D rays $v_i = (v_{i,1}^{(B)}, v_{i,2}^{(B)}, 2, 3)$ can be vertices of $\tilde{\nabla}$ only if $v_i^{(B)}$ are associated with curves of self-intersection $D_i \cdot D_i > -2$ (see table 6). We now wish to check that $\tilde{\nabla}$ is reflexive, so it can be used as the reflexive polytope ∇ in Batyrev's construction of a Calabi-Yau threefold. In some cases $\tilde{\nabla}$ is immediately reflexive, and in other more complicated cases it must be modified to make it reflexive.

We start with the simplest case, in which we have a generic elliptically fibered Calabi-Yau over a toric base B that contains no non-Higgsable clusters (i.e., no curves with self-intersection less than -2). In this case, the Weierstrass/Tate model of the Calabi-Yau is smooth and there is no gauge group in the 6D supergravity theory. In this context, lattice points associated to curves of self-intersection -2 lie on the 1D faces of $\tilde{\nabla}$ that are boundaries of the 2D face θ_B, which is the 2D face associated with the base; and there are no interior points in θ_B other than $(0,0,2,3)$. We can now check directly that in these simple cases $\tilde{\nabla}$ is reflexive without further modification. The vertices of the polytope dual to the convex hull of the set of vertices (4.1), in any case, are

$$\left\{ \left(\frac{6(v_{i,2}^{(B)} - v_{j,2}^{(B)})}{\mathrm{Det}[v_i^{(B)}, v_j^{(B)}]}, -\frac{6(v_{i,1}^{(B)} - v_{j,1}^{(B)})}{\mathrm{Det}[v_i^{(B)}, v_j^{(B)}]}, 1, 1 \right) \right\} \cup \{(0,0,-2,1), (0,0,1,-1)\}, \qquad (4.2)$$

where (i, j) are taken to run over all pairs of labels of base rays that correspond to adjacent vertices of θ_B. The vertices in (4.2) will lie on the M lattice only when the denominators $\mathrm{Det}[v_i^{(B)}, v_j^{(B)}]$ are cleared so that all entries are integers. For a smooth 2D base fan, $\mathrm{Det}[v_i^{(B)}, v_{i+1}^{(B)}] = 1$, so we have a lattice point whenever $j = i + 1$ (including the boundary case $j = 1, i = n$); i.e., we get lattice points as long as there are no non-convex base rays, which would be skipped. We also get a lattice point as long as $v_i^{(B)}$ and $v_j^{(B)}$ are separated only by some number k of -2 curves. In this case $v_i^{(B)} - v_j^{(B)} = kw$, where w is a primitive vector, and $\mathrm{Det}[v_i^{(B)}, v_j^{(B)}] = k$, so we again have a cancellation and the vertex

of the dual polyhedra is an integral lattice point. Thus, as long as the base B contains no non-Higgsable clusters, the set of vertices (4.1) immediately provides a reflexive polytope.[14]

Simple examples of polytopes realized in this way are the elliptically fibered Calabi-Yau threefolds over the toric bases $\mathbb{P}^2, \mathbb{F}_{n=0,1,2}$, whose vertex sets of the M polytopes Δ are (4.2), with the first set of vertices respectively being $\{(-6, -6, 1, 1), (12, -6, 1, 1), (-6, 12, 1, 1)\}$, $\{(-6, -6, 1, 1), (6(1+n), -6, 1, 1), (6(-n+1), 6, 1, 1), (-6, 6, 1, 1)\}$, given the respective base rays $\{(1, 0), (0, 1), (-1, -1)\}$, $\{(1, 0), (0, 1), (-1, -n), (0, -1)\}$. The $\mathbb{P}^2$ model gives the only polytope (up to lattice automorphism) with Hodge numbers H:2,272 in the KS database and the $\mathbb{F}_{n=0,1,2}$ models give exactly the three data points with Hodge numbers H:3,243.

The bases described by toric varieties with no curves of self-intersection less than -2 are *weak Fano* varieties, and correspond to reflexive 2D polytopes, as we have just verified explicitly. We now want to describe the generalization of this construction to situations where there is a gauge group arising either from a non-Higgsable cluster in the base or a Tate tuning. The realization of reflexive 4D polytopes in these cases arises from a general relationship between Tate tunings and "tops" in the toric language.

4.2 Tate tuning and polytope tops

We saw in section 3.4 that for a standard $\mathbb{P}^{2,3,1}$-fibered polytope, the lattice points of Δ that project to each of the different lattice points of Δ_2 (figure 1) correspond precisely to the sets of monomials in the coefficients of the Tate form (2.14). The lattice points of Δ are thus divided into 5 groups corresponding to the 5 sections $a_n \in \mathcal{O}(-nK_B)$ and another 2 points corresponding to the constant coefficients of y^2 and x^3. In the previous subsection we described generic elliptic fibrations over weak Fano bases, where the "standard stacking" procedure immediately gives a reflexive 4D polytope, and no additional rays are needed in ∇, corresponding to a physics model with no nonabelian gauge group. We now wish to consider how this story changes when there is a nontrivial nonabelian gauge group due either to an NHC in the base or a Tate tuning of the monomials in the Tate form.

The presence of an NHC in the base or an explicit Tate tuning can force some of the coefficients in the a_ns to vanish to some specified order along a particular base divisor $D_i^{(B)}$. This absence of monomials in Δ gives rise to a corresponding enlargement of ∇ from the standard stacking. The additional lattice points in the fan polytope ∇ correspond to the exceptional divisors that resolve the singularities of the associated fibered geometry. These additional lattice points form the "top" [21, 56, 58, 59] of the enhanced gauge symmetries over $D_i^{(B)}$. In coordinate representation, a lattice point in the top of $D_i^{(B)}$ is of the form

$$\left((lv_i^{(B)})_{1,2}, (pt_{1, 2, 3, 4, 5, 6, \text{ or } 7})_{3,4} \right), \tag{4.3}$$

where

$$pt_{1,2,3,4,5,6,7} = (2,3), (1,2), (1,1), (0,1), (0,0), (-1,0), (0,-1) \tag{4.4}$$

---

[14]As we will discuss in section 4.3.1, the set (4.1) still gives a reflexive polytope in certain cases when the base contain NHCs, but those lattice points corresponding to the curves in the base that carry the NHCs are not vertices.

n	Tate form	Top/Affine Dynkin nodes
7	$\{0, 1, 3, 4, 7\}$	$\{pt'_1, pt'_2, pt'_3, pt'_4, pt'_5, pt'_6, pt'_8\}$
8	$\{0, 1, 4, 4, 8\}$	$\{pt'_1, pt'_2, pt'_3, pt'_4, pt'_5, pt'_6, pt'_8, pt'_9\}$
9	$\{0, 1, 4, 5, 9\}$	$\{pt'_1, pt'_2, pt'_3, pt'_4, pt'_5, pt'_6, pt'_8, pt'_9, pt'_{11}\}$
10	$\{0, 1, 5, 5, 10\}$	$\{pt'_1, pt'_2, pt'_3, pt'_4, pt'_5, pt'_6, pt'_8, pt'_9, pt'_{10}, pt'_{11}\}$
11	$\{0, 1, 5, 6, 11\}$	$\{pt'_1, pt'_2, pt'_3, pt'_4, pt'_5, pt'_6, pt'_8, pt'_9, pt'_{10}, pt'_{11}, pt'_{14}\}$
12	$\{0, 1, 6, 6, 12\}$	$\{pt'_1, pt'_2, pt'_3, pt'_4, pt'_5, pt'_6, pt'_8, pt'_9, pt'_{10}, pt'_{11}, pt'_{12}, pt'_{14}\}$
13	$\{0, 1, 6, 7, 13\}$	$\{pt'_1, pt'_2, pt'_3, pt'_4, pt'_5, pt'_6, pt'_8, pt'_9, pt'_{10}, pt'_{11}, pt'_{12}, pt'_{14}, pt'_{17}\}$

Table 7. The tops of $\mathfrak{su}(n)$ algebras. The coordinates of the points $pt_{1,2,3,4,5,6,7,8,9,10,11,12,13,14,15,16,17}$ are given in equations (4.4) and (4.5). All lattice points in these tops are of level one, and correspond to affine Dynkin nodes. The rank of each algebra is the number of the nodes minus one.

are the 7 lattice points in the 2D reflexive fiber subpolytope $\mathbb{P}^{2,3,1}$, $v_i^{(B)}$ is the associated 2D ray, and $l \in \mathbb{N}$ specifies the "level" of the point away from the fiber plane (see figure 2). We adopt the shorthand notation $pt_j^{(l)}$ or $pt_j^{'\cdots'}$, where the number of primes specifies the level parameter l. When we denote a top, the points with fewer than the maximal number of primes over each point are omitted and implied by the point of most primes with the same index; e.g. $\{pt'''_1, pt''_2, pt'_3, pt'_4\} = \{pt'_1, pt''_1, pt'''_1, pt'_2, pt''_2, pt'_3, pt'_4\}$. The tops of the various gauge algebras have been worked out in the previous literature. Tops for gauge algebras of rank no greater than eight that arise in reflexive polytopes can be looked up for example in table 3.2 in [21]. We have explicitly calculated a few more cases, including the tops of $\mathfrak{so}(n)$ and $\mathfrak{su}(n)$ gauge algebras to rank 12 in both cases and list the results in tables table 7 and table 8, respectively. In [22], Vincent Bouchard and Harald Skarke generalized the notion of tops (including those which may not have a completion to reflexive polytopes) to include all fiber types, and they classified all such "tops in the dual space" (i.e., the M lattice space), including higher rank $\mathfrak{so}(n)$ and $\mathfrak{su}(n)$ tops. The tops in table 7 and table 8 were explicitly obtained from reflexive polytope constructed from successive Tate tunings, and we have cross-checked the $\mathfrak{so}(n)$ cases with the results of [22] in the dual space, which agree up to a $\mathrm{GL}(2, \mathbb{Z})$ transformation. Note that for higher rank $\mathfrak{so}(n)$ and $\mathfrak{su}(n)$ algebras, the ∇ polytope grows in the fiber subpolytope direction (as opposed to the level direction), and more pts projecting to the fiber plane are involved. We list the ones we need in table 7 and table 8:

$$pt_{8,9,10,11,12,13,14,15,16,17} = (-1,-1), (-2,-1), (-3,-2), (-2,-2), (-4,-3), (-5,-4), (-3,-3),$$
$$(-6,-5), (-7,-6), (-4,-4). \tag{4.5}$$

There is a simple and precise correspondence between tunings of the Tate form and tops. This correspondence holds independent of whether the Tate form corresponds to an NHC or an explicit tuning. Consider for example a situation where the standard $\mathbb{P}^{2,3,1}$-fibered polytope ∇ contains the lattice point $pt'_2 = (v^{(B)}_{1,2}, 1, 2)$. Recall that the lattice point $pt'_1 = (v^{(B)}_{1,2}, 2, 3)$ imposes the conditions on the dual lattice points $(m_{1,2}, 1, 1)$ associated

n	Tate form	Top	Affine Dynkin nodes
13	$\{1,1,3,4,6\}$	$\{pt''_1,pt''_2,pt'_3,pt''_4,pt'_5,pt''_6\}$	$\{pt'_1,pt''_1,pt''_2,pt'_3,pt''_4,pt'_6,pt''_6\}$
14	$\{1,1,3,4,7\}$	$\{pt''_1,pt''_2,pt'_3,pt''_4,pt'_5,pt''_6,pt'_8\}$	$\{pt'_1,pt''_1,pt''_2,pt'_3,pt''_4,pt'_6,pt''_6,pt'_8\}$
15	$\{1,1,4,4,7\}$	$\{pt''_1,pt''_2,pt'_3,pt''_4,pt'_5,pt''_6,pt'_8,pt''_9\}$	$\{pt'_1,pt''_1,pt''_2,pt'_3,pt''_4,pt'_6,pt'_8,pt''_9\}$
16	$\{1,1,4,4,8\}$	$\{pt''_1,pt''_2,pt'_3,pt''_4,pt'_5,pt''_6,pt'_8,pt''_9\}$	$\{pt'_1,pt''_1,pt''_2,pt'_3,pt''_4,pt''_6,pt'_8,pt'_9,pt''_9\}$
17	$\{1,1,4,5,8\}$	$\{pt''_1,pt''_2,pt'_3,pt''_4,pt'_5,pt''_6,pt'_8,pt''_9,pt''_{10}\}$	$\{pt'_1,pt''_1,pt''_2,pt'_3,pt''_4,pt''_6,pt'_9,pt''_9,pt''_{10}\}$
18	$\{1,1,4,5,9\}$	$\{pt''_1,pt''_2,pt'_3,pt''_4,pt'_5,pt''_6,pt'_8,pt''_9,pt''_{10},$ $pt'_{11}\}$	$\{pt'_1,pt''_1,pt''_2,pt'_3,pt''_4,pt''_6,pt'_9,pt''_9,$ $pt''_{10},pt'_{11}\}$
19	$\{1,1,5,5,9\}$	$\{pt''_1,pt''_2,pt'_3,pt''_4,pt'_5,pt''_6,pt'_8,pt''_9,pt''_{10},$ $pt'_{11},pt''_{12}\}$	$\{pt'_1,pt''_1,pt''_2,pt'_3,pt''_4,pt''_6,pt'_9,pt''_{10},$ $pt'_{11},pt''_{12}\}$
20	$\{1,1,5,5,10\}$	$\{pt''_1,pt''_2,pt'_3,pt''_4,pt'_5,pt''_6,pt'_8,pt''_9,pt''_{10},$ $pt'_{11},pt''_{12}\}$	$\{pt'_1,pt''_1,pt''_2,pt'_3,pt''_4,pt''_6,pt'_9,pt''_{10},$ $pt''_{10},pt'_{11},pt''_{12}\}$
21	$\{1,1,5,6,10\}$	$\{pt''_1,pt''_2,pt'_3,pt''_4,pt'_5,pt''_6,pt'_8,pt''_9,pt''_{10},$ $pt'_{11},pt''_{12},pt''_{13}\}$	$\{pt'_1,pt''_1,pt''_2,pt'_3,pt''_4,pt''_6,pt'_9,pt''_{10},$ $pt''_{10},pt''_{12},pt''_{13}\}$
22	$\{1,1,5,6,11\}$	$\{pt''_1,pt''_2,pt'_3,pt''_4,pt'_5,pt''_6,pt'_8,pt''_9,pt''_{10},$ $pt'_{11},pt''_{12},pt''_{13},pt'_{14}\}$	$\{pt'_1,pt''_1,pt''_2,pt'_3,pt''_4,pt''_6,pt'_9,pt''_{10},$ $pt''_{10},pt''_{12},pt''_{13},pt'_{14}\}$
23	$\{1,1,6,6,11\}$	$\{pt''_1,pt''_2,pt'_3,pt''_4,pt'_5,pt''_6,pt'_8,pt''_9,pt''_{10},$ $pt'_{11},pt''_{12},pt''_{13},pt'_{14},pt''_{15}\}$	$\{pt'_1,pt''_1,pt''_2,pt'_3,pt''_4,pt''_6,pt'_9,pt''_{10},$ $pt''_{12},pt''_{13},pt'_{14},pt''_{15}\}$
24	$\{1,1,6,6,12\}$	$\{pt''_1,pt''_2,pt'_3,pt''_4,pt'_5,pt''_6,pt'_8,pt''_9,pt''_{10},$ $pt'_{11},pt''_{12},pt''_{13},pt'_{14},pt''_{15}\}$	$\{pt'_1,pt''_1,pt''_2,pt'_3,pt''_4,pt''_6,pt'_9,pt''_{10},$ $pt'_{12},pt''_{12},pt''_{13},pt'_{14},pt''_{15}\}$
25	$\{1,1,6,7,12\}$	$\{pt''_1,pt''_2,pt'_3,pt''_4,pt'_5,pt''_6,pt'_8,pt''_9,pt''_{10},$ $pt'_{11},pt''_{12},pt''_{13},pt'_{14},pt''_{15},pt''_{16}\}$	$\{pt'_1,pt''_1,pt''_2,pt'_3,pt''_4,pt''_6,pt'_9,pt''_{10},$ $pt'_{12},pt''_{12},pt''_{13},pt''_{15},pt''_{16}\}$

Table 8. The tops of $\mathfrak{so}(n)$ algebras. The coordinates of the points $pt_{1,2,3,4,5,6,7,8,9,10,11,12,13,14,15,16}$ are given in equations (4.4) and (4.5). (Only the highest level point for each pt is listed in each top, and the lattice points of the lower levels are implied.) $\mathfrak{so}(4n-1)$ and $\mathfrak{so}(4n)$ in the table have the same top but different (numbers of) affine Dynkin nodes as the ranks (which differ from the number of the nodes by one) are different. These tops match those found in [22] after an appropriate coordinate transformation.

with monomials in a_6 that $v^{(B)} \cdot m + 5 \geq -1 \Rightarrow v^{(B)} \cdot m \geq -6$ as expected for a section of $\mathcal{O}(-6K)$. The point pt'_2 imposes the stronger condition $v^{(B)} \cdot m + 3 \geq -1 \Rightarrow v^{(B)} \cdot m \geq -6 + 2$, corresponding to the condition that a_6 vanish to order 2 over the corresponding $D^{(B)}$. A similar calculation shows that $(a_1, a_2, a_3, a_4, a_6)$ vanish to orders at least $(0, 0, 1, 1, 2)$ respectively when the point pt'_2 is present in ∇. Indeed, this goes both ways: only when the a_ns vanish at least to orders $(0, 0, 1, 1, 2)$, associated with the absence of a certain set of lattice points in Δ, can the point pt'_2 appear in ∇, and indeed if all the a_ns vanish to these orders then the point pt'_2 must appear in the polytope ∇ dual to Δ. Thus, there is a precise local correspondence between Tate tunings of the a_n coefficients over a certain ray in the base, associated with lattice points absent from Δ, and the toric top in ∇ over that ray. We tabulate a few examples of this correspondence in table 9. Note that just as multiple Tate

point	$\mathrm{ord}(a_1, a_2, a_3, a_4, a_6)$	group	type
pt'_2	$(0, 0, 1, 1, 2)$	SU(2)	I_2
pt'_3	$(0, 1, 1, 2, 3)$	SU(3)	I_3^s
pt''_1	$(1, 1, 2, 2, 3)$	G_2	I_0^{*ns}
pt'_4	$(0, 0, 2, 2, 4)$	Sp(2)	I_4^{ns}

Table 9. Some examples of the correspondence between additional lattice points in ∇ associated with a ray $v^{(B)}$ in the base and the associated tuning of the Tate coefficients $(a_1, a_2, a_3, a_4, a_6)$ over the associated divisor.
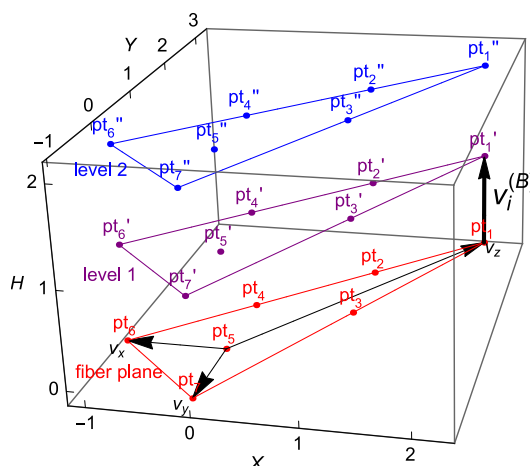

Figure 2. A 3D visualization of the lattice points that appear in a top over $v_i^{(B)}$: in standard $\mathbb{P}^{2,3,1}$ models, a top over a ray in the base $v_i^{(B)}$ (in the direction H) is a set of lattice points stacked over the 7 lattice points of the fiber subpolytope $\mathbb{P}^{2,3,1}$ (in the X-Y plane). The level (the multiple of $v_i^{(B)}$) where points are located is indicated by the number of primes. When the gauge algebra is trivial over the associated divisor $D_i^{(B)}$, pt'_1 (equation (3.13)) is the only point in the top; while otherwise there are additional points (cf. table 11) forming the extended Dynkin diagram of the gauge algebra with pt'_1 the affine node.

tunings can correspond to the same gauge algebra, the corresponding multiple tops also correspond to the same gauge algebra. The multiplicity of constructions for a given gauge algebra was studied from the point of view of tops in [23]. One particular situation in which multiple tops are possible for a fixed gauge algebra corresponds to monodromy-dependent Tate tuning configurations, which we discuss further in section 4.4.

This correspondence leads to a natural association of reflexive polytopes with elliptic fibrations over toric bases that have Tate forms. Over a given base, various gauge groups can arise from a combination of non-Higgsable clusters and Tate tunings. The interplay between extra vertices in ∇ over nearby divisors and the absence of monomials in Δ leads to local interactions between the sets of lattice points in the polytope that are affected by adjacent rays in the base. We consider more explicitly in the following section how this leads to consistent reflexive polytopes in both the NHC and Tate tuning cases.

4.3 Reflexive polytopes for NHCs and Tate tunings

In this subsection we describe the construction of reflexive polytopes from elliptic fibrations corresponding to F-theory models with gauge groups from non-Higgsable clusters or tuning. We give the construction of generic models over bases with NHCs in section 4.3.1 and section 4.3.2, and constructions with tunings in section 4.3.3.

4.3.1 NHCs with immediately reflexive polytopes

Now consider models where the base has a non-Higgsable cluster. We begin with the simplest cases, where the NHC contains a single curve of negative self-intersection $-m$, and $m|12$. In these cases, the standard stacking construction described in section 4.1 leads directly to a reflexive polytope. This can be understood from several points of view. Due to the factor 6 in the numerators of the first two coordinates in (4.2), those cases where a ray is skipped and $\mathrm{Det}[v_i^{(B)}, v_j^{(B)}] = 3$, or 6 also give lattice points; i.e., when the skipped rays are NHCs -3 and -6; furthermore, the NHCs -4 and -12 are fine as well because of extra factors of 2 that arise from the difference terms in the numerators. Therefore the set (4.2) should also be sufficient to give the Δ polytopes of the models with the NHCs $-3, -4, -6, -12$, so that the standard stacking polytope ∇ defined through (4.1) is reflexive. The values of m compatible with the standard stacking can also be understood from the bounds on the set of monomials in a_6 controlled by the $-m$ curve. Other than the vertices from x^3, y^2, all vertices of Δ come from lattice points associated with monomials in a_6. Choosing local toric coordinates for a set of adjacent rays $v_1^{(B)}, v_2^{(B)}, v_3^{(B)}$ in the base B so that the ray v_2 corresponds to the $-m$ curve,

$$v_1^{(B)} = (1,0), v_2^{(B)} = (0,-1), v_3^{(B)} = (-1,-m), \tag{4.6}$$

the monomials (m_1, m_2) in $a_6 \in \mathcal{O}(-6K_B)$ are then bounded by $m_1 \geq -6, m_2 \leq 6$, and $6 - mm_2 \geq m_1$. The first and the third constraints intersect at an integral point precisely when $m|12$. This intersection point is a vertex of Δ, so Δ can only be a lattice polytope when $m|12$. Note that $6 - 12/m$ is the order of vanishing of a_6 over the divisor associated with $v_2^{(B)}$ since there are no points in the dual lattice with $m_2 > 12/m$.

As an example, the reflexive polytope model for the generic elliptically fibered CY over the base $\mathbb{F}_{12}$ has $\{v_i^{(B)}\} = \{(1,0), (0,-1), (-1,-12), (0,1)\}$ (the self-intersection numbers of the toric divisors are $\{0, -12, 0, 12\}$); the vertices of the 2D convex polygon are $i = 1, 3, 4$, and the dual vertices arise from the pairs $\{(i,j)\} = \{(1,3), (3,4), (4,1)\}$, so with these pairs, (4.2) gives the vertices of the dual polytope Δ, which is a lattice polytope. Indeed, this polytope has vertices

$$\{(-6,1,1,1), (78,-6,1,1), (-6,-6,1,1), (0,0,-2,1), (0,0,1,-1)\}, \tag{4.7}$$

and is the only reflexive polytope in the M lattice (up to lattice automorphism) associated with the Hodge pair H:11,491 in the KS database.

We can understand the reflexive polytopes formed in this way in terms of the dual Tate tunings and tops described in the previous subsection. For example, consider the case of the -3 curve NHC. Using again the local toric coordinates (4.6) with $m = 3$, the polytope ∇

has vertices from (4.1), $(1, 0, 2, 3)$ and $(-1, -3, 2, 3)$. Considering a 3D slice of ∇ that contains the fiber polytope ∇_2 and the ray $v_2^{(B)} = (0, -1)$, we have a picture like figure 2, where $v_i^{(B)}$ is identified with $v_2^{(B)}$. The boundary of the polytope ∇ intersects the vertical line $\{X = 2, Y = 3\}$, which is perpendicular to the $\{H = 0\}$ plane, at $(X, Y, H) = (2, 3, 3/2)$; this corresponds in the polytope to the midpoint $(0, -3/2, 2, 3)$ of the line between the two vertices $(1, 0, 2, 3)$ and $(-1, -3, 2, 3)$. The boundary of the polytope in the 3D slice is therefore the 2-plane passing through the points $(2, 3, 3/2), (0, -1, 0), (-1, 0, 0)$. This plane passes through the point pt_2' $((X, Y, H) = (1, 2, 1)$ in the figure), so the reflexive polytope associated with a standard stacking from a base with a -3 curve automatically has the point $pt_2' = (0, -1, 1, 2)$ in the top in ∇. Using the same methodology as in the $n = 6$ example above, we see that the orders of vanishing of the a_ns in the dual polytope are $(1, 1, 1, 2, 2)$. From table 4, we see that this is a type IV singularity; in this case the monodromy condition for the gauge algebra $\mathfrak{su}(3)$ is automatically satisfied, so this actually corresponds to an $\mathfrak{su}(3)$ top, as indicated in the first line of table 11.

4.3.2 Other NHCs: reflexive polytopes from the dual of the dual

The rest of the NHCs have the issue that there are fractions in the vertices of the dual polytope described by (4.2). Let us denote the convex hull of the set of vertices defined by (4.1) by $\tilde{\nabla}$, and its dual by $\tilde{\Delta}$. If $\tilde{\Delta}$ is not a lattice polytope then $\tilde{\nabla}$ is not a reflexive polytope. We have to supply $\tilde{\nabla}$ with additional lattice points to make it into a reflexive polytope ∇ so that $\Delta = \nabla^*$ is a lattice polytope.

We can turn $\tilde{\nabla}$ into a reflexive polytope in a minimal fashion by taking the "dual of the dual". We begin by defining the lattice polytope $\Delta^\circ = \text{convex hull}(\tilde{\nabla}^* \cap M)$ to be the polytope defined by the convex hull of the set of integral points of $\tilde{\Delta}$; the polytope Δ° then has itself a dual $\nabla = (\Delta^\circ)^*$. This gives us the minimal reflexive polytope $\nabla \supset \tilde{\nabla}$ in the N lattice that we are looking for; for any base with NHCs, as we have confirmed by explicit computation in each case, the resulting ∇ indeed has a dual $\Delta = \nabla^*$ that is a lattice polytope.

This "dual of the dual" procedure adds points in the N lattice that are needed to complete the tops associated with the gauge symmetries coming from the NHCs in all cases other than those of a single curve with self-intersection $n|12$. For example, take the generic model over $\mathbb{F}_5$ described by the set of rays $\{(1, 0), (0, 1), (-1, -5), (0, -1)\}$; if we took just (4.1) as the set of vertices, we would have $\{(i, j)\} = \{(1, 2), (2, 3), (3, 1)\}$ in (4.2) and there would be a non-lattice point vertex $(-6, 12/5, 1, 1)$ from $(i, j) = (3, 1)$. This problem can be seen as arising from the absence of a sufficient set of lattice points in $\tilde{\nabla}$ over the NHC -5-curve $v_4^{(B)}$ to form a complete $\mathfrak{f}_4$ top. While the top in $\tilde{\nabla}$ (the convex hull of the standard stacking polytope) over $v_4^{(B)}$ is $\{pt_1', pt_1'', pt_2', pt_3'\}$, it is $\{pt_1', pt_1'', pt_1''', pt_2', pt_2'', pt_3', pt_4'\}$ in ∇; the latter is exactly the $\mathfrak{f}_4$ top as described in earlier literature, which is obtained explicitly via the Δ° construction we just described above.

For each of the NHC's, table 11 describes the tops that arise over the divisors supporting the NHC, the corresponding Tate forms, and the vanishing orders of f, g, Δ along with the resulting gauge algebra. The minimal top associated with the Δ° construction of ∇ as the dual of the dual is in each case the first top listed. In a number of cases there are other

higher Tate tunings that give different tops but the same gauge algebra, as discussed further in section 4.4. The global models describing generic elliptic fibrations over the Hirzebruch surfaces that incorporate each of the single-curve NHC's are also described explicitly in table 10, showing how this construction works in the context of the global polytopes. While in this paper we focus on the systematic construction of polytopes through tuning of Tate forms (corresponding to the structure of Δ), one could also construct general polytopes by considering the different tops over each base and thus classifying polytopes ∇; in table 11 we also list the possible new vertices that may arise in the polytope ∇ for each top.

4.3.3 Reflexive polytopes from Tate tunings

We can understand Tate tunings in the polytope in a similar fashion. Consider starting with the reflexive polytope ∇ associated with the generic elliptic fibration over a given toric base B, constructed as above using the standard stacking procedure and the dual of the dual if needed for NHC's. We take Δ to be the dual polytope of ∇, which is also a lattice polytope. We can produce an additional gauge group beyond the minimum imposed from the NHC's by performing a tuning in the Tate description of the model, which corresponds to removing certain vertices from the polytope Δ. Using a Tate tuning from table 4 gives us the set of lattice points that should be removed from Δ associated with certain coefficients in the a_ns over the divisor(s) in B. Calling the new M polytope that results from removing these lattice points $\hat{\Delta}$, we get an enlarged N polytope $\hat{\nabla} = (\hat{\Delta})^*$, which has extra lattice points. In general, each Tate tuning in Δ gives a corresponding top in ∇, giving a new reflexive polytope $\hat{\nabla}$. This gives a large class of constructions for Tate tunings that should have reflexive polytope analogues in the KS database.

As a simple example, consider the polytope ∇ associated with the generic elliptic fibration over $\mathbb{F}_2$. As discussed in section 4.1 this polytope follows from the standard stacking procedure and has vertices given by

$$\nabla = \text{Conv}\{(1,0,2,3),(-1,-m,2,3),(0,1,2,3),(0,0,-1,0),(0,0,0,-1)\} \qquad (4.8)$$

with $m = 2$. This is a reflexive polytope, identified in the Kreuzer-Skarke database as M:335 5 N:11 5 H:3,243. The dual polytope Δ has vertices

$$\{(-6,-6,1,1),(0,0,-2,1),(18,-6,1,1),(0,0,1,-1),(-6,6,1,1)\}. \qquad (4.9)$$

Now consider a Tate tuning of the algebra $\mathfrak{su}(2)$ over the -2 curve C in the base, which corresponds to the 2D toric vector $(0,-1)$. This is achieved by setting a_1, a_2, a_3, a_4, a_6 to vanish to orders $\{0,0,1,1,2\}$ in the coordinate associated with C, which is the second coordinate in Δ. The set of the lattice points that have to be removed from Δ to achieve the required vanishing orders is $\{(-6,5,1,1),(-6,6,1,1),(-5,5,1,1),(-4,4,0,1),(-4,5,1,1),(-3,3,1,0)\}$. The resulting new M polytope after the reduction is

$$\hat{\Delta} = \text{Conv}\{(-6,-6,1,1),(-6,4,1,1),(-2,2,-1,1),(-2,4,1,1),(0,0,-2,1),(0,0,1,-1),$$
$$(18,-6,1,1)\}. \qquad (4.10)$$

This gives the reflexive polytope $\hat{\nabla}$ given by augmenting ∇ from (4.8) with the additional lattice point $(0, -1, 1, 2)$, which gives the $\mathfrak{su}(2)$ top over C, as described in table 9. The resulting polytope corresponds to the example M:329 7 N:12 6 H:4,238 in the KS database. The Hodge numbers from the polytope data are consistent with those from the anomaly cancellation calculation in equations (2.6) and (2.7) with a tuning of $\mathfrak{su}(2)$ on the isolated -2 curve: $\Delta h^{1,1} = \mathrm{rank}(\mathfrak{su}(2)) = 1, \Delta h^{2,1} = \dim(\mathfrak{su}(2)) - 4 \times \mathbf{2} = 3 - 8 = -5$.

In general, we find that the correspondence described in the last few subsections between Tate tunings and tops immediately provides reflexive polytopes for most Tate tuning constructions. There are several subtleties in this construction, which we elaborate in the remainder of this section.

4.4 Multiple tops

One thing that we have found in considering the variety of Tate tunings and the corresponding models in the KS database is that for many gauge algebras there are multiple distinct tops that can arise in the N-polytope ∇. This multiplicity of tops was also discussed in [23]. These different tops correspond to distinct Tate tunings of the same gauge algebra. In many cases these arise in situations where the gauge algebra in the Weierstrass model depends upon some monodromy condition, which may be satisfied automatically in certain cases by the Tate tuning.

As an example of this phenomenon, consider the generic model over the $\mathbb{F}_{m=3}$ base,

$$\nabla = \mathrm{Conv}\{(1, 0, 2, 3), (-1, -3, 2, 3), (0, 1, 2, 3), (0, 0, -1, 0), (0, 0, 0, -1)\}. \qquad (4.11)$$

This is already a reflexive polytope, M:348 5 N:12 5 H:5,251, with the top over the -3-curve $\{pt'_1, pt'_2\}$ that we found at the end of section 4.3.1. Naively from table 9, this might appear to be an "$\mathfrak{su}(2)$" top; however looking explicitly at the Tate form associated to the polytope Δ, the vanishing orders along the -3-curve are $\{1,1,1,2,2\}$ in terms of the five sections a_n, and $\{2, 2, 4\}$ in terms of $\{f, g, \Delta\}$, and the $\mathfrak{su}(3)$ monodromy condition is satisfied — hence the gauge algebra is indeed $\mathfrak{su}(3)$ (indeed, we know from the presence of the -3 NHC that $\mathfrak{su}(2)$ is not possible in this geometry.) In section 2.3 (see in particular table 4), we described two distinct Tate tunings for $\mathfrak{su}(3)$. In this case, the geometry matches the alternate Tate form for IV^s associated with vanishing of a_6 to order 2 and an additional monodromy condition, and the "top" is a non-standard $\mathfrak{su}(3)$ top. There also exists a polytope model with the "usual" $\mathfrak{su}(3)$ top: adding pt'_3 $((0, -1, 1, 1))$ to the top gives another polytope model M:347 7 N:13 6 H:5,251, which has the standard $\mathfrak{su}(3)$ top; on the Tate side this model can be obtained by the reduction of the M polytope such that the vanishing orders along the -3-curve become $\{1, 1, 1, 2, 3\}$ — the standard Tate form for IV^s. Analogous situations arise for the NHCs -4 and -6 as well: in these cases, as discussed above, ∇ in equation (4.11) is already a reflexive polytope model of the generic CY over $\mathbb{F}_{m=4,6}$. The tops over the $-m$ curves in these cases look like those appearing in the literature for gauge algebras $\mathfrak{g}_2, \mathfrak{f}_4$ respectively, and the vanishing orders along the $-m$-curves are $\{1, 1, 2, 2, 3\}, \{1, 2, 2, 3, 4\}$ for $m = 4, 6$, which would naively be tunings for $\mathfrak{g}_2, \mathfrak{f}_4$. In these cases, however, the gauge algebras are actually $\mathfrak{so}(8), \mathfrak{e}_6$ with monodromy

conditions satisfied. Just like the case for $\mathbb{F}_3$, there are also generic polytope models over $\mathbb{F}_{4,6}$ that have the usual $\mathfrak{so}(8), \mathfrak{e}_6$ tops and Tate vanishing orders of $\mathfrak{so}(8), \mathfrak{e}_6$. The extra lattice points in the tops of these ∇ polytopes precisely correspond to the reduction in Tate monomials of the M polytope Δ.

In addition to multiple tops associated with monodromy conditions in Tate tunings, there are also other Tate tuning/top combinations that can arise for certain gauge groups. We have not attempted a systematic analysis of all possibilities, but we have encountered a range of possibilities simply in analyzing the polytopes of the KS database with fixed Hodge numbers and associated Tate tunings for the dual polytopes. To give a sense of the possibilities that arise, we list the structures of the polytopes in the KS database that have the Hodge numbers of generic elliptically fibered CYs over $\mathbb{F}_m$ bases for $0 \leq m \leq 12$ in table 10. The details of the corresponding Tate forms for the $-m$ NHCs are given in table 11. Note in particular, that in addition to those models mentioned above, there is a third polytope model associated with the Hodge numbers of the generic elliptic fibration over $\mathbb{F}_6$ in addition to the monodromy construction and the standard construction discussed above. This third possibility involves a further specialization of the vanishing orders of the standard construction along the -6-curve, giving a further reduced M polytope Δ. Another interesting case of multiple tops that arises in these tables is the possibility of a second type of Tate tuning/top for $\mathfrak{e}_7$ on a -8 curve. In this case there is no monodromy issue,[15] but a second Tate tuning where the degree of vanishing of a_6 is enhanced, associated with a second $\mathfrak{e}_7$ top and corresponding reflexive polytopes.

In the analysis in the remainder of this paper we focus on classifying the possible elliptic fibrations constructions through the set of Tate tunings. One could also, however, imagine classifying different reflexive polytopes by considering all ways of augmenting the set of vertices (4.1) associated with the "standard stacking" with all possible tops. Proceeding in this fashion would require a systematic way of identifying the complete set of tops for each possible tuned gauge group.

We will not deal systematically with the explicit triangulation of ∇, corresponding to the resolution of the Calabi-Yau threefold, but make some comments here on the relationship between extra rays in ∇ and the resolution of the singular fiber associated with a tuned or non-Higgsable gauge group. Many of the details of this correspondence were worked out in [58, 59]. When the gauge algebra is non-trivial over a divisor $D^{(B)}$, there are lattice points in the top over $v^{(B)}$ in addition to just pt_1'. Specifically, in the cases where there are no lattice points in the top lying in the interior of the 2-dimensional faces of ∇, the lattice points in the top that do not lie in the interior of the 3-dimensional faces of ∇ form the Dynkin diagram of the gauge algebra. These correspond to the exceptional divisors that arise in the resolution of the corresponding singularities. However, when there are lattice points lying in the interior of the 3-dimensional and the 2-dimensional faces of ∇, they contribute to the second and third terms, respectively, in Batyrev's $h^{1,1}$ formula (3.11). The second term corresponds to components that miss the hypersurface, and contributions to the third term arise when the singularity is not resolved by a toric divisor but rather

---

[15]However, note that the same Tate vanishing orders $\{1, 2, 3, 3, 5\}$ may also give the $\mathfrak{e}_7$ algebra over -7 curves where there is also charged matter.

Hodge pair	Mult. in KS	$\mathbb{F}_n$ base	Gauge symmetry	Top over the $-n$-curve
(3,243)	3	$\mathbb{F}_2$	trivial	$\{pt'_1\}$ (affine node)
		$\mathbb{F}_1$	trivial	$\{pt'_1\}$ (affine node)
		$\mathbb{F}_0$	trivial	$\{pt'_1\}$ (affine node)
(5,251)	3	$\mathbb{F}_3$	$\mathfrak{su}(3)$	$\{pt'_1, pt'_2\}$ ("$\mathfrak{su}(2)$")
		$\mathbb{F}_3$	$\mathfrak{su}(3)$	$\{pt'_1, pt'_2, pt'_3\}$
		$\mathbb{F}_3$	$\mathfrak{g}_2$ enhanced on -3	$\{pt''_1, pt'_2, pt'_3\}$
(7,271)	4	$\mathbb{F}_4$	$\mathfrak{so}(8)$	$\{pt''_1, pt'_2, pt'_3\}$ ("$\mathfrak{g}_2$")
		$\mathbb{F}_4$	$\mathfrak{so}(8)$	$\{pt''_1, pt'_2, pt'_3, pt'_4\}$ ("$\mathfrak{so}(7)$")
		$\mathbb{F}_4$	$\mathfrak{f}_4$ enhanced on -4	$\{pt'''_1, pt''_2, pt'_3, pt'_4\}$
		$\mathbb{F}_4$	$\mathfrak{so}(9)$ enhanced on -4	$\{pt''_1, pt''_2, pt'_3, pt'_4\}$
(7,295)	1	$\mathbb{F}_5$	$\mathfrak{f}_4$	$\{pt'''_1, pt''_2, pt'_3, pt'_4\}$
(9,321)	3	$\mathbb{F}_6$	$\mathfrak{e}_6$	$\{pt'''_1, pt''_2, pt'_3, pt'_4\}$ ("$\mathfrak{f}_4$")
		$\mathbb{F}_6$	$\mathfrak{e}_6$	$\{pt'''_1, pt''_2, pt'_3, pt'_4, pt'_5, pt'_7\}$
		$\mathbb{F}_6$	$\mathfrak{e}_6$	$\{pt'''_1, pt''_2, pt'_3, pt'_4, pt'_5\}$
(10,348)	1	$\mathbb{F}_7$	$\mathfrak{e}_7$ (w/ matter $\frac{1}{2}56$)	$\{pt''''_1, pt'''_2, pt''_3, pt''_4, pt'_5\}$
(10,376)	2	$\mathbb{F}_8$	$\mathfrak{e}_7$ w/o matter	$\{pt''''_1, pt'''_2, pt''_3, pt''_4, pt'_5, pt'_6\}$
		$\mathbb{F}_8$	$\mathfrak{e}_7$ w/o matter	$\{pt''''_1, pt'''_2, pt''_3, pt''_4, pt'_5\}$
(11,491)	1	$\mathbb{F}_{12}$	NHC -12 curve: $\mathfrak{e}_8$	$\{pt_1^{(6)}, pt''''_2, pt'''_3, pt''_4, pt'_5\}$

Table 10. Polytope models associated with generic elliptic fibrations over the Hirzebruch surfaces $\mathbb{F}_{0,1,\ldots,8,12}$, as well as all other models with the same Hodge numbers. Alternate constructions include multiple tops, some due to monodromy conditions in Tate tunings, as well as rank-preserving tunings (section 4.4).

by a non-toric deformation, so the Dynkin diagram is not fully visible from the top. This happens exactly in those gauge algebras with an additional monodromy condition that is automatically satisfied.

In summary, ∇ models are divided into two types according to whether there is a nonzero third term in the $h^{1,1}$ formula (3.11): (1) Trivial third term: there is no lattice point lying in the interior of any two-dimensional face. Gauge algebras can be read off directly from tops (the nodes of the Dynkin diagram are given by the lattice points in the top that do not lie in interior of facets), which are those in the literature. The Tate forms are those with no additional monodromy condition, which again match those in the literature. The nodes also correspond to exceptional divisors resolving the singular fiber. (2) Non-vanishing third term: there are lattice points lying in the interior of two-dimensional faces. These cases give rise to the additional Tate forms we have described. For example, in the gauge algebras involved with monodromy conditions, there are Tate forms of lower degrees, which achieve the gauge algebras by satisfying the additional monodromy conditions automatically. The singular fiber is (partially) resolved by deformation. Therefore, there are fewer exceptional

NHC	Tops	Possible vertices	Tate form	(f,g,Δ)	G
-3	$\{pt'_1, pt'_2\}$	none	$\{1,1,1,2,2\}$	$(2,2,4)$	$\mathfrak{su}(3)$
	$\{pt'_1, pt'_2, pt'_3\}$	pt'_3	$\{1,1,1,2,3\}$		
-4	$\{pt''_1, pt'_2, pt'_3\}$	none	$\{1,1,2,2,3\}$	$(2,3,6)$	$\mathfrak{so}(8)$
	$\{pt''_1, pt'_2, pt'_3, pt'_4\}$	pt'_4	$\{1,1,2,2,4\}$		
-5	$\{pt'''_1, pt''_2, pt'_3, pt'_4\}$	pt'''_1	$\{1,2,2,3,4\}$	$(3,4,8)$	$\mathfrak{f}_4$
-6	$\{pt'''_1, pt''_2, pt'_3, pt'_4\}$	none	$\{1,2,2,3,4\}$		
	$\{pt'''_1, pt''_2, pt''_3, pt'_4, pt'_5\}$	pt''_3, pt'_5	$\{1,2,2,3,5\}$	$(3,4,8)$	$\mathfrak{e}_6$
	$\{pt'''_1, pt''_2, pt''_3, pt'_4, pt'_5, pt'_7\}$	pt'_7	$\{1,2,2,4,6\}$		
-7	$\{pt''''_1, pt'''_2, pt''_3, pt''_4, pt'_5\}$	pt''''_1, pt''_4	$\{1,2,3,3,5\}$	$(3,5,9)$	$\mathfrak{e}7$
-8	$\{pt''''_1, pt'''_2, pt''_3, pt''_4, pt'_5\}$	pt''_4	$\{1,2,3,3,5\}$	$(3,5,9)$	$\mathfrak{e}_7$
	$\{pt''''_1, pt'''_2, pt''_3, pt''_4, pt'_5, pt'_6\}$	pt'_6	$\{1,2,3,3,6\}$		
-12	$\{pt_1^{(6)}, pt''''_2, pt'''_3, pt''_4, pt'_5\}$	none	$\{1,2,3,4,5\}$	$(4,5,10)$	$\mathfrak{e}8$
-2,	$\{pt'_1, pt'_2\}$,	$\{pt'_2\}$,	$\{1,1,1,1,2\}$,	$(1,2,3)$,	$\mathfrak{su}(2)$
-3	$\{pt''_1, pt'_2, pt'_3\}$	$\{pt''_1\}$	$\{1,1,2,2,3\}$	$(2,3,6)$	$\oplus\mathfrak{g}_2$
-2,	$\{pt'_1\}$,	none,	$\{1,1,1,1,1\}$,	$(1,1,2)$,	
-2,	$\{pt'_1, pt'_2\}$,	none,	$\{1,1,2,2,2\}$,	$(2,2,4)$,	$\mathfrak{su}(2)$
-3	$\{pt''_1, pt'_2, pt'_3\}$	$\{pt''_1\}$	$\{1,1,2,2,3\}$	$(2,3,6)$	$\oplus\mathfrak{g}_2$
-2,	$\{pt'_1, pt'_2\}$,	none,	$\{1,1,1,1,2\}$,	$(1,2,3)$,	$\mathfrak{su}(2)$
-3,	$\{pt''_1, pt'_2, pt'_3, pt'_4\}$,	$\{pt'_4\}$,	$\{1,2,2,2,4\}$,	$(2,4,6)$,	$\oplus\mathfrak{so}(7)$
-2	$\{pt'_1, pt'_2\}$	none	$\{1,1,1,1,2\}$	$(1,2,3)$	$\oplus\mathfrak{su}(2)$

-9 blown up at 3pts	$\{pt_1^{(6)}, pt''''_2, pt'''_3, pt''_4, pt'_5\}$	$pt_1^{(6)}$	$\{1,2,3,4,5\}$	$(4,5,10)$	$\mathfrak{e}8$
-10 blown up at 2pts	$\{pt_1^{(6)}, pt''''_2, pt'''_3, pt''_4, pt'_5\}$	$pt_1^{(6)}$	$\{1,2,3,4,5\}$	$(4,5,10)$	$\mathfrak{e}8$
-11 blown up at 1pt	$\{pt_1^{(6)}, pt''''_2, pt'''_3, pt''_4, pt'_5\}$	$pt_1^{(6)}$	$\{1,2,3,4,5\}$	$(4,5,10)$	$\mathfrak{e}8$

Table 11. Tops over NHCs and the corresponding Tate vanishing orders. In each case the first example is the top and associated minimal Tate tuning associated with the "dual of the dual" construction described in section 4.3.2.

divisors in the top, in which the "Dynkin diagram" would seem to be the lower rank gauge algebra counterpart.

Finally, recall from table 1 that there are *rank-preserving* tunings of certain gauge algebras that leave the Hodge numbers of an elliptic Calabi-Yau unchanged. These are also associated with further Tate tunings on Δ and additional tops in ∇ that do not change the Hodge numbers from the generic elliptic fibration over a given base. The polytopes listed in table 10 include rank-preserving tunings of $\mathfrak{g}_2$ over the -3 curve in $\mathbb{F}_3$, and $\mathfrak{f}_4, \mathfrak{so}(9)$ over the -4 curve in $\mathbb{F}_4$. A detailed example of the polytopes associated with different tunings of $\mathfrak{su}_3$ and $\mathfrak{g}_2$ over $\mathbb{F}_2$ is given in appendix B.

4.5 Combining tunings

A final important issue that we must consider in attempting to systematically construct global models associated with polytopes is whether given a generic model over a given base, all combinations of Tate tunings that are each possible locally can be combined into an allowed global model. This depends on the global structure of the base and can be tested by the Tate-Zariski decomposition discussed in section 2.5. As discussed there, we can perform a Zariski decomposition, with the initial values of $\{c_{j,n}|n\}$ over each curve set to be the initial values we want in table 11. We then carry out the Tate-Zariski iteration procedure and if the Zariski decomposition with the desired vanishing values and corresponding gauge groups does not exist, there will not be a corresponding polytope model. In general, if the Zariski decomposition works out, there is a corresponding polytope. We do not have a proof of this in general but as we see later, at least the Hodge numbers of every elliptic Calabi-Yau threefold constructed in this way arise from a polytope in the KS database. This analysis of combined tunings through Tate-Zariski is the essential analysis we carry out in our systematic enumeration of Tate tunings that should have corresponding polytopes. To illustrate the issues that can arise we give a couple of simple examples here, where one but not all of the possible Tate tunings over a given curve in the base are consistent with a global model.

Let us consider first as a concrete example the generic model over the base with toric curves of self-intersection numbers $\{-3, -2, -2, -1, -6, -1, -2, -3, -1, -1, -1, -1\}$, for which the toric rays take coordinates $\{v_i^{(B)}\}=\{(1, 1), (3, 2), (5, 3), (7, 4), (2, 1), (5, 2), (3, 1), (1, 0), (0, -1), (-1, -1), (-1, 0), (0, 1)\}$ (figure 3). We consider Tate tunings that keep the gauge group the same as in the generic model, determined by the NHCs. From table 11 and the discussion in the preceding subsection, we see that there are three different possible Tate tunings over the -6 curve: $\{1, 2, 2, 3, 4\}$, $\{1, 2, 2, 3, 5\}$, $\{1, 2, 2, 4, 6\}$. We wish to know which of these three tunings leads to a consistent Tate-Zariski decomposition, and which corresponding polytopes exist.

For the polytope ∇ in each of these three cases, we have the vertices from the fiber

$$\{(0, 0, -1, 0), (0, 0, 0, -1)\}, \tag{4.12}$$

the vertices from the base, which come from the -1's:

$$\{(7, 4, 2, 3), (5, 2, 2, 3), (0, -1, 2, 3), (-1, -1, 2, 3), (-1, 0, 2, 3), (0, 1, 2, 3)\}, \tag{4.13}$$

and vertices from the tops of the NHCs

- $-3, -2, -2$: $\{(2, 2, 2, 3)\}$,

- $-2, -3$: $\{(3, 1, 1, 2), (2, 0, 2, 3)\}$,

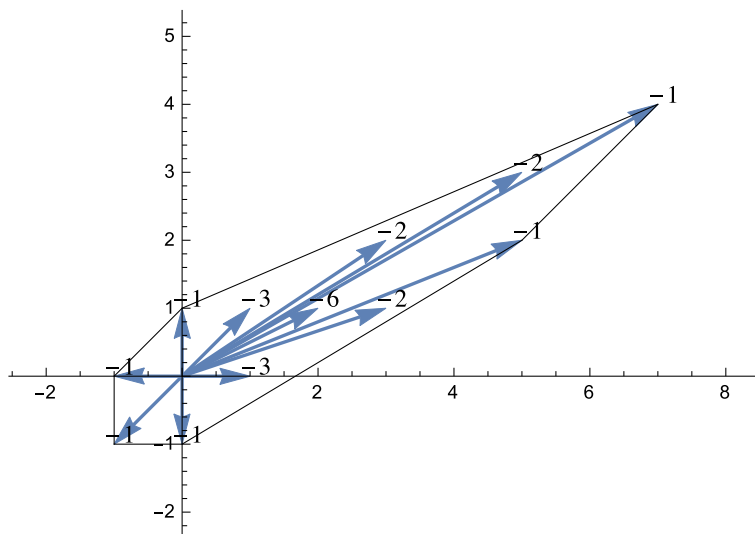- -6 with three choices of different possible top vertices.

Figure 3. The toric fan of the base of a generic model with small $h^{1,1}$: {23, 107, {-3, -2, -2, -1, -6, -1, -2, -3, -1, -1, -1, -1}}. Each -1-curve in the base corresponds to a vertex of ∇.

We now consider each of the tunings in turn over the -6 curve:

1. Minimal tuning $\{1, 2, 2, 3, 4\}$, corresponding to no additional top vertex from table 11. This construction leads to a consistent Zariski decomposition, which gives rise to the generic polytope model M:148 11 N:33 11 H:23,107[2]: we start with the initial configuration

$$\{\{1, 1, 2, 2, 3\}, \{1, 1, 2, 2, 2\}, \{1, 1, 1, 1, 1\}, \{0, 0, 0, 0, 0\}, \{1, 2, 2, 3, 4\}, \{0, 0, 0, 0, 0\},$$
$$\{1, 1, 1, 1, 2\}, \{1, 1, 2, 2, 3\}, \{0, 0, 0, 0, 0\}, \{0, 0, 0, 0, 0\}, \{0, 0, 0, 0, 0\}, \{0, 0, 0, 0, 0\}\}.$$

(4.14)

After the iteration procedure, the configuration becomes

$$\{\{1, 1, 2, 2, 3\}, \{1, 1, 2, 2, 2\}, \{1, 1, 1, 1, 1\}, \{1, 1, 0, 0, 0\}, \{1, 2, 2, 3, 4\}, \{1, 1, 0, 0, 0\},$$
$$\{1, 1, 1, 1, 2\}, \{1, 1, 2, 2, 3\}, \{0, 0, 0, 0, 0\}, \{0, 0, 0, 0, 0\}, \{0, 0, 0, 0, 0\}, \{0, 0, 0, 0, 0\}\},$$

where each curve still has their suitable Tate vanishing orders, which persist as $\{1, 2, 2, 3, 4\}$ on -6.

2. Tate tuning $\{1, 2, 2, 3, 5\}$, corresponding to the additional top vertices $\{pt_3'', pt_5'\} = \{(2, 1, 0, 0), (4, 2, 1, 1)\}$ over the -6 curve. This works as well and gives the generic polytope model M:147 12 N:35 13 H:23,107[1]: we start with the initial configuration in (4.14) but with the vanishing orders along -6 replaced by $\{1,2,2,3,5\}$. The configuration after iteration becomes

$$\{\{1, 1, 2, 2, 3\}, \{1, 1, 2, 2, 2\}, \{1, 1, 1, 1, 1\}, \{1, 1, 0, 0, 0\}, \{1, 2, 2, 3, 5\}, \{1, 1, 0, 0, 1\},$$
$$\{1, 1, 1, 1, 2\}, \{1, 1, 2, 2, 3\}, \{0, 0, 0, 0, 0\}, \{0, 0, 0, 0, 0\}, \{0, 0, 0, 0, 0\}, \{0, 0, 0, 0, 0\}\},$$

where each curve still has their suitable Tate vanishing orders, which persist as $\{1, 2, 2, 3, 5\}$ on -6.

3. Tate tuning $\{1, 2, 2, 4, 6\}$, which would correspond to the additional top vertex $\{pt_7'\} = \{(2, 1, 0, -1)\}$. This does not give a consistent polytope. The iteration of the initial configuration

$$\{\{1, 1, 2, 2, 3\}, \{1, 1, 2, 2, 2\}, \{1, 1, 1, 1, 1\}, \{0, 0, 0, 0, 0\}, \{1, 2, 2, 4, 6\}, \{0, 0, 0, 0, 0\},$$
$$\{1, 1, 1, 1, 2\}, \{1, 1, 2, 2, 3\}, \{0, 0, 0, 0, 0\}, \{0, 0, 0, 0, 0\}, \{0, 0, 0, 0, 0\}, \{0, 0, 0, 0, 0\}\}$$

becomes

$$\{\{1, 1, 2, 2, 3\}, \{1, 1, 2, 2, 3\}, \{1, 1, 1, 2, 3\}, \{1, 1, 0, 2, 3\}, \{1, 2, 2, 4, 6\}, \{1, 1, 0, 2, 3\},$$
$$\{1, 1, 1, 2, 3\}, \{1, 1, 2, 2, 3\}, \{0, 0, 0, 0, 0\}, \{0, 0, 0, 0, 0\}, \{0, 0, 0, 0, 0\}, \{0, 0, 0, 0, 0\}\},$$

where the vanishing orders over the NHC $-2, -2, -3$ are disturbed. Hence, unlike the case of the $\mathbb{F}_6$ base where there is a generic polytope model of vanishing order $\{1, 2, 2, 4, 6\}$ on -6, the third Tate tuning and corresponding top realization does not exist for this base.

As another illustrative example, consider the polytopes associated with Hodge numbers H:416,14, which match those of the generic elliptic Calabi-Yau threefold over the base $\{416, 14, \{-12//-11//-12//-12//-12//-12//-12//-12//-12//-12//-12//-12//- 12, -1, -2, -2, -3, -1, -5, -1, -3, -2, -1, -8, -1, -2, -3, -2, -1, -8, 0\}\}$ (see figure 4, by $//$ we denote the sequence of curves $-1, -2, -2, -3, -1, -5, -1, -3, -2, -2, -1$; there are in total 163 toric curves in the base, with curves 153 and 162 being the -8 curves). There are only two polytope models in the KS database with H:416,14, and both give polytope models of the CY with generic gauge group over the given base, with different detailed Tate tuning/top structure. Naively one might expect four models, since there are two different $\mathfrak{e}_7$ tunings possible over each -8 curve. Analyzing the structure of the polytopes, however, we find:

1. M:26 6 N:576 6 H:416,14

   - A vertex from the 0-curve in the base. In particular, note that all -1 curves in $//$ do not contribute to vertices.
   - Vertices from NHC tops
     (a) D_{B13} ([-11]): $pt_1^{(6)}$
     (b) D_{B153} (-3 in [-3 -2]): pt_1''
     (c) D_{B162} ([-8]): pt_6'
   - and vertices v_x, v_y.

2. M:29 7 N:575 7 H:416,14

   - Vertex contributions from the base and the fiber are the same as the first case.
   - Vertices from NHC tops
     (a) D_{B13} ([-11]): $pt_1^{(6)}$
     (b) D_{B153} (-3 in [-3 -2]): pt_1''
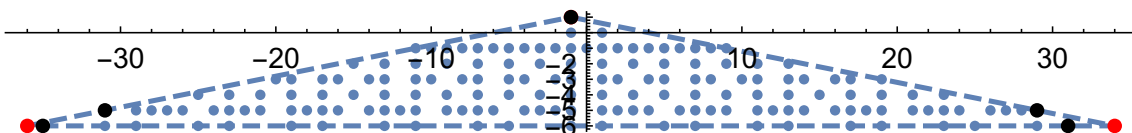   (c) D_{B156} ([-8]): pt_4''
     (d) D_{B162} ([-8]): pt_4''

Figure 4. The toric fan (arrows indicating rays are simplified to points for clarity) of the base of a generic model with large $h^{1,1}$ {416,14,{-12,-1,-2,-2,-3,-1,-5,-1,-3,-2,-2,**−1**,-11,**−1**,-2,-2,-3,-1,-5,-1,-3,-2,-2,-1,-12//-12//-12//-12//-12//-12//-12//-12//-12//-12//-12,**−1**,-2,-2,-3,-1,-5,-1,-3,-2,**−1**,-8,-1,-2,-3,-2,-1,-8,**0**}, where the five curves corresponding to vertices of the base are in boldface, and are denoted by black dots in the fan diagram. The point at the top $(-1, 1)$ corresponds to the zero curve, which is also a vertex of ∇. Two red dots in the fan diagram correspond to points in the tops: $pt_1^{(6)}$ of D_{B13} and pt_1'' of D_{B153}, respectively; these points thus do not correspond to rays of the base fan.

In the first model, the top over the first -8-curve (D_{B156}) is $\{pt_1'''', pt_2''', pt_3'', pt_4'', pt_5'\}$ while over the second (D_{B162}) is $\{pt_1'''', pt_2''', pt_3'', pt_4'', pt_5', pt_6'\}$; in the second model, it is $\{pt_1'''', pt_2''', pt_3'', pt_4'', pt_5'\}$ over both -8-curves; however there is no model of top $\{pt_1'''', pt_2''', pt_3'', pt_4'', pt_5', pt_6'\}$ over D_{B156}. This matches with the observation that there is no corresponding Zariski decomposition — the vanishing orders can not be $\{1, 2, 3, 3, 6\}$ along D_{B156}.

Note that these models also illustrate another point: a vertex of the base can only come from curves with self-intersection number m greater than -2, but all curves with $m > -2$ will not necessarily be vertices. Though this generally is the case for small $h^{1,1}$, exceptions increase as $h^{1,1}$ increases, since additional rays can expand the convex hull of the base polytope. Also, a vertex associated with a top can only come from those possibilities listed in the third column of table 11, but the entries in that column are not always vertices, though they are always lattice points in the N polytope ∇. This fact can be seen in the first model in the second example: pt_4'' over D_{B156} ([-8]) is not a vertex point.

4.6 Tate tunings and polytope models of $\mathfrak{so}(n)$ gauge algebras

As described in section 4.4, for some gauge algebras such as $\mathfrak{su}_3$ and $\mathfrak{e}_6$ there are multiple tops associated with distinct Tate tunings, where one tuning involves an additional monodromy condition. This also occurs for the gauge algebras $\mathfrak{so}(n)$. We discuss in this subsection some particular aspects of $\mathfrak{so}(n)$ tunings and the associated reflexive polytopes, which have some unique features.

As can be seen from table 4, for each of the $\mathfrak{so}(n)$ gauge algebras with n even, starting with $n = 8$, there are two distinct Tate tunings that realize the algebra, with one (both in the case of $\mathfrak{so}(8)$) involving a monodromy condition. (Note that these forms in the table expand on earlier versions of the table appearing in the literature, which did not include all these possibilities.) As discussed in section 4, the monodromy condition for the weaker Tate tuning can be realized automatically when the leading terms in certain a_is are powers of a single monomial, corresponding in the polytope language to a condition that the associated set of lattice points contain only a single element with appropriate multiplicity properties.

As for $\mathfrak{su}_3$, $\mathfrak{e}_6$, we find that both kinds of Tate tunings of the $\mathfrak{so}(2n)$ gauge algebras can arise in corresponding polytopes in the KS database, corresponding to the usual condition

that a global Tate-Zariski decomposition is possible. We also note, however, that when the algebra $\mathfrak{so}(2n-1)$ can be realized on one polytope over a given curve, then the monodromy realization of $\mathfrak{so}(2n)$ is generally not possible, though the higher Tate tuning generally is. This basically corresponds geometrically to the question of whether the minimally tuned Tate model with the weaker vanishing condition has the appropriate single monomials in the a_is, or not. By the same token, the gauge algebra $\mathfrak{so}(8)$, which has only monodromy realizations, can only be realized when neither $\mathfrak{g}_2$ or $\mathfrak{so}(7)$ is possible over a given curve, which essentially reduces the appearance of this algebra to the NHC structure of -4 curves.

To illustrate these points we give a few examples.

For a first example, consider a chain of curves $\{-1, -4, -1, -4, -1, -4, 0\}$; by requiring Tate vanishing orders $\{0, 0, 1, 1, 2\}$ ($\mathfrak{sp}(1)$ gauge algebra) on D_{B3} and D_{B5}, the Tate vanishing orders on each of the curves become $\{\{0, 0, 0, 0, 0\}, \{1, 1, 2, 3, 4\}, \{1, 0, 1, 2, 2\}, \{1, 1, 2, 3, 4\}, \{1, 0, 1, 2, 2\}, \{1, 1, 2, 3, 4\}, \{0, 0, 0, 0, 0\}\}$. Without taking into account the monodromy conditions, it would appear in this case that the enhanced algebras were $\{\cdot \oplus \mathfrak{so}(9) \oplus \mathfrak{sp}(1) \oplus \mathfrak{so}(9) \oplus \mathfrak{sp}(1) \oplus \mathfrak{so}(9) \oplus \cdot\}$; explicitly analysis of the monomials, however, shows that while D_{B2} and D_{B6} are indeed $\mathfrak{so}(9)$ algebras, there is really a $\mathfrak{so}(10)$ algebra on D_{B4}, since the $\mathfrak{so}(10)$ monodromy condition is automatically satisfied. This can also be understood from the perspective of global symmetry constraints [47]; when the gauge algebra is $\mathfrak{so}(9)$ on a -4-curve, the maximal global symmetry algebra is $\mathfrak{sp}(1)$, so it is not possible for $\mathfrak{so}(9)$ to appear on D_{B4} next to two $\mathfrak{sp}(1)$'s. Thus, D_{B4} indeed must carry the gauge algebra $\mathfrak{so}(10)$, for which the maximal global symmetry algebra is $\mathfrak{sp}(2) \supset \mathfrak{sp}(1) \oplus \mathfrak{sp}(1)$.

For a similar example, for tunings of $\mathfrak{so}(4k+3)$ and $\mathfrak{so}(4k+4)$ consider the sequence of curves $\{-1, -3, -1, -4, -1, 0\}$; by requiring vanishing orders of $\{1, 1, 3, 3, 5\}$ on D_{B4} and $\{0, 0, 3, 3, 6\}$ on D_{B5}, the other vanishing orders are forced to $\{\{0, 0, 0, 0, 0\}, \{1, 1, 2, 2, 3\}, \{1, 0, 2, 1, 2\}, \{1, 1, 3, 3, 5\}, \{0, 0, 3, 3, 6\}, \{0, 0, 0, 0, 2\}\}$, which gives the gauge algebras $\{\cdot \oplus \mathfrak{g}_2 \oplus \mathfrak{sp}(1) \oplus \mathfrak{so}(12) \oplus \mathfrak{sp}(3) \oplus \cdot\}$; the algebra $\mathfrak{so}(11)$ is not possible on D_{B4} by global symmetry constraints. Examples of these tunings in the context of global constructions are given in tables 12 and 13.

In the examples just given, on certain curves the $\mathfrak{so}(2n-1)$ gauge algebra cannot arise, and the lower Tate tuning with the monodromy condition is realized. As mentioned above, when the $\mathfrak{so}(2n-1)$ tuning is allowed, there is not generally a polytope in the KS database with the same Tate tuning and the monodromy condition automatically satisfied, and one has to use the higher Tate tuning to guarantee the condition. These facts can be seen in contrasting the polytope models, for example, of $\mathfrak{so}(9)$ and the two realizations of $\mathfrak{so}(10)$ in table 12. There is only one model in the KS database with the Hodge pair $\{339, 21\}$, M:36 9 N:467 9 H:339,21, which corresponds to tuning of the generic model $\{335, 23, \{-12//-11//-12//-12//-12//-12//-12//-12//-12//-12//-12, -1, -2, -2, -3, -1, -4, -1, -4, -1, -4, 0\}\}$ on $\{-1, -4, -1, -4, -1, -4, 0\}$ to gauge algebras $\{\cdot \oplus \mathfrak{so}(9) \oplus \mathfrak{sp}(1) \oplus \mathfrak{so}(10) \oplus \mathfrak{sp}(1) \oplus \mathfrak{so}(10) \oplus \cdot\}$. The Tate tuning along the last -4-curve is $\{1, 1, 2, 3, 5\}$. There is not a second polytope with the same Hodge numbers corresponding to the weaker Tate realization $\{1, 1, 2, 3, 4\}$ of the gauge algebra $\mathfrak{so}(10)$ along the last -4-curve. This matches with the observation that the absence of multiple data in the KS database for a given tuning is due to the existence of the

Generic models NHCs	$\cdot \oplus \mathfrak{so}(8) \oplus \cdot \oplus \mathfrak{so}(8) \oplus \cdot \oplus \mathfrak{so}(8) \oplus \cdot$
M:41 5 N:457 5 H:335,23	{{1,0,1,0,0},{1,1,2,2,3},{1,0,1,0,0} ,{1,1,2,2,3}, {1,0,1,0,0},{1,1,2,2,3},{0,0,0,0,0}}
M:40 7 N:460 7 H:335,23	{{1,0,1,0,1},{1,1,2,2,4},{1,0,1,0,2} ,{1,1,2,2,4}, {1,0,1,0,2},{1,1,2,2,4},{0,0,0,0,0}}
Tuned symmetries	$\cdot \oplus \mathfrak{so}(9) \oplus \mathfrak{sp}(1) \oplus \mathfrak{so}(10) \oplus \mathfrak{sp}(1) \oplus \mathfrak{so}(9) \oplus \cdot$
M:39 7 N:465 7 H:338,22	{{1,0,1,2,1},{1,1,2,3,4},{1,0,1,2,2},{1,1,2,3,4}, {1,0,1,2,2},{1,1,2,3,4},{0,0,0,0,0}}
M:38 8 N:466 8 H:338,22	{{1,0,1,2,1},{1,1,2,3,4},{1,0,1,2,3},{1,1,2,3,5}, {1,0,1,2,3},{1,1,2,3,4},{0,0,0,0,0}}
Tuned symmetries	$\cdot \oplus \mathfrak{so}(9) \oplus \mathfrak{sp}(1) \oplus \oplus \mathfrak{so}(11) \oplus \mathfrak{sp}(1) \oplus \mathfrak{so}(9) \oplus \cdot$
M:37 7 N:467 7 H:338,22	{{1,0,3,2,1},{1,1,3,3,4},{1,0,3,2,3},{1,1,3,3,5}, {1,0,2,2,3},{1,1,2,3,4},{0,0,0,0,0}}
Tuned symmetries	$\cdot \oplus \mathfrak{so}(9) \oplus \mathfrak{sp}(1) \oplus \mathfrak{so}(10) \oplus \mathfrak{sp}(1) \oplus \mathfrak{so}(10) \oplus \cdot$
M:36 9 N:467 9 H:339,21	{{1,0,1,2,1},{1,1,2,3,4},{1,0,1,2,3},{1,1,2,3,5}, {1,0,1,2,4},{1,1,2,3,5},{0,0,0,0,0}}

Table 12. An example contrasting the absence and the existence of multiple realizations: successive Tate tunings of generic CYs over the toric base $\{-12//-11//-12//-12//-12//-12//-12//-12//-12//-12//-12, -1, -2, -2, -3, -1, -4, -1, -4, -1, -4, 0\}$. The Tate vanishing orders on the last seven curves $\{-1, -4, -1, -4, -1, -4, 0\}$ are indicated. All polytope models in the KS database with the Hodge pairs $\{225, 23\}, \{338, 22\}, \{339, 21\}$ are listed in each of the three blocks. In models with Hodge pair $\{338, 22\}$, both the weaker and the stronger versions of the tuning of $\mathfrak{so}(10)$ on the middle -4-curve exist — the weaker version can not correspond to $\mathfrak{so}(9)$ by the global symmetry constraint on the -4-curve. On the other hand, there is only one model with Hodge pair $\{339, 21\}$, the weaker version of the tuning of $\mathfrak{so}(10)$ on the last -4-curve does not exist in the KS database — the same Tate tuning gives $\mathfrak{so}(9)$ on the last -4-curve in the model M:38 8 N:466 8 H:338,22.

same Tate tuning appearing in the lower rank gauge algebras: there is already the case M:38 8 N:466 8 H:338,22, corresponding to tuning of the same generic model to gauge algebras $\{\cdot \oplus \mathfrak{so}(9) \oplus \mathfrak{sp}(1) \oplus \mathfrak{so}(10) \oplus \mathfrak{sp}(1) \oplus \mathfrak{so}(9) \oplus \cdot\}$, and the Tate tuning along the last -4-curve is $\{1, 1, 2, 3, 4\}$ giving an $\mathfrak{so}(9)$ there. On the other hand, there are two models with H:338,22, M:39 7 N:465 7 and M:38 8 N:466 8, corresponding to the tuning $\{\cdot \oplus \mathfrak{so}(9) \oplus \mathfrak{sp}(1) \oplus \mathfrak{so}(10) \oplus \mathfrak{sp}(1) \oplus \mathfrak{so}(9) \oplus \cdot\}$ giving the two different Tate realizations of the $\mathfrak{so}(10)$. In this case, the weaker tuning satisfies the monodromy condition automatically, which is expected as $\{\cdot \oplus \mathfrak{so}(9) \oplus \mathfrak{sp}(1) \oplus \mathfrak{so}(9) \oplus \mathfrak{sp}(1) \oplus \mathfrak{so}(9) \oplus \cdot\}$ is not allowed as mentioned.

There is a similar story between $\mathfrak{so}(11)$ and $\mathfrak{so}(12)$. For example, we can tune an $\mathfrak{so}(11)$ on the -3-curve of the generic model over $\mathbb{F}_3$ by requiring Tate vanishing orders of $\{1, 1, 3, 3, 5\}$, which gives rise to M:328 8 N:18 7 H:8,242 in KS database. Then to get a polytope corresponding to a tuning of $\mathfrak{so}(12)$, we need to use $\{1, 1, 3, 3, 6\}$, which has a good

Generic model, in KS	$\cdot \oplus \mathfrak{su}(3) \oplus \cdot \oplus \mathfrak{so}(8) \oplus \cdot \oplus \cdot$
M:85 6 N:379 6 H:274,58	$\{\{1,1,0,1,0\}, \{1,1,1,2,2\}, \{1,0,0,0,0\},$ $\{1,1,2,2,3\}, \{0,0,0,0,0\}, \{0,0,0,0,0\}\}$
Tuned model, in KS	$\cdot \oplus \mathfrak{g}_2 \oplus \mathfrak{sp}(1) \oplus \mathfrak{so}(12) \oplus \mathfrak{sp}(3) \oplus \cdot$
M:35 7 N:387 7 H:280,22	$\{\{1,1,3,1,1\}, \{1,1,3,2,3\}, \{1,0,3,1,2\},$ $\{1,1,3,3,5\}, \{0,0,3,3,6\}, \{0,0,0,0,0\}\}$

Table 13. An example of the non-existence of the stronger version of the Tate form: a tuning of a generic model over the base $\{-12// - 11// - 12// - 12// - 12// - 12// - 12// - 12, -1, -2, -2, -3, -1, -5, -1, -3, -1, -4, -1, 0\}$ on the last -4-curve with a $\mathfrak{so}(12)$ gauge algebra (which forces gauge algebras on nearby curves). The Tate vanishing orders on the last six curves $\{-1, -3, -1, -4, -1, 0\}$ are indicated. While the weaker version of the Tate form $\{1,1,3,3,5\}$ exists in the KS database, the stronger version $\{1,1,3,3,6\}$ does not give rise to a Tate-Zariski decomposition with the desired gauge algebras.

Zariski decomposition, and therefore a corresponding reflexive polytope exists, M:318 10 N:19 8 H:9,233. The Hodge numbers of all these examples are consistent with calculations from anomalies.

As we have mentioned, there is a special situation for the $\mathfrak{so}(8)$ algebra and related polytopes in the KS database: all realizations of $\mathfrak{so}(8)$ involve monodromy constraints. Thus, there are no polytopes where there is a Tate tuning of the algebra $\mathfrak{so}(8)$, and this algebra only arises over the NHC -4. In the case of the NHC -4, $\mathfrak{so}(8)$ is the minimal gauge algebra, so either vanishing orders $\{1,1,2,2,3\}$ or $\{1,1,2,2,4\}$ will automatically satisfy the $\mathfrak{so}(8)$ monodromy condition in any Tate tuning over a base with a -4 curve. This unique aspect of $\mathfrak{so}(8)$ matches with the observation that a tuned $\mathfrak{so}(7)$ cannot be ruled out through the global symmetry group since the global symmetry group on a tuned $\mathfrak{so}(7)$ curve contains that on a tuned $\mathfrak{so}(8)$ curve. Thus, any Tate tuning of $\{1,1,2,2,3\}$ or $\{1,1,2,2,4\}$ over a curve with self-intersection greater than -4 will lead to a model with, if not $\mathfrak{g}_2$, $\mathfrak{so}(7)$ enhancement.

4.7 Multiplicity in the KS database

Given a pair of Hodge numbers $h^{1,1}, h^{2,1}$, there are in general many distinct polytopes in the KS database. There are many ways in which such a multiplicity may arise. Of course, generic or tuned elliptic fibrations over distinct bases may coincidentally give the same Hodge numbers. As discussed above, however, there are also many closely related constructions that give identical Hodge numbers. Different realizations of the same gauge algebra through different Tate tunings may contribute, often related to monodromy tunings as discussed in the preceding subsections. There are also rank-preserving tunings that change the gauge algebra but not the Hodge numbers. And in some cases there are non-toric deformations that can give additional multiplicity. A complete analysis of the KS database that accounts for these multiplicities exactly would require a complete and systematic tracking of all distinct possible Tate tunings for each gauge algebra combination and a clear

and systematic analysis of the non-toric deformation possibilities. We have not attempted such a systematic analysis here. Rather, in the analysis in the remainder of the paper we focus on constructing distinct possible gauge groups through Tate tunings and identifying the distinct Hodge numbers that can arise for reflexive polytopes in this way. In this section we discuss in a bit more detail some aspects of the multiplicity question.

To systematically analyze multiplicities of different Tate tunings of the same algebra, we would need to consider all combinations of monodromy and non-monodromy tunings of algebras like $\mathfrak{su}_3, \mathfrak{e}_6, \mathfrak{so}(n)$ etc. Over bases with many curves allowing such tunings this could give a large combinatorial multiplicity. For example, consider the two polytope models in the first block of table 12. We start with the minimal $\{1, 1, 2, 2, 3\}$ Tate vanishing orders for all three -4 curves, which together do have a corresponding Tate-Zariski decomposition, so there is a corresponding polytope construction. Then we tune the vanishing orders on the middle -4-curve alone to be $\{1, 1, 2, 2, 4\}$. After iteration, the other two -4-curves are forced to also have $\{1, 1, 2, 2, 4\}$ vanishing, giving the second generic model with all -4 curves reaching the second realization. This exhausts the possibilities. So from what might appear to in principle be 8 possible combinations of tunings, only two are actually consistent. It can also happen that only the lower-order realization exists, while the higher-order realization does not have an acceptable Zariski decomposition and there is no corresponding polytope, as we have seen for example in the failure to realize the third model of H:23,107 with the generic gauge group over a -6 curve in section 4.5. In general, the realization of any given combination must be checked by performing a global Tate-Zariski decomposition, as local information may not be completely adequate to rule in or out a possible tuning. An example is given by the models in table 13, where there is no global Zariski decomposition of the $\{1, 1, 3, 3, 6\}$ realization of $\mathfrak{so}(12)$, and the reflexive polytope model does not exist over the given global base, though it would seem to be fine if we were to analyze the tuning pattern with the focus on the local sequence $\{-1, -3, -1, -4, -1, 0\}$ only.

Note also that further Tate tunings of a given algebra may not give rise to a new reflexive polytope, even if the higher vanishing orders still have a valid Zariski decomposition. We describe briefly several examples here: there is only one polytope in the KS database with H:4,226, which corresponds to the type I_2 $\mathfrak{su}(2)$ tuning $\{0, 0, 1, 1, 2\}$ on the -2-curve of the $\mathbb{F}_2$ base, but there is no polytope that corresponds to the type III $\mathfrak{su}(2)$ $\{1, 1, 1, 1, 2\}$. It is even more interesting to compare the H:5,233 models discussed in appendix A and H:5,251 in table 10: there is no IV $\mathfrak{su}(3)$ for the former since it is just a specialization of the type I_3 $\mathfrak{su}(3)$ tuning, while there are two different IV $\mathfrak{su}(3)$ realizations for the latter; and both of these sets have the rank-preserving tuning $\mathfrak{g}_2$ model. Similarly, type I_{2n}^{ns} and type I_{2n+1}^{ns} $\mathfrak{sp}(n)$ tunings do not give rise to different polytopes. Also for three different types I_0, I_1, II of the trivial algebra, only the one with the lowest vanishing orders that has a Tate-Zariski decomposition has a reflexive polytope construction. An amusing exercise is illustrated in table 14, where we can see the changes in three different types of trivial algebra under various tunings.

Another source of multiplicity comes from tunings of rank-preserving type as described in the end of section 2.1. We have seen several examples in global models: H:7,271 of rank 4 $\mathfrak{so}(8), \mathfrak{so}(9)$, and $\mathfrak{f}_4$ tunings in table 10, and H:338,22 of rank 5 $\mathfrak{so}(10)$ and $\mathfrak{so}(11)$ tunings

-1	0	1	0	KS data
$\{0,0,0,1,1\}$ I_0	$\{0,1,1,2,3\}$ I_3 $\mathfrak{su}(3)$	$\{0,0,0,0,0\}$ I_0	$\{1,1,2,3,4\}$ $\mathfrak{so}(9)$	M:165 11 N:18 9 H:9,129[1]
$\{0,1,1,1,1\}$ I_1	$\{0,1,1,2,3\}$ I_3 $\mathfrak{su}(3)$	$\{0,0,0,0,0\}$ I_0	$\{1,2,2,3,4\}$ $\mathfrak{f}_4$	M:160 9 N:19 8 H:9,129
$\{1,0,1,1,1\}$ I_1	$\{1,1,2,2,3\}$ $\mathfrak{g}_2$	$\{0,0,0,0,0\}$ I_0	$\{1,1,2,3,4\}$ $\mathfrak{so}(9)$	M:155 7 N:19 6 H:9,129
$\{1,1,1,1,1\}$ II	$\{1,1,2,2,3\}$ $\mathfrak{g}_2$	$\{0,0,0,0,0\}$ I_0	$\{1,2,2,3,4\}$ $\mathfrak{f}_4$	M:150 5 N:20 5 H:9,129
$\{1,1,1,1,1\}$ II	$\{1,1,1,2,3\}$ $IV^s\mathfrak{su}(3)$	$\{0,0,0,0,0\}$ I_0	$\{1,2,2,3,4\}$ $\mathfrak{f}_4$	no corresponding KS data

Table 14. Some rank-preserving tunings over the $\mathbb{F}_1$ base. Notice that the Tate vanishing orders of the trivial algebra on the -1-curve change in the Tate-Zariski decomposition as the vanishing orders of the two 0-curves get higher. The last row gives an example of a general observation that when the gauge algebra tuning is only a further specialization of an existing gauge algebra tuning (but not the case of gauge algebras realized by different monodromy tunings listed in table 4 with $\star$, which involves with the requirements of additional conditions), there would not be a corresponding polytope in the KS database even if the Tate-Zariski configuration is stable. The example illustrates that since there is the $\mathfrak{su}(3)$ model in the second row realized by I_3, there is no model realized by IV^s.

in table 12, and H:9,129 of different combinations of rank preserving tunings in table 14. Notice that it is not always true that tuning gauge algebras with the same rank will lead to the same $h^{2,1}$ shift. For example, $\mathfrak{su}(7)$ and $\mathfrak{e}_6$ are not subalgebras of each other, and the tunings give different $h^{2,1}$s.

Lastly, multiplicity can come from situations where the elliptic fibration over a toric base has $(4, 6)$ points that must be blown up. As discussed in section 2.8, over toric bases containing curves with self-intersection number $-9, -10, -11$ the generic elliptic fibration is non-flat and the base must be blown up at the $(4, 6)$ points to give -12-curves, over which there is a flat elliptic fibration. In general the base resulting from these blow-ups will be non-toric, and the blowups give extra tensor multiplets contributing to anomaly cancellation [9, 10]. In some cases, however, the base is still toric after blowing up one or more of the $(4, 6)$ points; in such cases there will be multiple entries in the KS database associated with these distinct bases. In general we expect that these all represent smooth Calabi-Yau threefolds that can be viewed as non-flat elliptic fibrations over toric bases or flat elliptic fibrations over the non-toric bases resolved at the non-toric $(4, 6)$ points, though we have not checked explicitly that this is true in all cases. Examples of some non-flat elliptic fibrations of this type are analyzed in [31, 40, 41]. To illustrate this structure, in appendix B we analyze the non-flat elliptic fibration structure of the toric hypersurfaces associated with (flat) toric fibrations of the reflexive fibered polytopes over the Hirzebruch surfaces $\mathbb{F}_9, \mathbb{F}_{10}, \mathbb{F}_{11}$. In these cases, we see explicitly that the fiber over the $(4, 6)$ points in the $-9, -10, -11$-curves contains extra irreducible components that may naturally be

associated with divisors in the blown up space. The multiplicity with which the Hodge pairs for the generic elliptic fibration models over the suitably blown up Hirzebruch surfaces $\mathbb{F}_{9/10/11}$ are listed in table 15, the tops over the -9/-10/-11-curves are listed in the second block in table 11. This illustrates the way in which the same smooth Calabi-Yau threefold can be realized as a non-flat elliptic fibration over one or more toric bases as well as sometimes a flat elliptic fibration over another toric base, with each fibration structure realized in a different polytope in the KS database. For example, as illustrated in the table there are 6 distinct polytopes at Hodge numbers H:14,404, which correspond to toric realizations of elliptic fibrations over different "semi-toric" bases that admit only a single $\mathbb{C}^*$ action (including various limits in which -2 curves arise).

4.8 Bases with large Hodge numbers

In this work we have confined our study to the simplest $\mathbb{P}^{2,3,1}$ fiber type polytopes. In part this is because the standard fiber type matches with the Tate structure of the Weierstrass model as discussed previously. Also, however, this fiber type dominates the structure at large Hodge numbers. In particular, we can explicitly identify constraints on the bases that can be used for the other 15 fiber types. These constraints are such that the other fiber types all lead to problematic codimension one $(4, 6)$ singularities on some divisor in the base when the base contains curves of sufficiently negative self-intersection. In particular, none of the other 15 fibers can be supported over any base that contains a curve of self-intersection less than -8. This immediately constrains the set of constructions at large Hodge number, since the generic elliptic fibrations with the largest Hodge numbers almost always involve -12 curves in the base (though there are notable exceptions to this general principle, including the other one of the two fibrations of the H:491:11 polytope).

We leave a more detailed analysis of the constraints on different fiber types for future work, but briefly outline the issue that arises for other fiber types besides the $\mathbb{P}^{2,3,1}$ fiber. Consider for example the $\mathbb{P}^2$ fiber type. Carrying out the analogue of the standard stacking procedure for a $\mathbb{P}^2$ fiber, we find that there are 10 dual monomials analogous to the coefficients $a_1, \ldots, a_6$. These 10 monomials are sections of line bundles $\mathcal{O}(-K), \mathcal{O}(-2K)$ and $\mathcal{O}(-3K)$. Any section of a line bundle $-nK$ must vanish over a -12 curve to at least degree n when $n < 5$ by the Zariski decomposition. This immediately leads to the presence of a codimension one $(4, 6)$ singularity over any -12 curve in the base. Similar issues arise for the other fiber types.

Considering the toric bases, we can simply consider the complete enumeration carried out in [9] and identify the bases with largest Hodge numbers that have curves of self-intersection no smaller than -8. The base of this type with the largest $h^{2,1}$ for the generic elliptic fibration is $\mathbb{F}_8$, over which the generic elliptic fibration has Hodge numbers $(10, 376)$. Even over $\mathbb{F}_8$, the largest $h^{2,1}$ value that can be achieved for a tuning with any fiber other than $\mathbb{P}^{2,3,1}$ is quite restricted; over this base, for example, there are 5 other fiber types including $\mathbb{P}^{1,1,2}$ that are possible; the generic fibration with each of these fiber types gives an elliptic Calabi-Yau threefold with Hodge numbers $(11, 227)$. Any other fibration with these or any other fibers other than $\mathbb{P}^{2,3,1}$ over any base would seem to give a Calabi-Yau threefold with an even smaller value of $h^{2,1}$. Thus, by restricting to Hodge numbers

Hodge pair	Mult. in KS	Bases	
(14,404)	6	{0, -9, 0, 9}	{-1, -1, -10, 0, 9}
		{-1, -1, -11, -1, -1, 9}	{-1, -2, -1, -11, 0, 9}
		{-1, -2, -1, -12, -1, -1, 9}	{-1, -2, -2, -1, -12, 0, 9}
(13,433)	4	{0, -10, 0, 10}	{-1, -1, -11, 0, 10}
		{-1, -1, -12, -1, -1, 10}	{-1, -2, -1, -12, 0, 10}
(12,462)	2	{0, -11, 0, 11}	{-1, -1, -12, 0, 11}

Table 15. A variety of polytope models arise for the Hodge pairs associated with the generic elliptic fibrations over the Hirzebruch surfaces $\mathbb{F}_{9/10/11}$. The possibilities are enumerated in this table. The first graph for each Hodge pair is the generic model, where the $(4, 6)$ singularities on the $-9, -10,$ or -11 curve are at non-toric points and the elliptic fibration is non-flat. In these cases the blow-ups are handled automatically by the resolution of the toric geometry, giving a resolved model corresponding to a flat elliptic fibration over a "semi-toric" base. There are also toric bases that arise by blowing up one or more of the $(4, 6)$ points at toric points, giving polytopes with toric fibrations over blow-ups of the Hirzebruch surfaces. When multiple $(4, 6)$ points coincide this corresponds to a limit with a -2 curve in the base. For each polytope the base of the fibration is a toric surface given by the curves on the outside of the diagram, with self-intersections as labeled.

above $h^{2,1} \geq 240$, we can expect that the threefolds in the KS database that admit elliptic fibrations should be all or almost all described by the $\mathbb{P}^{2,3,1}$ fiber type.

Similarly, the largest value of $h^{1,1}$ that can arise for a base with no curves of self-intersection below -8 is 224. The corresponding base has a set of toric curves of self-intersection $(0, -8//-7//-8//-8//-8//-8//-8//-8//-8//-8//-8//-7//-8)$, where $//$ denotes the sequence $-1, -2, -3, -2, -1$ associated with E_7 chains (see e.g. [9]), and a generic elliptic fibration with Hodge numbers (224,18). There is nothing that can be tuned over this base without producing a curve of self-intersection below -8 so it seems that confining attention to threefolds with $h^{1,1} \geq 240$ should again restrict us to primarily $\mathbb{P}^{2,3,1}$ fiber types. As we see in section 6, however, there are a few unusual cases in which bases that have generic elliptic fibrations with rather small values of $h^{1,1}$ admit extreme tunings that dramatically increase the value of $h^{1,1}$ without producing curves of highly negative self-intersection. In a companion paper [20], we study the fibration structure of the hypersurface models in the KS database more directly, and confirm both the prevalence of $\mathbb{P}^{2,3,1}$ fibers at large Hodge numbers and the existence of exceptions involving extreme tunings.

5 Systematic construction of Tate-tuned models in the KS database

Kreuzer and Skarke have classified all 473,800,776 4D reflexive polytope models, which give 30,108 distinct Hodge pairs. It was found in [39] that the set of Hodge pairs $\{h^{1,1}, h^{2,1}\}$ of all generic elliptically fibered CYs over toric bases is a subset of all the Hodge pairs in the KS database. We gave in section 4.3.2 a general construction of reflexive polytope models of these generic elliptic fibrations over toric bases with NHCs, and we expect that all generic elliptic fibration models over toric bases have these corresponding reflexive polytope models in the KS database. We wish to carry out a more comprehensive comparison by matching tuned Weierstrass models of CYs over 2D toric bases with 4D reflexive polytope models of Calabi-Yau hypersurfaces at large Hodge numbers.

Of the 30,108 distinct Hodge pairs in the KS database, 1,827 have either $h^{1,1} \geq 240$ or $h^{2,1} \geq 240$ (only the Hodge pair $\{251, 251\}$ satisfies both inequalities). To compare the two constructions at large Hodge numbers, the next step would be to construct roughly this number of distinct Weierstrass models of tuned CYs in these regions. Not all Weierstrass models correspond to reflexive polytope constructions, however. Nonetheless, as discussed in section 4, there is a close relation between Tate-tuned models and $\mathbb{P}^{2,3,1}$-fibered polytopes, which dominate at large Hodge numbers as argued in section 4.8. Therefore, our approach is to construct systematically all Tate-tuned models via tunings of generic Tate models over 2D toric bases. As a preliminary to this analysis, however, we begin with a simpler systematic analysis of which gauge group tunings may be possible based on more general Weierstrass tunings, and then we refine the analysis to Tate tunings. We describe the logic of this analysis in more detail in section 5.1.

All Hodge pairs of the Tate-tuned models from this algorithm fall within those in the KS database. However, there are certain Hodge numbers in the KS database in the regions of interest at which our initial analysis identified no matching Tate-tuned model. We therefore have analyzed directly, via the method described in section 3.5, the polytope

models with the Hodge numbers that were not found in our systematic tuning construction; the analysis of these cases is described in section 6. It turns out that all these remaining polytope models can be described as somewhat more exotic Weierstrass or Tate tunings over bases that are either toric bases or blow-ups thereof. This completes the comparison of the two constructions at the level of Hodge numbers. At a basic level the result of this analysis is that in the regions of interest all the Hodge pairs in the KS database are realized through generic or tuned elliptic fibrations. This matches with the results through a direct analysis of the fibration structure in the companion paper [20]. The more detailed analysis we carry out here, however, gives much more insight into the structure of these fibrations and the complex variety of Weierstrass tunings and geometries that are realized through simple toric hypersurface constructions.

We also discuss briefly the limits of Tate tuning in section 5.4, where we collect some results on tunings that are compatible with the global symmetry constraints but can't not be realized by Tate tunings. These tunings may be realized by Weierstrass models and in such cases give new Hodge pairs outside the KS database.

5.1 Algorithm: global symmetries and Zariski decomposition for Weierstrass models

We give an algorithm in this section to systematically construct all tunings of enhanced gauge groups over a given 2D toric base, starting with the generic model. Our goal is to construct all Tate-tuned models over toric bases that give elliptic Calabi-Yau threefolds with Hodge numbers in the regions $h^{1,1} \geq 240$ or $h^{2,1} \geq 240$. As we saw in section 2.7, global symmetry constraints on each curve put upper bounds on the gauge algebras that can be tuned on intersecting curves. On the other hand, as discussed in section 4.5, there is an issue of whether local tunings on subsets of curves can be combined into a global model over some toric base B_2. This can be tested by the Zariski decomposition. More specifically, our goal is to carry out explicitly arbitrary combinations of the Tate tunings from section 2.3 on the curves in the base, applying the variant of the Zariski decomposition described in section 2.5 to determine which combinations are globally compatible. While in principle we could simply iterate over all possible gauge algebra combinations, using the global symmetry constraints on what gauge algebras can arise on the curves intersecting a curve of negative self intersection helps prune the tree and make the algorithm more efficient. Global symmetries are also helpful in limiting the set of possible monodromy-dependent gauge groups that can arise on sequences of intersecting curves in ways that are not apparent at the level of the Zariski decomposition.

Although ultimately we wish to analyze Tate tunings, we perform an initial analysis of Weierstrass tunings using global symmetry constraints and the Zariski decomposition. This gives us a set of possible tunings that we expect may be possible at the level of the gauge algebras. Not all these constructions, however, are compatible with Tate tunings and with polytopes. We begin the discussion by focusing on the Weierstrass tunings and then in section 5.4 we use the results of the Weierstrass tunings to check which Tate tunings are possible.

Given a 2D toric base B, which is represented by a set of K irreducible toric curves $\{C_j, j = 1, 2, \ldots, K\}$ intersecting each other in a linear chain, we first obtain for the generic model over the base B the orders of vanishing $\{c_{j,4}, c_{j,6}, c_{j,12}\}$ of f, g, and Δ along each curve. The sets of values $\{c_{j,4}\}$, $\{c_{j,6}\}$, and $\{c_{j,12}\}$ can be determined by the Zariski decomposition via the procedure described in equations (2.27)–(2.30) with $n = 4$, $n = 6$, and $n = 12$, respectively, or can be directly read off from the non-Higgsable cluster structure of the curves $\{C_j\}$.

Now let us consider all possible (Weierstrass) tunings of the generic model. We describe a procedure to determine an allowed pattern $\{\mathfrak{g}_j\}$ of tuned algebras $\mathfrak{g}_j$ on each curve C_j in the base. Note that in this algorithm we assume that there are no toric $(4, 6)$ points in the base, even after the tuning; such a point would be blown up to form a different toric base, and the tunings over the blown up base would be found directly by tunings over that base. We do allow non-toric $(4, 6)$ points in the case where the base contains $-9, -10$ or -11 curves; in these cases we essentially treat the curve as a -12 curve supporting an $\mathfrak{e}_8$, understanding that the polytope hypersurface construction will automatically resolve these singularities and effectively blow up the non-toric points in the base, in accord with the discussions in section 2.8 and section 4.7.

5.2 Main structure of the algorithm: bases with a non-Higgsable $\mathfrak{e}_7$ or $\mathfrak{e}_8$

We consider first the simplest cases, where there is at least one curve in the toric base of self-intersection $m \leq -9$; such a curve necessarily carries a non-Higgsable $\mathfrak{e}_8$ gauge algebra. We start the procedure by choosing a specific curve with a non-Higgsable $\mathfrak{e}_8$ and first considering the possible tunings on one of the adjacent curves. Let us label the curve with the $\mathfrak{e}_8$ using the index $j = 1$, the curve we attempt the first tuning on by $j = 2$, the subsequent curve by $j = 3$, etc. This choice of the initial configuration is convenient to serve as the starting point of a branching algorithm because an $\mathfrak{e}_8$ algebra cannot be further enhanced; moreover, nothing can be tuned next to an $\mathfrak{e}_8$, without producing a $(4, 6)$ singularity at a toric point, which we are assuming does not happen as discussed above. Therefore, the gauge algebras on C_1 and C_2 are fixed: $\mathfrak{g}_1 = \mathfrak{e}_8$ and $\mathfrak{g}_2$ has to be a trivial algebra.

We then pass to tunings $\mathfrak{g}_3$ on C_3. The possible tunings on C_3 are constrained by the global symmetry group $\mathfrak{g}_2^{(\text{glob})}$ on C_2, which is determined by the self-intersection number of C_2 and the gauge algebra $\mathfrak{g}_2$ on C_2. Let the set $\{\mathfrak{g}_{3,\alpha}\}$ be the set of algebras that satisfy the constraint $\mathfrak{g}_1 \oplus \mathfrak{g}_{3,\alpha} = \mathfrak{e}_8 \oplus \mathfrak{g}_{3,\alpha} \subset \mathfrak{g}_2^{(\text{glob})}$. For the global symmetries, we used the results in table 6.1 and table 6.2 in [47] for the maximal global symmetry group $\mathfrak{g}_j^{(\text{glob})}$ on a curve C_j of negative self-intersection m carrying a gauge algebra $\mathfrak{g}_j$. Additionally, the curves of negative self-intersection that do not support an NHC can carry trivial gauge algebras, of types I_0, I_1, II; therefore in such cases when $\mathfrak{g}_j = \cdot$, we use $\mathfrak{g}_j^{(\text{glob})} = \mathfrak{e}_8$ and $\mathfrak{g}_j^{(\text{glob})} = \mathfrak{su}(2)$ for $m = -1$ and $m = -2$, respectively. We used the results tabulated in [61] for the subgroups of a global symmetry group $\mathfrak{g}_{j-1}^{(\text{glob})}$ to obtain the restricted set of algebras $\{\mathfrak{g}_{j,\alpha}\}$ satisfying the constraint $\mathfrak{g}_{j-2} \oplus \mathfrak{g}_{j,\alpha} \subset \mathfrak{g}_{j-1}^{(\text{glob})}$.

We attempt tunings one-by-one for each $\mathfrak{g}_{3,\alpha}$. For each possible algebra we replace the original orders of vanishing $\{c_{3,4}, c_{3,6}, c_{3,12}\}$ with the desired orders of vanishing corresponding to $\mathfrak{g}_{3,\alpha}$ using table 2. We then perform the Zariski iteration procedure on all curves with the new $\{c_{3,4}, c_{3,6}, c_{3,12}\}$ for $n = 4, 6$ and 12, respectively. If all the gauge algebras on the curves prior to and including C_3 stay unchanged after the iteration, tuning $\mathfrak{g}_{3,\alpha}$ is not ruled out. If any of the gauge algebras on the curves prior to C_3 have changed, or the vanishing orders $\{c_{3,4}, c_{3,6}, c_{3,12}\}$ do not produce the desired gauge algebra $\mathfrak{g}_{3,\alpha}$ in the new configuration after the iteration, tuning $\mathfrak{g}_{3,\alpha}$ is not allowed on C_3; in such cases we terminate the procedure with this $\mathfrak{g}_{3,\alpha}$ branch, and attempt the next tuning $\mathfrak{g}_{3,\alpha+1}$ on C_3. Note, however, that the fact that the gauge algebras stay unchanged does not mean that the set of values $\{c_{j\le 3,4}\}, \{c_{j\le 3,6}\}, \{c_{j\le 3,12}\}$ stay unchanged under the iterations. Indeed, often it is the case that the orders of vanishing on curves near C_3 are increased, but without modifying the gauge algebra on C_2. In other words, in this case $\mathfrak{g}_2$ should be the trivial algebra, but it may be type I_0, I_1, or II (cf. also examples in table 14.)

Note that the vanishing orders $\{c_{j>3,4}, c_{j>3,6}, c_{j>3,12}\}$ can obtain new values after the initial set of iterations just described. If these increase beyond those determined by the initial NHC configuration, we use the larger vanishing orders as the starting points in further iterations of the tuning. We denote by $\mathfrak{g}_{j[i]}$ the gauge algebra on curve j after the iteration procedure associated with curve C_i. For $i = j$, $\mathfrak{g}_{j[j]}$ denotes a choice of gauge algebra in a branch, $\mathfrak{g}_{j[j]} \in \{\mathfrak{g}_{j,\alpha}\}$, and $\mathfrak{g}_{j[j]} \supseteq \mathfrak{g}_{j[j-1]}$. Note that we must have $\mathfrak{g}_{j[k]} = \mathfrak{g}_{j[j]}$ for all $k > j$ as we require in the branch that the gauge algebra on C_j stays unchanged in tuning gauge algebras on $C_{k>j}$, but the orders of vanishing realizing the gauge algebra may be different. We can proceed with the new configuration to the next step of tuning algebras on C_4, as long as $\mathfrak{g}_{4[3]} \oplus \mathfrak{g}_{2[3]} \subset \mathfrak{g}_{3[3]}^{(\text{glob})}$ is satisfied, where now $\mathfrak{g}_{4[3]}$ is the gauge algebra on C_4 in the new configuration and $\mathfrak{g}_{3[3]}^{(\text{glob})}$ is determined by the self-intersection of C_3 and the gauge algebra $\mathfrak{g}_{3[3]} \in \{\mathfrak{g}_{3,\alpha}\}$. For example, let us start with $\mathfrak{g}_{3[3]} = \mathfrak{g}_{3,1}$. We terminate the procedure with the $\mathfrak{g}_{3,1}$ branch and attempt the next branch of tuning $\mathfrak{g}_{3,2}$ on C_3 if $\mathfrak{g}_{4[3]} \oplus \mathfrak{g}_{2[3]} \subset \mathfrak{g}_{3,1}^{(\text{glob})}$ is violated in the new configuration.

Assume $\mathfrak{g}_{3,1}$ passes the tests above. We then continue the procedure similarly to tune the curve C_4 in the $\mathfrak{g}_{3,1}$ branch with the new configuration: the set of possible tunings $\{\mathfrak{g}_{4,\beta}\}$ we attempt on C_4 is constrained by $\mathfrak{g}_{4,\beta} \oplus \mathfrak{g}_{2[3]} \subset \mathfrak{g}_{3[3]}^{(\text{glob})}$. The branch $\mathfrak{g}_{4,1}$ can be continued only if $\mathfrak{g}_{4,1}$ passes the two tests (1) the set of gauge algebras $\{\mathfrak{g}_{j\le 4}\} = \{\mathfrak{e}_8, \cdot, \mathfrak{g}_{3[4]}, \mathfrak{g}_{4,1}\}$ stays unchanged after performing Zariski iterations on $\{c_{j,4}\}, \{c_{j,6}\}$, and $\{c_{j,12}\}$ with the desired degrees of vanishing $\{c_{4,4}, c_{4,6}, c_{4,12}\}$ of the tuned gauge algebra plugged into the configuration, and (2) $\mathfrak{g}_{5[4]} \oplus \mathfrak{g}_{3[4]} \subset \mathfrak{g}_{4,1}^{(\text{glob})}$ is satisfied, where $\mathfrak{g}_{5[4]}$ is the gauge algebra on C_5 *after* the iterations in the newest updated configuration, and $\mathfrak{g}_{4,1}^{(\text{glob})}$ is again determined by the self-intersection of C_4 and $\mathfrak{g}_{4,1}$.

The procedure continues similarly until the second to the last curve C_{K-1} is met. As the last curve C_K is connected back to the first curve C_1, we need to consider also the global symmetry constraint on C_K to close the tuning pattern. The set of possible tunings $\{\mathfrak{g}_{K-1,\gamma}\}$ on C_{K-1} is constrained by $\mathfrak{g}_{K-1,\gamma} \oplus \mathfrak{g}_{K-3[K-2]} \subset \mathfrak{g}_{K-2[K-2]}^{(\text{glob})}$. First, the usual two conditions have to be satisfied for $\mathfrak{g}_{K-1,\gamma}$ to be allowed: in the new configuration after

the iterations associated with the tuning of $\mathfrak{g}_{K-1,\gamma}$ (1) the prior gauge algebras are held fixed, and (2) the global symmetry constraint on C_{K-1} is satisfied. Moreover, there is the additional third condition: (3) the global symmetry constraint on the curve C_K has to be satisfied; i.e., $\mathfrak{g}_{K-1,\gamma} \oplus \mathfrak{g}_1 \subset \mathfrak{g}_{K[K-1]}^{(\mathrm{glob})}$, where $\mathfrak{g}_1$ is held fixed and is $\mathfrak{e}_8$ in the simplest cases, and $\mathfrak{g}_{K[K-1]}^{(\mathrm{glob})}$ is determined by the self-intersection of the curve C_K and the gauge algebra $\mathfrak{g}_K$ after the Zariski interations for the tuning $\mathfrak{g}_{K-1,\gamma}$. In fact, $\mathfrak{g}_K$ is only allowed to be a trivial algebra in the simplest cases as C_1 carries an $\mathfrak{e}_8$ algebra, so no tuning is allowed on C_K. Hence, if the global symmetry constraint on C_K is satisfied, we are basically done to this point in the procedure searching for a tuning pattern. In this case, we obtain a tuning pattern $\{\mathfrak{e}_8, \cdot, \mathfrak{g}_{3[K-1]}, \mathfrak{g}_{4[K-1]}, \ldots, \mathfrak{g}_{K-3[K-1]}, \mathfrak{g}_{K-2[K-1]}, \mathfrak{g}_{K-1[K-1]}, \cdot\}$.

We check all $\mathfrak{g}_{K-1,\gamma}$'s in order similarly to complete the scan through all possible tuning patterns compatible with the initial viable possibility for $\mathfrak{g}_{3[3]}, \ldots, \mathfrak{g}_{K-2[K-2]}$. After all $\mathfrak{g}_{K-1,\gamma}$'s are processed, we proceed iteratively with a nested loop, continuing with the next possible value of $\mathfrak{g}_{K-2}$, etc. so that all possible combinations of gauge group tunings are considered.

All tunings increase $h^{1,1}$ and decrease $h^{2,1}$ with respect to the generic model over a given base. Thus, to classify all tuned models of $h^{2,1} \geq 240$, we need only consider toric bases for which the generic elliptic fibration has $h^{2,1} \geq 240$. In our initial scan, we also restricted to bases that have generic models with $h^{1,1} \geq 220$. As we describe in more detail in the following section, this misses a few cases where there is a large amount of tuning that significantly changes $h^{1,1}$. On the other hand, as bases associated with generic models having $h^{1,1} > 224$ always contain at least one curve carrying an $\mathfrak{e}_8$ algebra, the algorithm as described above is quite effective in dealing with tunings in the large $h^{1,1}$ region as we always have a simple starting point for the iteration. In fact, the algorithm actually can work in the same way for tunings of generic models with a curve carrying $\mathfrak{e}_7$ in the base; i.e., generic models with a curve of self-intersection $m \leq -7$ in the base. This is because $\mathfrak{e}_7$ algebras also cannot be further enhanced without modifying the base — an enhancement to an $\mathfrak{e}_8$ algebra would give additional $(4,6)$ points that must be blown up. And no non-trivial algebra can be tuned next to an $\mathfrak{e}_7$ algebra. Thus, in this case we similarly can make the convenient choice that the initial configuration is fixed to be $\mathfrak{g}_1 = \mathfrak{e}_7, \mathfrak{g}_2 = \cdot$.

We make some final comments on two technical issues in the tuning procedure. As mentioned above, in tuning the curve C_j, not only do the orders of vanishing on C_{j+1} (and in some cases on further curves $C_{j+2}, \ldots$) also change in general, but the new vanishing orders $\{c_{j+1,4}, c_{j+1,6}, c_{j+1,12}\}$ can in some cases correspond to a different gauge algebra. However, because the three Zariski iterations were performed independently, sometimes these vanishing orders do not correspond to any algebras in the Kodaira classification. We encountered a few cases of this type, for example where $\{c_{j+1,4}, c_{j+1,6}, c_{j+1,12}\} = \{1, 2, 4\}$; this can happen for example if a previous $\mathfrak{su}(n)$ tuning $(\{0, 0, n\})$ pushes up the order of vanishing of Δ more significantly than f, g (where some required orders of f, g already imposed on the curve); however, note that, this can never happen in a real Δ as calculated in a complete model from f and g in equation (2.10). In such situations, we modify the orders of vanishing on C_{j+1} to fit with those that correspond to the gauge algebra that

arises by increasing the values $c_{j+1,4}, c_{j+1,6}$ minimally. Then we perform the iteration again after the modification, and use the resulting configuration to test the conditions (1) and (2).

Another detail to take care is the tuning of algebras only distinguished by monodromy conditions. For those cases where there are distinct algebras associated with different monodromy conditions, we retain all the possibilities allowed by global symmetries; in the list of possible tunings we attach an additional label to the orders of vanishing using a fourth entry $\{c_{j,4}, c_{j,6}, c_{j,12}, \text{algebra}\}$ to ensure that all possible tunings are considered.

5.3 Special cases: bases lacking curves of self-intersection $m \leq -7$ and/or having curves of non-negative self intersection

The algorithm described in the preceding subsection relies on the presence of a curve of self-intersection $m \leq -7$ in the base, where we can begin the iteration process in a simple fashion as the gauge algebra on the initial curve is fixed. In the regions we are considering, there are very few bases that lack such curves; we describe here briefly how these cases are handled. Of course, one could simply use a brute force algorithm of choosing an arbitrary starting point and looping over all tunings on the initial curve C_1. In principle, however, for efficiency we would like to choose the curves C_1, C_2 such that there are fewer allowed combinations $\{\mathfrak{g}_1, \mathfrak{g}_2\}$. For example, for the generic model $\{11, 263, \{-1, -1, -6, -1, -1, 4\}\}$, we may choose to rotate the sequence of the curves to be $\{-6, -1, -1, 4, -1, -1\}$, so that there are only two initial configurations on the -6 curve C_1, which are the generic gauge algebra $\{\mathfrak{e}_6, \cdot\}$ and an enhancement on C_1 $\{\mathfrak{e}_7, \cdot\}$. Note that in this case there cannot be any enhancement on C_2 as the global symmetry algebra is always the trivial algebra on -6-curves without an further enhancement to $\mathfrak{e}_7$, so no tunings are allowed on any intersecting curves. In fact, in the Hodge number regions we are considering, there are very few cases that lack non-Higgsable $\mathfrak{e}_7$ or $\mathfrak{e}_8$ gauge algebras. Every base with a generic elliptic fibration having $h^{1,1} \geq 220$ has a curve of self-intersection -7 or below. In the region $h^{2,1} \geq 240$, there are 14 generic models that contain no curve in the base carrying an $\mathfrak{e}_7$ or $\mathfrak{e}_8$ algebra; the generic models over bases $\mathbb{F}_{0 \leq m \leq 6}$ and $\mathbb{P}^2$ compose 9 of these 14 models, and are discussed further below. In the remaining cases, there is no choice of the initial configuration that uniquely determines the initial configuration, and we have to enumerate and specify different initial configurations $\{\mathfrak{g}_1, \mathfrak{g}_2\}$ over a curve of minimal self-intersection to perform the algorithm.

A further issue arises for bases that have curves of non-negative self intersection. On such curves, there is no global constraint on the adjacent algebras from the SCFT point of view. While there are some analogous constraints in the case of curves of non-negative self intersection [13], the constraints are weaker and less completely understood. So we do not impose global constraints in these cases. In principle this can be handled by simply iterating over all gauge groups, however in practice the number of cases where this issue is relevant is rather limited and can be handled efficiently using more specific methods.

From the minimal model point of view we can fairly easily classify the types and configurations of non-negative self intersection curves that can arise. The minimal model bases $\mathbb{P}^2$ and $\mathbb{F}_m$ have three consecutive curves of non-negative self intersection. Any blow-up of one of these bases has either only one such curve or two adjacent such curves, since

blow-ups reduce the self-intersection of curves containing the blow-up point and do not introduce new curves of non-negative self intersection. Blow-ups of the resulting bases again have at most two curves of non-negative self intersection and when there are two they are always adjacent. So the possibilities are actually quite limited.

In general, the way we deal with the cases having one or two non-negative curves for bases with large $h^{2,1}$ is by performing the algorithm separately in both opposite directions from a good starting point (curve of maximally negative self intersection) to get two "half-patterns" of tunings, and connect them appropriately. In other words, we start from a chosen curve C_1, run the algorithm in both directions, and stop the tuning procedures when the first non-negative curve is met in both directions. We do not impose any global conditions for the curves of non-negative self intersection. The combination of the two sets of the half-patterns connected in this way gives all tuning patterns of a generic model with one or two non-negative curves in the base. For bases with large $h^{1,1}$, there is generally at most one non-negative self intersection curve and the nearby gauge group is generally constrained by global symmetries and nearby large negative self-interactions; in some of these cases we have used simpler heuristics to complete the analysis in the presence of non-negative self-intersection curves.

For the cases $\mathbb{P}^2$ and $\mathbb{F}_{0 \leq m \leq 12}$ that have three non-negative curves, most tunings in fact decrease the Hodge number $h^{2,1}$ below the value 240 of interest. For example [13], tuning an $\mathfrak{su}(2)$ on a $+1$ curve of $\mathbb{P}^2$ changes the Hodge numbers from $(2, 272)$ to $(3, 231)$. There are some exceptions: for example tuning an $\mathfrak{su}(2)$ on the $+12$ curve of $\mathbb{F}_{12}$ gives a Calabi-Yau with Hodge numbers $(12, 318)$. But it turns out (as we see explicitly from the analysis of the following section) that all these cases with $h^{2,1} \geq 240$ are also realized in other ways by generic or tuned models over other toric bases. So we do not need to explicitly include these in our analysis since we are not trying to reproduce the precise multiplicity of models at each Hodge number pair.

Although we have only focused on tuning models in the large Hodge number regions, one can in principle classify all allowed tuning patterns of non-abelian gauge algebras on any toric base with the algorithm described here; though slightly different methods are needed for tunings over the bases $\mathbb{P}^2$ and $\mathbb{F}_{0 \leq m \leq 12}$, an exhaustive search is straightforward in these cases as there are only a few curves in these bases (three curves in $\mathbb{P}^2$ and four curves in $\mathbb{F}_m$).

5.4 Tate-tuned models

The analysis described so far in terms of Weierstrass models gives a large collection of possible gauge algebra tunings over each toric base. Not all of these gauge algebra combinations correspond to hypersurfaces in reflexive polytopes. There are several reasons for this. First, not every Weierstrass tuning can be realized through a Tate form, so some of these tunings on toric curves will not have standard $\mathbb{P}^{2,3,1}$-fibered polytope constructions. Further, some of the combinations of gauge groups that are allowed by the Zariski analysis and global constraints still cannot be realized in practice in a global model — we alluded for example at the end of section 5.2 to the fact that monodromy conditions are not really taken care of properly in the Zariski decompositions of $n = 4, 6, 12$. Indeed, an explicit

check shows that not all the Hodge pairs calculated via equations (2.6) and (2.7) from the Weierstrass tuning patterns we got from section 5.2 and section 5.3 lie in the KS database.

We are interested in constraining to a subset of tuning constructions for which we expect direct polytope constructions. Hence, for each gauge algebra tuning combination that satisfies the Weierstrass Zariski analysis and global conditions, we attempt to construct an explicit Tate-type model by specifying Tate orders of vanishing according to table 4 for each tuning in a tuning pattern. We then perform the Zariski decomposition of the Tate tunings described in section 2.5. A tuning pattern gives a genuine Tate-tuned model if it has the Zariski decompositions of Tate tunings. In performing this analysis, we used in our systematic analysis only the stronger version of the Tate forms for the algebras with multiple realizations and/or monodromy conditions. In particular, we did not use any of the tunings marked with $\circ$ or $\star$ in table 4. The second version of the I_{2n}^s Tate tuning (marked with $\circ$) was in fact previously not known and was identified through the analysis of the next section. For the $\mathfrak{so}$ algebras, some of the alternate monodromy tunings were not previously known (for example, the non-$\star$ version of $\mathfrak{so}(4n+4)$ algebras); also, we wished to restrict attention to cases where the algebra is guaranteed simply by the order of vanishing of the Tate coefficients. In general, as we have noted in the examples in section 4.5 and section 4.6, the polytope constructions do not satisfy the monodromy conditions for the higher rank gauge algebras in these cases.

These principles give us a set of gauge group and Tate tunings over each toric base that we believe should have direct correspondents in the KS database through standard $\mathbb{P}^{2,3,1}$-fibered polytopes, given the correspondence that we established in section 4. We have carried out an explicit comparison of these two sets, and indeed the Hodge numbers of this more limited class of Tate-tuned gauge groups all correspond to values that appear in the KS database. Furthermore, the Hodge pairs from the original Weierstrass analysis that are not in the KS database are exactly those of the tuning patterns that can not be realized by Tate tuning. In fact, given this restricted set of tunings we reproduce almost all of the 1,827 distinct Hodge pairs in the range $h^{1,1} \geq 240$ or $h^{2,1} \geq 240$. Only 18 of the Hodge pairs in this range were not found by a "sieve" using the Tate constructions described above. In the next section we consider the analysis of these 18 outlying polytope constructions.

A question that we do not explore further here, but which is relevant to the more general problem of understanding the full set of Calabi-Yau threefolds and the classification of 6D F-theory models, is the extent to which tunings are possible that look like they should be allowed from the Weierstrass Zariski analysis and anomaly cancellation conditions, but do not correspond to Tate constructions. Various aspects of this "Tate tuning swampland" were analyzed in [13]. In the context of this project, we did a local analysis of the Weierstrass tuning patterns that are not Tate tuning patterns. We reproduced some parts of the known Tate tuning swampland and also found new obstructions. Some examples of the problematic tunings in the Tate construction are listed in table 16. An interesting question for further research is which of these can be realized through good global Weierstrass models when the indicated sequence of curves arises as part of a toric (or non-toric) base.

$\mathfrak{e}8$ Tate swamp	
$\mathfrak{su}(3) \oplus \mathfrak{sp}(3)$, $\mathfrak{su}(3) \oplus \mathfrak{sp}(4)$,	
$\mathfrak{g}_2 \oplus \mathfrak{so}(10)$,	
$\mathfrak{so}(9) \oplus \mathfrak{su}(4)$, $\mathfrak{so}(9) \oplus \mathfrak{sp}(2)$, $\mathfrak{so}(10) \oplus \mathfrak{su}(4)$, $\mathfrak{so}(10) \oplus \mathfrak{sp}(2)$,	
$\mathfrak{so}(11) \oplus \mathfrak{su}(3)$, $\mathfrak{so}(11) \oplus \mathfrak{sp}(2)$,	
$\mathfrak{so}(13) \oplus \mathfrak{sp}(1)$, $\mathfrak{so}(13) \oplus \mathfrak{su}(2)$	
Miscellaneous Tate swamp (some examples)	
Gauge groups	Local geometry
$\mathfrak{so}(7) \oplus \mathfrak{su}(2) \oplus \cdot$	-3, -2, -2
$\cdot \oplus \mathfrak{su}(2) \oplus \mathfrak{sp}(2)$(or $\mathfrak{su}(4)$)	-2, -2, -1/0
$\cdot \oplus \mathfrak{su}(2) \oplus \mathfrak{g}_2 \oplus \mathfrak{sp}(3)$	-2, -2, -2, -1/0

Table 16. Tate tuning swamp: we list all subalgebras allowed by the "E_8 rule" that however can not be realized by Tate tunings. We also give some examples of the tuning patterns we found that do not violate global symmetry constraints but that can not be realized by Tate tunings (i.e. violate Tate-Zariski decomposition).

6 Polytope analysis for cases missing from the simple tuning construction, and other exotic constructions

As discussed above, there are only 18 Hodge pairs in the regions $h^{1,1} \geq 240$ or $h^{2,1} \geq 240$ in the KS database that are not produced by our Tate tuning algorithm. One of these missing 18 Hodge pairs is in the large $h^{2,1}$ region, $\{45, 261\}$, and the other 17 (see table 17) are in the large $h^{1,1}$ region. In this section we analyze the polytopes in the Kreuzer-Skarke database associated with these 18 Hodge number pairs.

By studying these 18 classes of Calabi-Yau manifolds, we have identified new tuning constructions that we had not known previously; the KS database provides us with global models utilizing these constructions that we did not expect a priori in our original analysis. We study the fibration structure of the 18 outstanding classes by analyzing the polytopes in the way described in section 3.5. All the polytopes associated with these 18 Hodge pairs have a $\mathbb{P}^{2,3,1}$ fibered polytope structure (though in some cases it is really the more specialized $\text{Bl}_{[0,0,1]}\mathbb{P}^{2,3,1}$ fiber that occurs), but not all of them are the standard $\mathbb{P}^{2,3,1}$-fibered polytopes that we have defined in section 3.4. In particular, the CY hypersurface of a standard $\mathbb{P}^{2,3,1}$-fibered polytope (or $\text{Bl}_{[0,0,1]}\mathbb{P}^{2,3,1}$-fibered polytope) has a Tate form, while this is not the case for other fibration structures that use the same fiber but a different "twist". We analyze the two different types of polytopes arising from the 18 Hodge pairs separately. In section 6.1 we analyze the standard $\mathbb{P}^{2,3,1}$-fibered polytopes in the KS database that we have not obtained in our systematic construction of Tate-tuned models. In section 6.2 we analyze the polytopes that do not have the standard $\mathbb{P}^{2,3,1}$-fibered structure. We also include in section 6.2 some further examples in the KS database that are outside the range of focus of this paper but that illustrate some further interesting exotic structure associated with gauge groups on non-toric curves in the base.

Standard $\mathbb{P}^{2,3,1}$-	huge tuning	$\{240, 48\}, \{244, 10\}, \{250, 10\}, \{261, 9\}$
fibered polytopes	non-toric base	$\{258, 60\}$ ("$\mathfrak{e}_8$-tuning")
$\mathrm{Bl}_{[0,0,1]}\mathbb{P}^{2,3,1}$-	global $\mathfrak{u}(1)$ tuning and	$\{263, 32\}, \{251, 35\}, \{247, 35\}, \{240, 37\}$
fibered polytopes	non-toric base	("$\mathfrak{so}(n \geq 13)$-tuning" on a -3-curve)
Non-standard $\mathbb{P}^{2,3,1}$-	tuning on non-	$\{261, 51\}, \{261, 45\}, \{260, 62\}, \{260, 54\},$
fibered polytopes	toric curve	$\{259, 55\}, \{258, 84\}, \{254, 56\}, \{245, 57\}$

Table 17. The Hodge number pairs in the KS database at large $h^{1,1}$ that we did not obtain from straightforward Tate-tuned models. However, all these can be reproduced by some flat elliptic fibrations that we discuss in this section: the standard $\mathbb{P}^{2,3,1}$ models, which have a Tate form, are studied in section 6.1, and the non-standard $\mathbb{P}^{2,3,1}$ models, which involve tunings on non-toric curves in the base, are studied in section 6.2.

6.1 Fibered polytope models with Tate forms

Of the 18 missing Hodge pairs, there are $1 + 9$ Hodge pairs in the large $h^{2,1}, h^{1,1}$ regions respectively in which there is a standard $\mathbb{P}^{2,3,1}$-fibered polytope (or a standard $\mathrm{Bl}_{[0,0,1]}\mathbb{P}^{2,3,1}$-fibered polytope), which has a Tate form. Therefore, we analyze the Tate models explicitly from these polytopes to learn about the Tate tunings that we missed in our initial construction.

The Hodge pair in the large $h^{2,1}$ region, $\{45, 261\}$, has only one polytope. This polytope reveals a second tuning of the type I_{2n}^s singular fiber that is not just a specialization of the known Tate tuning. We also find that applying this novel Tate tuning $\mathfrak{su}(6)$ on a $m \geq -1$-curve gives models with the three-index antisymmetric representation as opposed to the generic fundamental and two-index antisymmetry representations. We describe this analysis in detail in section 6.1.1. The polytopes of the nine missing Hodge pairs at large $h^{1,1}$ with the standard fibration structure are either extremely tuned models, with bases having generic elliptic fibrations with $h^{1,1} < 220$ (described in section 6.1.2), or are non-flat elliptic fibration models over a toric base (described in section 6.1.3). In the non-flat elliptic fibration cases, as we have discussed at the end of section 4.7, the CY resolution of $(4,6)$ singularities in terms of the polytope model produces irreducible components of the ambient toric fiber (as the hypersurface equation restricted to the components is trivially satisfied over the $(4,6)$ points). Therefore, at these points the dimension of the fiber jumps to two giving the non-flat elliptic fibration structure. Associating the additional divisors with blow-ups in the base allows us to describe the resulting Calabi-Yau threefolds alternatively as flat elliptic fibrations over the blown up base. The resulting models in the cases found here give rise to $\mathfrak{e}_8$ tunings or $\mathfrak{so}(n \geq 13)$ tunings on -3-curves, and are also involved with tuned Mordell-Weil sections, which are associated with U(1) factors and U(1)-charged hypermultiplets.

6.1.1 Type I_{2n}^s Tate tunings and exotic matter

The polytope model M:357 8 N:65 8 H:45,261 is a standard $\mathbb{P}^{2,3,1}$-fibered polytope, and is a Tate-tuned model of the generic model

$$\{38, 290, \{-2, -2, -1, -6, -1, -3, -1, -5, -1, -3, -2, -2, -1, -12, 0, 6\}\}.$$

The data $\{a_1, a_2, a_3, a_4, a_6\}$ of the Tate form show the orders of vanishing along each curve

$$\{\{0,2,2,4,6\}, \{0,2,1,4,5\}, \{0,2,0,4,4\}, \{1,2,2,4,5\}, \{1,2,0,4,2\},$$
$$\{1,2,1,4,3\}, \{1,2,0,4,1\}, \{1,2,2,4,4\}, \{1,2,1,4,1\}, \{1,2,2,4,3\},$$
$$\{1,2,2,4,2\}, \{1,2,2,4,1\}, \{1,2,2,4,0\}, \{1,2,3,4,5\}, \{0,0,0,0,0\}, \{0,0,0,0,0\}\}. \quad (6.1)$$

In terms of $\{f, g, \Delta\}$ (equations (2.15)–(2.21)), the orders of vanishing are

$$\{\{0,0,6\}, \{0,0,3\}, \{0,0,0\}, \{3,4,8\}, \{1,0,0\}, \{2,2,4\}, \{1,0,0\}, \{3,4,8\},$$
$$\{2,1,2\}, \{3,3,6\}, \{3,2,4\}, \{3,1,2\}, \{3,0,0\}, \{4,5,10\}, \{0,0,0\}, \{0,0,0\}\},$$

which shows that there is an $\mathfrak{su}(6)$ enhanced on the first -2-curve, $D_1 \equiv \{b_1 = 0\}$, and an $\mathfrak{su}(3)$ on the second -2 curve. However, the corresponding Tate tuning is not just a specialization of the $\mathfrak{su}(6)$ Tate tuning $\{0,1,3,3,6\}$ in the literature. Via this example, we found the second version of the $\mathfrak{su}(2n)$ tuning, which we have included in the Tate tunings listed in table 4, indicated by $\mathfrak{su}(2n)^\circ$.

As this is the only polytope associated with the Hodge pair $\{45, 261\}$, it seems that the traditional $\mathfrak{su}(2n)$ tuning is somehow not allowed in this configuration. We checked explicitly by performing a tuning where we substitute in the vanishing order $\{0,1,3,3,6\}$ over D_1, and perform the Tate-Zariski decomposition. The vanishing orders after iteration become

$$\{\{0,1,3,3,6\}, \{0,1,3,2,5\}, \{0,1,3,1,4\}, \{1,2,3,3,5\}, \{1,2,3,1,2\},$$
$$\{1,2,3,2,3\}, \{1,2,3,1,1\}, \{1,2,3,3,4\}, \{1,2,3,2,1\}, \{1,2,3,3,3\},$$
$$\{1,2,3,3,2\}, \{1,2,3,3,1\}, \{1,2,3,3,0\}, \{1,2,3,4,5\}, \{0,0,0,0,0\}, \{0,0,0,0,0\}\};$$

or in terms of $\{f, g, \Delta\}$,

$$\{\{0,0,6\}, \{0,0,4\}, \{0,0,2\}, \{3,5,9\}, \{1,2,3\}, \{2,3,6\}, \{1,1,2\}, \{3,4,8\},$$
$$\{2,1,2\}, \{3,3,6\}, \{3,2,4\}, \{3,1,2\}, \{3,0,0\}, \{4,5,10\}, \{0,0,0\}, \{0,0,0\}\},$$

which is problematic as the global symmetry constraint on the -6-curve D_4 is violated. This confirms again that there has to be a Tate-tuned pattern that is consistent under the Tate-Zariski decomposition for a corresponding polytope to exist. And we cannot obtain a polytope of these Hodge numbers using the standard tuning methods because the $\mathfrak{su}(2n)^\circ$ tunings, $\{0,2,n-1,n+1,2n\}$, are not specializations of the standard $\mathfrak{su}(2n)$ tunings, $\{0,1,n,n,2n\}$.

In the case of a -2 curve, as in the example encountered at large $h^{2,1}$, the matter content associated with the physics of the exotic $\mathfrak{su}(6)^\circ$ tuning is equivalent to that of a standard $\mathfrak{su}(6)$ tuning over a -2 curve. After incorporating these alternative $\mathfrak{su}(2n)^\circ$-tunings into our algorithm, however, we discovered that this second Tate realization of $\{f, g, \Delta\} = \{0, 0, 2n\}$ gives rise to the non-generic three-index antisymmetric ($\mathbf{20}$) representation of $\mathfrak{su}(6)$ when the tuning is performed on curves of self-intersection $m \geq -1$. We describe an example of this explicitly, in the context of a global model that lies outside the regions of primary interest $h^{1,1}, h^{2,1} \geq 240$.

The polytope model M:280 11 N:28 9 H:18,206 is a Tate-tuned model of

$$\{11, 263, \{-1, -2, -1, -6, 0, 4\}\}. \tag{6.2}$$

There is an $\mathfrak{su}(6)^\circ$ tuned on the -1-curve D_1 and an $\mathfrak{su}(3)$ tuned on the -2-curve D_2. Interestingly, by explicit analysis, we find that the f, g from the polytope data automatically satisfy the conditions for the codimension-two singularity on D_1 to support the three-index antisymmetric representation of $\mathfrak{su}(6)$, as described in [30]. To see this, we fix the complex structure moduli of f, g to some general enough $\mathbb{Z}$ values to avoid accidental cancellations, expand f and g in terms of $\sigma \equiv b_1$ where the coefficients are in terms of a second local coordinate that we choose to be b_2

$$f(\sigma, b_2) = f_0(b_2) + f_1(b_2)\sigma + f_2(b_2)\sigma^2 + \cdots, \tag{6.3}$$
$$g(\sigma, b_2) = g_0(b_2) + g_1(b_2)\sigma + g_2(b_2)\sigma^2 + \cdots; \tag{6.4}$$

then we find (following the notation in [30])

- $\Delta_0 = 0$: $f_0 \sim -\frac{1}{48}\phi_0^4$ and $g_0 \sim \frac{1}{864}\phi_0^6$; we choose to set $\phi_0 = 57 + 46b_2$.

- $\Delta_1 = 0$: $g_1 = -\frac{1}{12}\phi_0^2 f_1$.

- $\Delta_2 = 0$: $f_1 \sim \frac{1}{2}\phi_0\psi_1 \Rightarrow \psi_1 = -(1/6)b_2(37 + 62b_2)\phi_0^2$ and $g_2 = \frac{1}{4}\psi_1^2 - \frac{1}{12}\phi_0^2 f_2$.

- $\Delta_3 = 0$: $\psi_1 \sim -\frac{1}{3}\phi_0\phi_1 \Rightarrow \phi_1 = (1/2)b_2(37+62b_2)\phi_0$ and $g_3 = -\frac{1}{12}\phi_0^2 f_3 - \frac{1}{3}\phi_1 f_2 - \frac{1}{27}\phi_1^3$.

- $\Delta_4 = 0$: $f_2 + \frac{1}{3}\phi_1^2 = \frac{1}{2}\phi_0\psi_2 \Rightarrow \psi_2 = -(1/12)b_2(-972 + 321867b_2 + 818194b_2^2 + 770316b_2^3 + 257716b_2^4)$ and $g_4 = \frac{1}{4}\psi_2^2 - \frac{1}{12}\phi_0^2 f_4 - \frac{1}{3}\phi_1 f_3$.

- $\Delta_5 = 0$: $\alpha = \mathrm{GCD}[\phi_0, \psi_2] = 1 \Rightarrow \beta = \phi_0, \phi_2 = -3\psi_2, \nu = (1/2)b_2(37 + 62b_2)$. $f_3 = -\frac{1}{3}\nu\phi_2 - 3\lambda\beta \Rightarrow \lambda = (1/72)b_2^3(358621 + 1496554b_2 + 1733688b_2^2 + 656328b_2^3)$ and $g_5 = -\frac{1}{12}\phi_0^2 f_5 - \frac{1}{3}\phi_1 f_4 + \phi_2\lambda$.

Hence, $\alpha \neq 0$ and $\beta = 0$ over the codimension-two point $\sigma = \phi_0 = 0$, which gives rise to a 3-index antisymmetric matter field. Indeed, we have to use the representations $15 \times \mathbf{6} + 1/2 \times \mathbf{20}$, as opposed to the ordinary $14 \times \mathbf{6} + 1 \times \mathbf{15}$ of $\mathfrak{su}(6)$ on -1-curves, to obtain the correct shifts of the Hodge number $h^{2,1}$ from anomaly cancellation: $\Delta h^{1,1} = 2 + 5 = 7$, and $\Delta h^{2,1} = (8 + 35) + (6 \times \mathbf{3} + 15 \times \mathbf{6} + 1/2 \times \mathbf{20} - \mathbf{3} \times \mathbf{6} \text{ (shared)}) = -57$.

The conclusion that the $\mathfrak{su}(6)^\circ$-tuning on the -1-curve leads to this exotic matter representations is not particular to this specific global model. Following the same steps, we performed a local analysis on an isolated -1 curve; when we tune the Tate form $\{0, 2, 2, 4, 6\}$ on the curve, we see that $\alpha \neq 0$ but $\beta = 0$ over a point on the curve, while the Tate form $\{0, 1, 3, 3, 6\}$ leads to $\alpha = 0$ over a point but $\beta \neq 0$. Although there is no corresponding polytope model with ordinary $\mathfrak{su}(6)$ matter in case of the global model studied above (there is no polytope in the KS database that gives a Calabi-Yau with Hodge numbers $\{18, 207\}$, and the tuning $\{0, 1, 3, 3, 6\}$ over the base (6.2) does not lead to a good global Zariski decomposition), we can contrast the two tunings of $\mathfrak{su}(6)$ on a -1-curve in polytopes that describe tunings of the generic model over the $\mathbb{F}_1$ base M:335 6 N:11 6 H:3,243. Both models

	Ordinary matter	Exotic matter
Tate form	$\{0, 1, 3, 3, 6\}$	$\{0, 2, 2, 4, 6\}$
Representations	$(16 + 2m)\mathbf{6} + (m + 2)\mathbf{15}$	$(16 + 3m + 2)\mathbf{6} + (m + 2)\frac{1}{2}\mathbf{20}$

Table 18. Representations of $\mathfrak{su}(6)$ and $\mathfrak{su}(6)^\circ$-tuning on curves of self-intersection $m \geq -2$.

exist in the KS database: the $\mathfrak{su}(6)$-tuning gives the model M:242 12 N:16 9 H:8,179 and the $\mathfrak{su}(6)^\circ$-tuning gives the model M:236 10 N:16 8 H:8,178.

The two different Tate forms of $\mathfrak{su}(6)$ automatically give different representations on all curves with self-intersection $m \geq -1$ (there is only matter in the fundamental representation on -2-curves). For example, consider tuning the generic model over $\mathbb{F}_1$ now with $\mathfrak{su}(6)$ and $\mathfrak{su}(6)^\circ$ respectively on a 0-curve. The $\mathfrak{su}(6)$-tuning gives the model with ordinary matter M:204 11 N:16 9 H:8,152 while the $\mathfrak{su}(6)$-tuning gives the model with exotic matter (two half-hypermultiplets in the $\mathbf{20}$ representation) M:197 9 N:16 8 H:8,150. The Hodge numbers from the polytope data are consistent with the calculation from anomaly cancellation with the respective matter representations (see table 18).

6.1.2 Large Hodge number shifts

Four of the "extra" Hodge number pairs in the region $h^{1,1} \geq 240$ turn out to come from standard Tate tunings of generic models that have $h^{1,1} < 220$, outside the region we considered for starting points. These are listed as "huge tunings" in table 17. These models each contain a chain of $\{-1, -4\}$s, which allows $\mathfrak{so}(n)$ with n very large to be enhanced on the -4-curves, producing huge shifts of the Hodge numbers. While there are only four specific models of this type among the 18 Hodge pairs in the region of interest not found by Tate tunings, it seems that this large tuning structure on chains of $-1, -4$ curves is a common feature and there are many other examples of this in the database, both increasing multiplicities at large Hodge numbers in cases that also have Tate tuned realizations, and also occurring at Hodge numbers outside the range of interest here.

We work out one example here in detail; the others have similar structure. The example with the largest $h^{1,1}$ (from the four "extra" models of this type) is the polytope M:20 6 N:352 7 H:261,9, which is a Tate-tuned model of the generic polytope model

$$
\begin{aligned}
\{135, 15, \{ & -12, -1, -2, -2, -3, -1, -4, -1, -4, -1, -4, -1, -4, -1, \\
& -4, -1, -4, -1, -4, -1, -4, -1, -4, -1, -4, -1, -4, -1, -4, -1, -4, \\
& -1, -4, -1, -4, -1, -4, -1, -4, -1, -3, -2, -2, -1, -12, 0 \}\},
\end{aligned} \tag{6.5}
$$

as can be determined by explicitly computing the base polytope of the toric fibration. Therefore, the enhanced tunings should give $\{\Delta h^{1,1}, \Delta h^{2,1}\} = \{126, -6\}$. Explicit analysis

of the polytope gives the data $\{m, \{a_1, a_2, a_3, a_4, a_6\}, \{f, g, \Delta\}\}$ of each m-curve

$\{\{-12, \{1, 2, 3, 4, 5\}, \{4, 5, 10\}\}, \{-1, \{1, 1, 5, 5, 0\}, \{2, 0, 0\}\},$ $\{-2, \{1, 1, 5, 5, 1\}, \{2, 1, 2\}\},$
$\{-2, \{1, 1, 5, 5, 2\}, \{2, 2, 4\}\}, \{-3, \{1, 1, 5, 5, 3\}, \{2, 3, 6\}\}, \{-1, \{1, 0, 7, 6, 1\}, \{0, 0, 1\}\},$
$\{-4, \{1, 1, 5, 5, 4\}, \{2, 3, 7\}\}, \{-1, \{1, 0, 7, 6, 3\}, \{0, 0, 3\}\}, \{-4, \{1, 1, 5, 5, 5\}, \{2, 3, 8\}\},$
$\{-1, \{1, 0, 7, 6, 5\}, \{0, 0, 5\}\}, \{-4, \{1, 1, 5, 5, 6\}, \{2, 3, 9\}\}, \{-1, \{1, 0, 7, 6, 7\}, \{0, 0, 7\}\},$
$\{-4, \{1, 1, 5, 5, 7\}, \{2, 3, 10\}\}, \{-1, \{1, 0, 7, 6, 9\}, \{0, 0, 9\}\}, \{-4, \{1, 1, 5, 5, 8\}, \{2, 3, 11\}\},$
$\{-1, \{1, 0, 7, 6, 11\}, \{0, 0, 11\}\}, \{-4, \{1, 1, 5, 5, 9\}, \{2, 3, 12\}\}, \{-1, \{1, 0, 7, 6, 12\}, \{0, 0, 12\}\},$
$\{-4, \{1, 1, 5, 5, 9\}, \{2, 3, 12\}\}, \{-1, \{1, 0, 7, 6, 12\}, \{0, 0, 12\}\}, \{-4, \{1, 1, 5, 5, 9\}, \{2, 3, 12\}\},$
$\{-1, \{1, 0, 7, 6, 12\}, \{0, 0, 12\}\}, \{-4, \{1, 1, 5, 5, 9\}, \{2, 3, 12\}\}, \{-4, \{1, 1, 5, 5, 9\}, \{2, 3, 12\}\},$
$\{-1, \{1, 0, 7, 6, 12\}, \{0, 0, 12\}\}, \{-4, \{1, 1, 5, 5, 9\}, \{2, 3, 12\}\}, \{-1, \{1, 0, 7, 6, 11\}, \{0, 0, 11\}\},$
$\{-4, \{1, 1, 5, 5, 8\}, \{2, 3, 11\}\}, \{-1, \{1, 0, 7, 6, 9\}, \{0, 0, 9\}\}, \{-4, \{1, 1, 5, 5, 7\}, \{2, 3, 10\}\},$
$\{-1, \{1, 0, 7, 6, 7\}, \{0, 0, 7\}\}, \{-4, \{1, 1, 5, 5, 6\}, \{2, 3, 9\}\}, \{-1, \{1, 0, 7, 6, 5\}, \{0, 0, 5\}\},$
$\{-4, \{1, 1, 5, 5, 5\}, \{2, 3, 8\}\}, \{-1, \{1, 0, 7, 6, 3\}, \{0, 0, 3\}\}, \{-4, \{1, 1, 5, 5, 4\}, \{2, 3, 7\}\},$
$\{-1, \{1, 0, 7, 6, 1\}, \{0, 0, 1\}\}, \{-3, \{1, 1, 5, 5, 3\}, \{2, 3, 6\}\}, \{-2, \{1, 1, 5, 5, 2\}, \{2, 2, 4\}\},$
$\{-2, \{1, 1, 5, 5, 1\}, \{2, 1, 2\}\}, \{-1, \{1, 1, 5, 5, 0\}, \{2, 0, 0\}\}, \{-12, \{1, 2, 3, 4, 5\}, \{4, 5, 10\}\},$
$\{0, \{0, 0, 0, 0, 0\}, \{0, 0, 0\}\}\}.$

The gauge algebras on -4 and -1 curves are only determined from this analysis up to monodromies. We can, however, determine the algebras without explicitly analyzing monomials. First, from the anomaly constraint analyzed in [13], $\mathfrak{su}$ cannot be adjacent to $\mathfrak{so}$, so the algebras on -1 curves have to be $\mathfrak{sp}$. The choice $\mathfrak{so}(2n-5)$ or $\mathfrak{so}(2n-4)$ on -4 is determined from global symmetry constraints. For example, it has to be $\mathfrak{so}(20)$ rather than $\mathfrak{so}(19)$ between two $\mathfrak{sp}(6)$ algebras for the global symmetry on the -4 curve to be satisfied; while the lower rank $\mathfrak{so}(17), \mathfrak{so}(19)$ has to be chosen for two -4's connecting to $\mathfrak{sp}(5)$ for the global symmetry constraint on the -1 curve to be satisfied. Hence, the corresponding gauge algebras are

$\{\{-12, \mathfrak{e}_8\}, \{-1, \cdot\}, \{-2, \cdot\}, \{-2, \mathfrak{su}(2)\}, \{-3, \mathfrak{g}_2\}, \{-1, \cdot\}, \{-4, \mathfrak{so}(9)\}, \{-1, \mathfrak{sp}(1)\},$
$\{-4, \mathfrak{so}(11)\}, \{-1, \mathfrak{sp}(2)\}, \{-4, \mathfrak{so}(13)\}, \{-1, \mathfrak{sp}(3)\}, \{-4, \mathfrak{so}(15)\}, \{-1, \mathfrak{sp}(4)\}, \{-4, \mathfrak{so}(17)\},$
$\{-1, \mathfrak{sp}(5)\}, \{-4, \mathfrak{so}(19)\}, \{-1, \mathfrak{sp}(6)\}, \{-4, \mathfrak{so}(20)\}, \{-1, \mathfrak{sp}(6)\}, \{-4, \mathfrak{so}(20)\}, \{-1, \mathfrak{sp}(6)\},$
$\{-4, \mathfrak{so}(20)\}, \{-1, \mathfrak{sp}(6)\}, \{-4, \mathfrak{so}(20)\}, \{-1, \mathfrak{sp}(6)\}, \{-4, \mathfrak{so}(20)\}, \{-1, \mathfrak{sp}(6)\}, \{-4, \mathfrak{so}(19)\},$
$\{-1, \mathfrak{sp}(5)\}, \{-4, \mathfrak{so}(17)\}, \{-1, \mathfrak{sp}(4)\}, \{-4, \mathfrak{so}(15)\}, \{-1, \mathfrak{sp}(3)\}, \{-4, \mathfrak{so}(13)\}, \{-1, \mathfrak{sp}(2)\},$
$\{-4, \mathfrak{so}(11)\}, \{-1, \mathfrak{sp}(1)\}, \{-4, \mathfrak{so}(9)\}, \{-1, \cdot\}, \{-3, \mathfrak{g}_2\}, \{-2, \mathfrak{su}(2)\}, \{-2, \cdot\},$
$\{-1, \cdot\}, \{-12, \mathfrak{e}_8\}, \{0, \cdot\}\},$

which give the correct Hodge number shifts (in particular, one can quickly check that according to the rank of the gauge algebras $\Delta h^{1,1} = 126$ as expected above).

6.1.3 Tate-tuned models corresponding to non-toric bases

We have not considered tuning an $\mathfrak{e}_8$ algebra on any curve of self-intersection $m \geq -8$, as it leads to a violation of the anomaly conditions that corresponds to the appearance of a $(4,6)$ singularity. Similarly, tunings of $\mathfrak{so}(n \geq 13)$ on -3-curves are also ruled out by anomaly cancellation. Nonetheless, there are polytope models in the KS database that appear to contain these tunings, which give rise to Hodge pairs that we have not obtained in Tate tunings of Kodaira type. This set of tunings can be understood as more complicated generalizations of the non-flat structure we have already described for fibrations over $-9, -10$ and -11 curves. As we discussed already in that context, over $(4,6)$ points the resolved fiber in the polytope model is two-dimensional, but we can understand the Calabi-Yau geometry by resolving the base at these points to obtain a corresponding flat elliptic fibration model over a blown up base that is generally non-toric. In this section we describe models that involve $\mathfrak{e}_8$ algebras tuned on -8 curves and models involving tunings of $\mathfrak{so}(n \geq 13)$ on -3-curves. In the latter case, the "extra" models in the KS database in our region of interest involve a further complication in which a nontrivial Mordell-Weil group is generated associated with an abelian U(1) factor in the F-theory gauge group; a detailed example with that additional structure is relegated to appendix C.

We begin with an example of a tuned $\mathfrak{e}_8$ on a -8-curve. This occurs in the model M:88 8 N:356 8 H:258,60. The ∇ polytope has vertices $\{(0,0,0,-1),(7,6,2,3),(-1,-1,2,3),$ $(-1,-1,1,2), (0,6,2,3), (0,0,-1,0), (-42,-36,2,3), (-15,-13,2,3)\}$. It describes a non-flat Tate-tuning of the generic elliptic fibration

$$\{252, 78, \{-12// -11// -12// -12// -12// -12// -12// -12//-8, -1, -2, -1, 0\}\}$$

where $//$ stands for $\{-1, -2, -2, -3, -1, -5, -1, -3, -2, -2, -1\}$, and there are in total 101 curves D_i in the base. There is an $\mathfrak{e}_8$ tuned on D_{97} and an $\mathfrak{su}(2)$ tuned on D_{100}, where the orders of vanishing are enhanced to $\{1,2,3,4,5\}$ and $\{0,0,1,1,2\}$, respectively. As it needs four blowups for a -8-curve to become a -12-curve, which carries the $\mathfrak{e}_8$ gauge algebra without $(4,6)$ points, we expect that there are four $(4,6)$ points on the D_{97} over which the resolved fiber become two-dimensional.

The $(4,6)$ points and the 2D fiber can be understood by an explicit analysis of the hypersurface p in equation (3.7) restricting to each irreducible component, which corresponds to a lattice point in the $\mathfrak{e}_8$ top in equation (B.2) of the non-generic toric fiber over D_{97}. Analogous to the models over Hirzebruch surfaces $\mathbb{F}_9/\mathbb{F}_{10}/\mathbb{F}_{11}$ in appendix B, we find in this case that over a generic point on the -8-curve, p intersects the 9 components in equation (B.3) that are the boundary of the 3-dimensional face in a locus comprising nine $\mathbb{P}^1$'s, which form the $\mathfrak{e}_8$ extended Dynkin diagram, but over four distinct $(4,6)$ points on D_{97}, p intersects also the whole irreducible component corresponding to $((v_{97}^{(B)})_{1,2}, 0, 0)$ (pt_5') in the top; i.e., $p|_{D_{97}} = 0$ is trivially satisfied over these four points, and the elliptic fiber over the toric base contains this irreducible component, which is two-dimensional, at these four points.

The corresponding flat elliptic fibration model has a non-toric base where the four points on D_{97} are blown up and the proper transform -12-curve intersects with the four exceptional divisor -1-curves. Now we can calculate the Hodge number shifts of the flat

n	Tate form	polytope model	top over the -3-curve
7	$\{1,1,2,2,4\}$	M:342 8 N:15 7 H:6,248	$\{pt_1'', pt_2', pt_3', pt_4'\}$
9	$\{1,1,2,3,4\}$	M:339 8 N:16 7 H:7,247	$\{pt_1'', pt_2'', pt_3', pt_4'\}$
10	$\{1,1,2,3,5\}$	M:332 10 N:17 8 H:8,242	$\{pt_1'', pt_2'', pt_3', pt_4', pt_5'\}$
11	$\{1,1,3,3,5\}$	M:328 8 N:18 7 H:8,242	$\{pt_1'', pt_2'', pt_3', pt_4'', pt_5'\}$
12	$\{1,1,3,3,6\}$	M:318 10 N:19 8 H:9,233	$\{pt_1'', pt_2'', pt_3', pt_4'', pt_5', pt_6'\}$

Table 19. Polytope tunings of M:348 5 N:12 5 H:5,251 (generic model over $\mathbb{F}_3$): $\mathfrak{so}(n)$-tunings on the -3-curve with $n < 13$. These are flat elliptic fibration models, where the Hodge numbers can be directly calculated from the anomaly cancellation conditions.

elliptic fibration model via anomaly cancellation: $\Delta T = 4$ (each blowup contributes one additional tensor multiplet), $\Delta r = (8 - 7) + 1$, $\Delta V = (248 - 133) + 3$, and $\Delta H_c = 10 \times \mathbf{2}$; therefore, by equations (2.6) and (2.7), $\Delta h^{1,1} = 6$ and $\Delta h^{2,1} = -18$, which gives $\{252, 78\} + \{6, -18\} = \{258, 60\}$, as needed.

The remaining four Hodge pairs corresponding to standard $\mathbb{P}^{2,3,1}$-fibered polytopes at large $h^{1,1}$ that were missed in our Tate tuning set have a combination of two novel features: they have apparent $\mathfrak{so}(n \geq 13)$ tunings on -3 curves, and also have extra sections associated with a nontrivial Mordell-Weil rank and corresponding U(1) factors in the F-theory physics. For clarity, we delegate a complete example of one of the "extra" models of this type to appendix C, and focus in the rest of this section on the issue of $\mathfrak{so}(n \geq 13)$-tunings on -3-curves in the context of simpler models with relatively small $h^{1,1}$ that do not also involve the U(1) issue.

As mentioned above, $\mathfrak{so}(n)$-tunings on -3-curves give rise to $(4,6)$ singularities and two-dimensional resolved fibers when $n \geq 13$. While the anomaly conditions impose an upper bound of $n = 12$ for $\mathfrak{so}(n)$-tunings over -3-curves, there is no bound on -4-curves from anomaly conditions [13]. Therefore, in these cases the corresponding flat elliptic fibration models can be obtained by resolving the -3-curves to -4-curves that support $\mathfrak{so}(n \geq 13)$ without suffering from (4,6) points.

We start with a generic polytope model over the Hirzebruch surface $\mathbb{F}_3$, M:348 5 N:12 5 H:5,251, and perform successive tunings of $\mathfrak{so}(n)$ on the -3-curve. For $7 \leq n \leq 12$, all these polytope tunings, except $\mathfrak{so}(8)$,[16] give a model in the KS database as expected, and the Hodge numbers of these polytope models agree with the Hodge numbers calculated from anomalies. We list these polytope models in table 19. Note that the tuning from $\mathfrak{so}(10)$ to $\mathfrak{so}(11)$ is a rank-preserving tuning (see table 1), so the Hodge numbers for these cases are identical.

Consider now the $\mathfrak{so}(13)$ polytope tuning on the -3-curve. This also gives a reflexive polytope, M:312 8 N:20 7 H:10,232, which is still of the standard $\mathbb{P}^{2,3,1}$-fibered form over the $\mathbb{F}_3$ base. But this is a non-flat elliptic fibration. In fact, we know immediately from the Hodge numbers that there is some additional subtlety in this tuning. Naively, $\mathfrak{so}(12)$ to $\mathfrak{so}(13)$ would be a rank-preserving tuning, and, as for the $\mathfrak{so}(10)$ to $\mathfrak{so}(11)$ tuning, in

---

[16]We do not expect tuned $\mathfrak{so}(8)$ in reflexive polytope models; see section 4.6 for discussion.

the absence of other issues these should have the same Hodge numbers, but they clearly do not. An explicit analysis shows that over a generic point on the -3-curve, the hypersurface equation intersects with seven components associated with the seven lattice points $\{pt_1', pt_1'', pt_2'', pt_3', pt_4'', pt_6', pt_6''\}$ in the $\mathfrak{so}(13)$ top in a locus containing $\mathbb{P}^1$'s which form the $\mathfrak{so}(13)$ extended Dynkin diagram, and there is a $(4,6)$ point on the -3-curve, over which the fiber contains the whole irreducible component associated with the lattice point pt_5' in the top.

Again, we can calculate the Hodge numbers by considering the corresponding flat elliptic fibration model over the base where the $(4,6)$ point on the -3-curve is blown up. This blow-up produces an exceptional -1-curve that intersects the proper transform -4-curve, and which can support any $\mathfrak{so}(n)$ tunings without producing $(4,6)$ points. Therefore, $\Delta h^{1,1} = \Delta T + \Delta r = 1 + (6-2) = 5$ and $\Delta h^{2,1} = \Delta V - 29\Delta T - \Delta H_c = (78-8) - 29 - 5 \times (\mathbf{13}-\mathbf{1}) = -19,^{[17]}$ which agrees with $\{10, 232\} - \{5, 251\}$.

In the flat elliptic fibration model over the resolved base, as we keep increasing the $\mathfrak{so}(n)$ tuning, an additional gauge factor $\mathfrak{sp}(m)$ is forced to arise on the exceptional -1-curve starting at $n = 17$: a simple local analysis shows that tuning $\mathfrak{so}(n)$ on a -4-curve forces $\mathfrak{sp}(\lceil n/4 \rceil - 4)$ on an intersecting -1-curve. The forced $\mathfrak{sp}(m)$ is not apparent in the (f, g, Δ) of the polytope model, which is the non-flat model over the original $\mathbb{F}_3$ base where the -1-curve does not exist. But we have to carefully consider this forced gauge algebra on the exceptional -1-curve in computing the Hodge numbers from the anomaly equations (2.1) and (2.5). For example, tuning $\mathfrak{so}(22)$ on the -3-curve gives rise to the model M:179 10 N:29 8 H:17,143. The corresponding flat fibration model has a -4-curve intersecting an exceptional -1-curve replacing the -3-curve, and the $\mathfrak{so}(22)$ is tuned on the -4-curve, which forces an $\mathfrak{sp}(2)$ on the -1-curve. Therefore, the shifts of the Hodge numbers are $\Delta h^{1,1} = \Delta T + \Delta r = 1 + ((11-2)+2) = 12$ and $\Delta h^{2,1} = \Delta V - 29\Delta T - \Delta H_c = ((231-8)+10) - 29 - (14 \times \mathbf{22} + 12 \times \mathbf{4} - 1/2 \times 22 \times 4 \text{ (shared)}) = -108$, which agree with the Hodge numbers from the polytope. The Hodge numbers of the polytope models from the successive tunings can be calculated this way up to $\mathfrak{so}(26)$, at which point all monomials in a_6 are tuned off, and a U(1) global factor comes into play. See appendix C for an explicit analysis of one of the models associated with the missing Hodge pairs where such a U(1) becomes relevant. We list the non-flat polytope models of tuning $\mathfrak{so}(n)$, $13 \le n < 26$, over the -3 curve of $\mathbb{F}_3$ in table 20.

6.2 Weierstrass models from non-standard $\mathbb{P}^{2,3,1}$-fibered polytopes

For the remaining eight Hodge pairs with large $h^{1,1}$ in the KS database that were missed by our Tate construction (see table 17), the CY hypersurface equations (3.7) with suitable homogeneous coordinates cannot be in Tate form, although the ∇ polytopes are still $\mathbb{P}^{2,3,1}$ fibered. The failure to be in the Tate form arises from the feature that there are lattice

---

[17]Note that although the representations of $\mathfrak{so}(13)$ tuning on an -4-curve are $5 \times \mathbf{13}$, the components that are charged under the Cartan are $5 \times (\mathbf{13}-\mathbf{1})$ (the Cartan subgroup of SO(2N + 1) is the same as SO(2N)). As $\mathfrak{so}(13)$ is a rank-preserving tuning of $\mathfrak{so}(12)$, we can also do the calculation as if it were a $\mathfrak{so}(12)$ tuning, in which case $\Delta h^{1,2} = \Delta V - 29\Delta T - \Delta H_c = (66-8) - 29 - 4 \times \mathbf{12} = -19$. The two Hodge number shifts are the same.

n	polytope model	{2D component, $(4,6)$ point}
13	M:312 8 N:20 7 H:10,232	$\{\{pt'_5,\ c_3b_1 + c_4b_3\}\}$
14	M:299 10 N:21 8 H:11,221	$\{\{pt'_5,\ c_4b_1 + c_5b_3\}\}$
15	M:292 8 N:22 7 H:11,221	$\{\{pt'_5,\ c_3b_1 + c_4b_3\}\}$
16	M:276 10 N:23 8 H:12,206	$\{\{pt'_5,\ c_4b_1 + c_5b_3\}\}$
17	M:267 8 N:24 7 H:13,205	$\{\{pt'_5,\ c_3b_1 + c_4b_3\},\{pt'_8,\ c_3b_1 + c_4b_3\}\}$
18	M:248 10 N:25 8 H:14,188	$\{\{pt'_5,\ c_4b_1 + c_5b_3\},\{pt'_8,\ c_4b_1 + c_5b_3\}\}$
19	M:238 8 N:26 7 H:14,188	$\{\{pt'_5,\ c_3b_1 + c_4b_3\},\{pt'_8,\ c_3b_1 + c_4b_3\}\}$
20	M:216 10 N:27 8 H:15,167	$\{\{pt'_5,\ c_4b_1 + c_5b_3\},\{pt'_8,\ c_4b_1 + c_5b_3\}\}$
21	M:204 8 N:28 7 H:16,166	$\{\{pt'_5,\ c_3b_1 + c_4b_3\},\{pt'_8,\ c_3b_1 + c_4b_3\},$ $\{pt'_{11},\ c_3b_1 + c_4b_3\}\}$
22	M:179 10 N:29 8 H:17,143	$\{\{pt'_5,\ c_4b_1 + c_5b_3\},\{pt'_8,\ c_4b_1 + c_5b_3\},$ $\{pt'_{11},\ c_4b_1 + c_5b_3\}\}$
23	M:166 8 N:30 7 H:17,143	$\{\{pt'_5,\ c_3b_1 + c_4b_3\},\{pt'_8,\ c_3b_1 + c_4b_3\},$ $\{pt'_{11},\ c_3b_1 + c_4b_3\}\}$
24	M:138 8 N:31 7 H:18,116	$\{\{pt'_5,\ c_3b_1 + c_4b_3\},\{pt'_8,\ c_3b_1 + c_4b_3\},$ $\{pt'_{11},\ c_3b_1 + c_4b_3\}\}$
25	M:123 6 N:32 6 H:19,115	$\{\{pt'_5,\ c_2b_1 + c_3b_3\},\{pt'_8,\ c_2b_1 + c_3b_3\},$ $\{pt'_{11},\ c_2b_1 + c_3b_3\},\{pt'_{14},\ c_2b_1 + c_3b_3\}\}$

Table 20. Polytope tunings of M:348 5 N:12 5 H:5,251 (generic model over $\mathbb{F}_3$): $\mathfrak{so}(n)$-tunings on the -3-curve with $13 \leq n < 26$. These are non-flat elliptic fibration models. The last column gives the $(4,6)$ points and the corresponding 2D toric fiber components contained in the hypersurface CY (see table 8 for pt in tops). The Hodge numbers can be calculated from the associated flat elliptic fibration model over the non-toric base where the $(4,6)$-point are blown up.

points in Δ that give rise to non-trivial base dependence in the coefficients of the monomials x^3 or y^2; i.e., these should be sections of non-trivial line bundles over the base.

These ∇ polytopes do not the form of standard $\mathbb{P}^{2,3,1}$-fibered polytopes that we have defined in section 3.4, although they still have $\mathbb{P}^{2,3,1}$ fibers. We refer to such polytopes as *non-standard* $\mathbb{P}^{2,3,1}$-fibered polytopes. In fact, the feature of having base-dependent terms in x^3 or y^2 is equivalent to being a non-standard $\mathbb{P}^{2,3,1}$-fibered polytope. Geometrically this feature corresponds to the condition that there is only a single lattice point in Δ that projects to each of the vertices associated with these monomials. We prove this equivalence as follows: without loss of generality, we choose a coordinate system such that the three vertices of the $\mathbb{P}^{2,3,1}$ subpolytope ∇_2 are as given in equation (3.12), and such that the projection matrix to the base is $\pi = \{\{1,0,0,0\},\{0,1,0,0\},\{0,0,0,0\},\{0,0,0,0\}\}$. Therefore, the set of the vertices of the dual subpolytope Δ_2 is $\{(-2,1),(1,-1),(1,1)\}$, and the lattice points in Δ are all in one of the forms in the set $\{(\_,\_,1,-1),(\_,\_,-2,1),(\_,\_,0,0),(\_,\_,-1,1),(\_,\_,1,0),(\_,\_,0,1),(\_,\_,1,1)\}$. Let us first show the forward direction: we already showed in section 3.4 that the standard $\mathbb{P}^{2,3,1}$-fibered polytope construction in the coordinates given

in (3.13) gives a dual polytope Δ that contains at most the single points corresponding to $\mathcal{O}(0)$ at the vertices $(-2, 1), (1, -1)$ associated with the y^2, x^3 terms (assuming that the base is compact), and both of these points must be present for the polytope Δ to contain the origin as an interior point. Thus, any standard $\mathbb{P}^{2,3,1}$-fibered polytope can be put in a coordinate system where it has only the points $(0, 0, -2, 1)$ and $(0, 0, 1, -1)$ that project to $(-2, 1)$ and $(1, -1)$ in Δ_2. We can prove the backward direction as follows: assume there is only a single lattice point in Δ taking each of the forms $(\_, \_, -2, 1)$ and $(\_, \_, 1, -1)$. There is always a linear transformation that leaves the last two coordinates fixed that moves these to the points $(0, 0, -2, 1)$ and $(0, 0, 1, -1)$; this linear transformation will also leave the form of the fiber fixed as (3.12). The presence of these two points in Δ shows that every lattice point $(v_{i,1}^{(B)}, v_{i,2}^{(B)}, \xi, \eta)$ has coordinates ξ, η that satisfy $\eta \leq \xi + 1, \eta \geq 2\xi - 1$. For each ray in the base, however, the presence of any such lattice point imposes conditions on the points in Δ over each of the points other than $(-2, 1)$ and $(1, -1)$ that are at least as strong as those imposed by the ray $(v_{i,1}^{(B)}, v_{i,2}^{(B)}, 2, 3)$; the conditions over these two points can be weaker, but as long as there is only the one point $(0, 0, -2, 1)$, $(0, 0, 1, -1)$ over these two points in the dual fiber, the ray $(v_{i,1}^{(B)}, v_{i,2}^{(B)}, 2, 3)$ will be included in the polytope. Thus, for each ray in the base $(v_{i,1}^{(B)}, v_{i,2}^{(B)}, 2, 3) \in \nabla$ in this coordinate system. This proves that the presence of a single lattice point of each of the forms $(\_, \_, -2, 1)$ and $(\_, \_, 1, -1)$ implies that the polytope ∇ has the form of a standard $\mathbb{P}^{2,3,1}$-fibered polytope.

We would like to have a Weierstrass description of the non-standard $\mathbb{P}^{2,3,1}$-fibered polytopes so that we can use the methodology of F-theory to understand and analyze the geometry. To this end, we treat the $\mathbb{P}^{2,3,1}$ fiber as a twice blown up $\mathbb{P}^{1,1,2}$ fiber, as depicted in figure 5a; following the procedure in appendix A of [31] to obtain the Weierstrass model of the associated Jacobian fibration model of a $\mathbb{P}^{1,1,2}$-fibered polytope, we can obtain similarly that of the blownup $\mathbb{P}^{1,1,2}$-fibered polytope. Note that because even non-standard $\mathbb{P}^{2,3,1}$-fibered polytopes give elliptic Calabi-Yau hypersurfaces that have a global section, the Jacobian fibration should have the same geometry as the original Calabi-Yau hypersurface; this would not be true for example if the original elliptic fibration had no section [33]. Explicitly in coordinates, instead of treating the elliptic fiber as being embedded in the $\mathbb{P}^{2,3,1}$ ambient fiber with $v_x = (0, 0, -1, 0), v_y = (0, 0, 0, -1)$, $v_z = (0, 0, 2, 3)$, we treat the $\mathbb{P}^{2,3,1}$ fiber as a blownup $\mathbb{P}^{1,1,2}$, and embed the elliptic fiber in this blownup $\mathbb{P}^{1,1,2}$ ambient fiber with $v_x = (0, 0, -1, 0), v_y = (0, 0, 0, -1)$, $v_z = (0, 0, 1, 2)$. The blowup rays of $\mathbb{P}^{1,1,2}$ reflect the fact that two of the nine sections of a $\mathbb{P}^{1,1,2}$-fibered polytope model are completely tuned off (see figure 5b) — the hypersurface equation of a non-standard $\mathbb{P}^{2,3,1}$-fibered polytope is a specialization of that of a generic $\mathbb{P}^{1,1,2}$-fibered polytope, and the blowups of the $\mathbb{P}^{1,1,2}$ fiber resolve the singularities of the tunings.

The Weierstrass models obtained in this way from non-standard $\mathbb{P}^{2,3,1}$-fibered polytopes have the novel feature that they can have gauge groups tuned over non-toric curves in the base. Moreover, unlike the toric curves, which are always genus zero curves (isomorphic to $\mathbb{P}^1$), non-toric curves can be of higher genus, and this class of global Weierstrass models gives examples of tunings of gauge groups over higher genus curves in the bases. As a check on this picture, we can verify that the Hodge numbers of these Weierstrass models calculated from anomaly cancellation match with those of the polytope data.
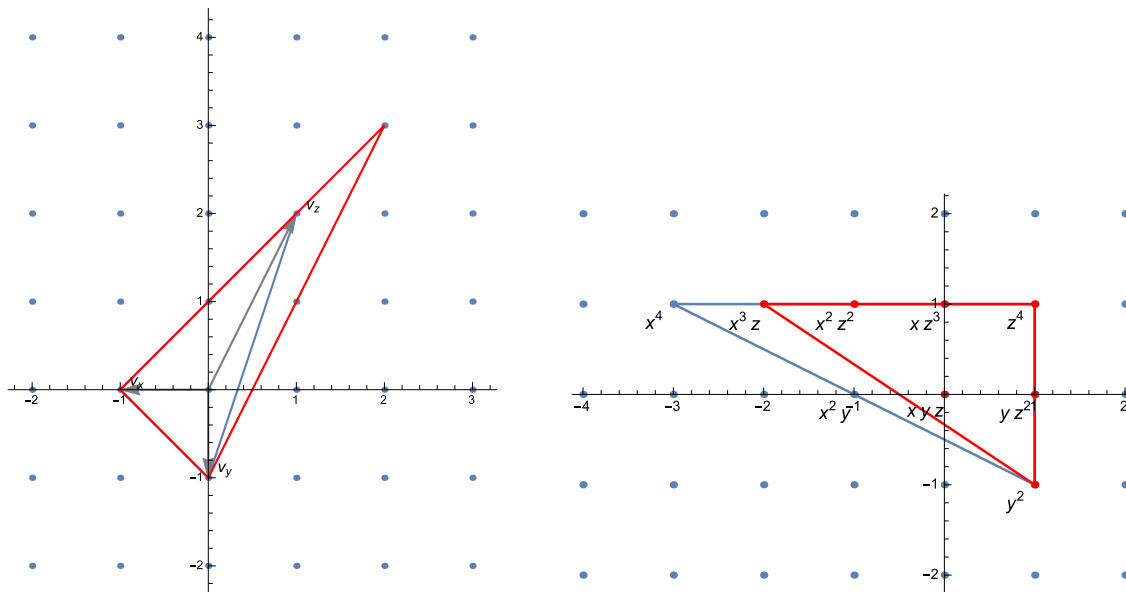
(a) Comparing the polytopes for $\mathbb{P}^{2,3,1}$ (red) and $\mathbb{P}^{1,1,2}$ (blue). The red triangle ∇_{231} comes from blowing up the (fiber) fan of ∇_{112} twice (cf. indicated rays in figure 1a for standard $\mathbb{P}^{2,3,1}$-fibered polytopes).

(b) The blue triangle Δ_{112} is the dual of ∇_{112} and the red triangle Δ_{231} is the dual of ∇_{231}. The monomials in different sections are categorized by projection to the different lattice points in Δ_{112}, labeled in terms of the homogeneous coordinates x, y, z in the fiber. The equations describing the hypersurface Calabi-Yau for a non-standard $\mathbb{P}^{2,3,1}$ polytope can be characterized as tunings for a $\mathbb{P}^{1,1,2}$-fibered polytope, in which there are no nonzero monomials in the sections labeled x^4 and x^2y. This interpretation allows the possibility of having sections in y^2 or x^3.

Figure 5. The reflexive polytope pairs for the $\mathbb{P}^{1,1,2}$ ambient toric fiber (in blue) and the $\mathbb{P}^{2,3,1} = \text{Bl}_2\mathbb{P}^{1,1,2}$ ambient toric fiber (in red).

We give some examples of Weierstrass models from non-standard $\mathbb{P}^{2,3,1}$-fibered polytopes in the following subsections. In section 6.2.1, we give a simple example that illustrates the non-toric curve enhancement feature. In section 6.2.2, we analyze the eight remaining polytope data with large $h^{1,1}$ from the KS database that were missing in the Tate-tuned construction. We also give some further examples of interesting geometries from the KS database at smaller Hodge numbers to illustrate the unusual nature of the non-standard $\mathbb{P}^{2,3,1}$-fibered polytope construction. In section 6.2.3, we give a model with an $\mathfrak{su}(2)$ tuning on a non-toric curve of genus one in the base.

6.2.1 A warmup example

As an illustration of the two different types of $\mathbb{P}^{2,3,1}$-fibered polytopes, we contrast the two polytopes in the KS database associated with Calabi-Yau threefolds having Hodge numbers $\{8, 250\}$: M:346 8 N:16 7 H:8,250 and M:345 8 N:17 7 H:8,250.

The second $\nabla_{2\mathrm{nd}}$ polytope is a standard $\mathbb{P}^{2,3,1}$-fibered polytope, with vertices (in the standard coordinates) $\{(0,0,-1,0), (-1,-4,2,3), (0,-2,1,2), (0,1,2,3), (1,0,1,2), (1,0,2,3), (0,0,0,-1)\}$. This is a Tate-tuned model over the base $\mathbb{F}_4$, with $\mathfrak{so}(9) \oplus \mathfrak{sp}(1)$ enhanced on the -4-curve and the 0-curve $\{b_2 = 0\}$. The base rays are $\{(0,1), (1,0), (0,-1), (-1,-4)\}$, and in particular, $\{(0,1,2,3),(1,0,2,3),(0,-1,2,3),(-1,-4,2,3)\}$ are lattice points. This polytope can be obtained by tuning the $\Delta_{\mathfrak{so}(8)}$ polytope of either one of the $\mathfrak{so}(8)$ KS models (a generic elliptic fibration over $\mathbb{F}_4$) by requiring the vanishing orders with respect to the coordinate $b_2 \leftrightsquigarrow (1,0,2,3)$ to be $\{0,0,1,1,2\}$ and those for the coordinate $b_3 \leftrightsquigarrow (0,-1,2,3)$ to be $\{1,1,2,3,4\}$. The $\nabla_{2\mathrm{nd}}$ polytope, which is then the dual of the reduction of the $\Delta_{\mathfrak{so}(8)}$ polytope, has an $\mathfrak{so}(9)$ top over the base ray $(0,-1)$ and an $\mathfrak{sp}(1)$ top over $(1,0)$.

The first $\nabla_{1\mathrm{st}}$ polytope is, on the other hand, of a non-standard $\mathbb{P}^{2,3,1}$-fibered form. The data of this polytope can be obtained by removing the vertex $(1,0,2,3)$ from $\nabla_{2\mathrm{nd}}$ or equivalently by adding the lattice point $(-1,0,-2,1)$ to $\Delta_{2\mathrm{nd}}$, which becomes a vertex of $\Delta_{1\mathrm{st}}$. The one lattice point reduction of $\nabla_{2\mathrm{nd}}$ corresponds to the one lattice point enhancement of $\Delta_{2\mathrm{nd}}$. Let us now show explicitly that $\nabla_{1\mathrm{st}}$ is a non-standard $\mathbb{P}^{2,3,1}$-fibered polytope and check that it satisfies each of the two equivalent conditions (i.e., the absence of an appropriate preimage of the base in ∇ and the condition that Δ has lattice points associated with monomials in x^3 or y^2 that have base dependence): the base rays of $\nabla_{1\mathrm{st}}$ are the same as those of $\nabla_{2\mathrm{nd}}$, but the ray $(1,0)$ lacks the preimage $(1,0,2,3)$ that we have removed; instead, the base ray $(1,0)$ comes from the projection of the 4D ray $(1,0,1,2)$; nonetheless $\nabla_{1\mathrm{st}}$ still has $\mathbb{P}^{2,3,1}$ as a subpolytope, and therefore $\nabla_{1\mathrm{st}}$ is a non-standard $\mathbb{P}^{2,3,1}$-fibered polytope. The equivalent condition for a non-standard $\mathbb{P}^{2,3,1}$-fibered polytope is also satisfied from the Δ point of view: let us associate base coordinates $\{b_1, b_2, b_3, b_4\}$ to the set of 4D rays $\{(0,1,2,3),(1,0,1,2),(0,-1,2,3),(-1,-4,2,3)\}$, and calculate the set of monomials. The two lattice points $(-1,0,-2,1),(0,0,-2,1)$ give monomials of the form x^3 with base-dependent coefficients, $b_4 x^3$ and $b_2 x^3$ respectively.

Although we do not have a Weierstrass model from a Tate form for this polytope, we instead have a Weierstrass form for the hypersurface in the $\mathrm{Bl}_2\mathbb{P}^{1,1,2}$-fibered polytope (where we have substituted some generic $\mathbb{Z}$ values in the complex structure moduli):

$$
\begin{aligned}
f = {} & 1/48 b_3^2 (-1009274573279509056 + 346222371062059303350000 b_3 \\
& - 2745890658512627779075253906 25 b_3^2 \cdots - 528582381600 b_3^6 b_4^{22} \\
& - 22258660320 b_3^6 b_4^{23} + 388841808 b_3^6 b_4^{24}),
\end{aligned}
$$
$$
\begin{aligned}
g = {} & -(1/864) b_3^3 (344205633835899813888000 \\
& + 192654770654227763688364004147200 b_3 \cdots + 6291082311776640 b_3^9 b_4^{35} \\
& + 27125536688271 b_3^9 b_4^{36}),
\end{aligned}
$$
$$
\begin{aligned}
\Delta = {} & 19683/2 b_3^7 (35 b_2 + 24 b_4)^2 (109370724968448 b_1^{17} b_2^2 \\
& + 588208065199776 b_1^{16} b_2^6 b_3 + 1344055426083360 b_1^{15} b_2^{10} b_3^2 \\
& + \cdots + 681083735457852 b_2 b_3^{17} b_4^{69} + 217077176379771 b_3^{17} b_4^{70}).
\end{aligned}
$$

According to this analysis, there is an $\mathfrak{so}(9)$ enhancement on the -4-curve ($b_3 = 0$) and an $\mathfrak{sp}(1)$ enhancement on the non-toric 0-curve $\{35b_2 + 24b_4 = 0\}$. Note that this non-toric curve is a (rational) 0-curve because it is in the same class as the two toric 0-curves. The curve supporting the $\mathfrak{sp}(1)$ algebra intersects both the -4- and the 4-curve at one point. This is essentially the same configuration as the second model, so the Hodge numbers from an anomaly calculation also give the same result, $\{8, 250\}$, in both cases. While in this case, the non-toric curve supporting the $\mathfrak{sp}(1)$ can be trivially transformed into a toric curve by a simple linear change of variables, this is not the case in the more complicated examples that we consider in the later subsections.

6.2.2 The eight remaining missing cases at large $h^{1,1}$

Now let us come back to the polytopes of the eight Hodge pairs in the large $h^{1,1}$ region that we did not obtain through Tate tunings and that have non-standard $\mathbb{P}^{2,3,1}$ fibration structure. We go through one example in detail; the others have similar structure.

As a specific example, we consider the polytope M:65 8 N:357 8 H:261,45. The vertex set of Δ is

$$\{(-3, -3, 1, 1), (0, 0, -2, 1), (1, -7, 1, 1), (-3, 1, 1, 1), (-1, 1, -1, 1), (0, 1, 1, 1),$$
$$(-1, 1, 1, -1), (0, 0, 1, -1)\}, \quad (6.6)$$

where both the lattice points in the second line contribute to a y^2 term but with base dependence. Performing the projection we find that ∇ is a non-standard $\mathbb{P}^{2,3,1}$-fibered polytope over the base

$$\{-12// -11// -12// -12// -12// -12// -12// -12// -9, -1, -2, -2, -1, 0\}. \quad (6.7)$$

There are in total 102 base rays, and all rays but $v^{(B)}_{i=98,99,100,101}$ have a preimage of the form $(\_, \_, 2, 3)$.

The generic Weierstrass model over this base has the Hodge numbers $\{257, 77\}$, so the tunings must be such that the shifts are $\{4, -32\}$. We analyze the Weierstrass model of the non-standard $\mathbb{P}^{2,3,1}$ polytope; as in the preceding example we treat ∇ as a Bl_2 $\mathbb{P}^{1,1,2}$-fibered polytope (in particular, the fiber coordinates are associated to $\{v_x, v_y, v_z\} = \{(0,0,-1,0), (0,0,0,-1), (0,0,1,2)\}$), and find the associated tuned Weierstrass model. The resulting computation of $\{f, g, \Delta\}$ shows that

- Over the toric curve $D_{100} \equiv \{b_{100} = 0\}$ the vanishing order is enhanced to $\{0, 0, 2\}$, which corresponds to an $\mathfrak{su}(2)$ gauge symmetry on the -2-curve.

- Over the non-toric curve $D_{\text{non-toric}} \equiv \{b_{\text{non-toric}} = 0\}$, where

$$\begin{aligned}
b_{\text{non-toric}} = {} & c_7 b_{100} b_{101} b_{98} b_{99} \\
& + c_6 b_1 b_{10}^{22} b_{11}^{29} b_{12}^{36} b_{13}^{7} b_{14}^{41} b_{15}^{34} b_{16}^{27} b_{17}^{20} b_{18}^{33} b_{19}^{13} b_{2}^{12} b_{20}^{32} b_{21}^{19} b_{22}^{25} b_{23}^{31} b_{24}^{37} b_{25}^{6} b_{26}^{35} b_{27}^{29} b_{28}^{23} b_{29}^{17} b_{3}^{11} b_{30}^{28} b_{31}^{11} \\
& b_{32}^{27} b_{33}^{16} b_{34}^{21} b_{35}^{26} b_{36}^{31} b_{37}^{5} b_{38}^{29} b_{39}^{24} b_{4}^{10} b_{40}^{19} b_{41}^{14} b_{42}^{23} b_{43}^{9} b_{44}^{22} b_{45}^{13} b_{46}^{17} b_{47}^{21} b_{48}^{25} b_{49}^{4} b_{5}^{9} b_{50}^{23} b_{51}^{19} b_{52}^{15} b_{53}^{11} b_{54}^{18} \\
& b_{55}^{7} b_{56}^{17} b_{57}^{10} b_{58}^{13} b_{59}^{16} b_{6}^{17} b_{60}^{19} b_{61}^{3} b_{62}^{17} b_{63}^{14} b_{64}^{11} b_{65}^{8} b_{66}^{13} b_{67}^{5} b_{68}^{12} b_{69}^{7} b_{7}^{8} b_{70}^{9} b_{71}^{11} b_{72}^{13} b_{73}^{2} b_{74}^{11} b_{75}^{9} b_{76}^{7} b_{77}^{5} \\
& b_{78}^{8} b_{79}^{3} b_{8}^{23} b_{80}^{7} b_{81}^{4} b_{82}^{5} b_{83}^{6} b_{84}^{7} b_{85} b_{86}^{5} b_{87}^{4} b_{88}^{3} b_{89}^{2} b_{9}^{15} b_{90}^{3} b_{91} b_{92}^{2} b_{93} b_{94} b_{95} b_{96}, \quad (6.8)
\end{aligned}$$

the vanishing order is enhanced to $\{0, 0, 3\}$, which corresponds to an $\mathfrak{su}(3)$ gauge symmetry on the non-toric curve. In this expression, c_i are constant coefficients, while b_k are the variables associated with toric divisors D_k. Note that the non-toric curve intersects the two toric curves $\{b_{102} = 0\}$ and $\{b_{97} = 0\}$ (b_{102} and b_{97} are the only coordinates that do not appear in equation (6.8), and there are no intersections between the divisors associated with the variables in the first and second terms). As in the preceding example, this non-toric curve is a 0-curve, and is linearly equivalent to the combination of curves $D_{98} + D_{99} + D_{100} + D_{101}$, as can be seen from the first term in (6.8). The complicated combination of powers in the second term in (6.8) arise from the structure of the toric rays and the sequence of blow-ups needed to build those rays from a fiber of a minimal model Hirzebruch base.

- Over the curve $D_{97} \equiv \{b_{97} = 0\}$ (a -9-curve), there is a two-dimensional resolved fiber; due, however, to the enhancement over the non-toric curve intersecting the -9-curve, there are some differences between the fiber structure over this -9-curve and the one in an isolated -9-curve such as we discussed in section 4.7 (see also appendix B): the top is the same as that in equation (B.2), so the 9 components that are the boundary of the 3-dimensional face intersect with the CY over a generic point in the -9-curve in a locus of $\mathbb{P}^1$s that compose the extended E_8 Dynkin diagram, just as in equation (B.3). However, as opposed to having three distinct $(4, 6)$-points, as occur in the isolated -9-curve, there is only one $(4, 6)$ point. Over this point the CY intersects the four irreducible components interior to the 3-face (while in the previous case, there is only one irreducible component that intersects the CY)

$$S = \{(-3, -3, 1, 2), (-2, -2, 1, 2), (-1, -1, 1, 2), (-1, -1, 0, 1)\}. \tag{6.9}$$

Explicitly,

$$
\begin{aligned}
p|_I = {} & c_7 b_{100} b_{101} b_{98} b_{99} \\
& + c_6 b_1 b_{10}^{22} b_{11}^{29} b_{12}^{36} b_{13}^{7} b_{14}^{41} b_{15}^{34} b_{16}^{27} b_{17}^{20} b_{18}^{33} b_{19}^{13} b_2^{12} b_{20}^{32} b_{21}^{19} b_{22}^{25} b_{23}^{31} b_{24}^{37} b_{25}^{6} b_{26}^{35} b_{27}^{29} b_{28}^{23} b_{29}^{17} b_3^{11} b_{30}^{28} b_{31}^{11} \\
& b_{32}^{27} b_{33}^{16} b_{34}^{21} b_{35}^{26} b_{36}^{31} b_{37}^{5} b_{38}^{29} b_{39}^{24} b_4^{10} b_{40}^{19} b_{41}^{14} b_{42}^{23} b_{43}^{9} b_{44}^{22} b_{45}^{13} b_{46}^{17} b_{47}^{21} b_{48}^{25} b_{49}^{4} b_5^{9} b_{50}^{23} b_{51}^{19} b_{52}^{15} b_{53}^{11} b_{54}^{18} \\
& b_{55}^{7} b_{56}^{17} b_{57}^{10} b_{58}^{13} b_{59}^{16} b_6^{17} b_{60}^{19} b_{61}^{3} b_{62}^{17} b_{63}^{14} b_{64}^{11} b_{65}^{8} b_{66}^{13} b_{67}^{5} b_{68}^{12} b_{69}^{7} b_7^{8} b_{70}^{9} b_{71}^{11} b_{72}^{13} b_{73}^{2} b_{74}^{11} b_{75}^{9} b_{76}^{7} b_{77}^{5} \\
& b_{78}^{8} b_{79}^{3} b_8^{23} b_{80}^{7} b_{81}^{4} b_{82}^{5} b_{83}^{6} b_{84}^{7} b_{85}^{5} b_{86}^{4} b_{87}^{3} b_{88}^{2} b_{89}^{15} b_9^{3} b_{90}^{3} b_{91} b_{92}^{2} b_{93} b_{94} b_{95} b_{96}, \forall I \in S.
\end{aligned}
\tag{6.10}
$$

Moreover, by comparing equations (6.8) and (6.10), we know that the $(4, 6)$ point is exactly at the intersection of the divisors $\{b_{97} = 0\}$ and $\{b_{\text{non-toric}} = 0\}$.

We now find the associated flat elliptic fibration model, so that we can use F-theory techniques to compute the Hodge number shifts. We first identify the resolved base, which is semi-toric, and then determine the tunings. Since there is the only one $(4, 6)$ point, we blow up successively three times at this point to turn the -9-curve into a -12-curve, and the non-toric 0-curve is replaced by a chain of curves of self-intersection numbers $-1, -2, -2, -1$ (similar to the last graph of the Hodge pair $\{14, 404\}$ in table 15). The divisor classes of
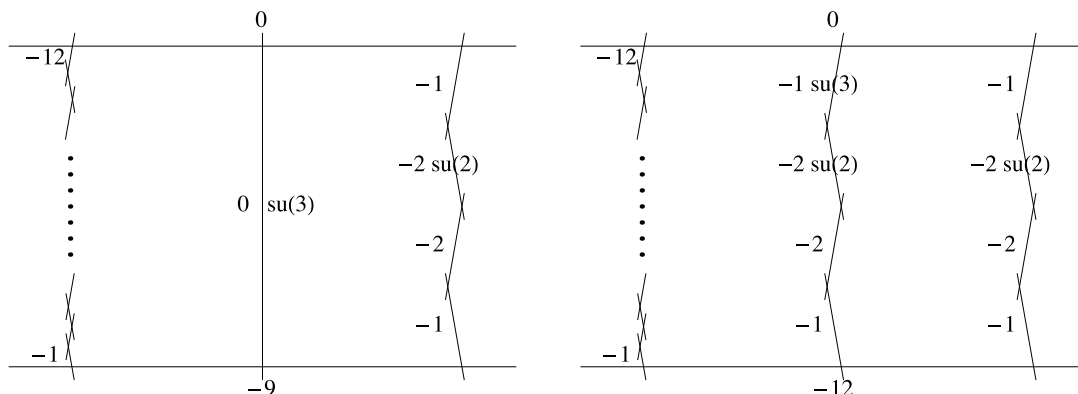
Figure 6. The base of the example with Hodge numbers $\{261, 45\}$. Left: before resolution. Right: after resolving $(4,6)$ points in the base. The top curve is D_{102} and the bottom curve is $\tilde{D}_{97}$. The curves in the left chain from top to down are in the order $\{D_1, D_2, \ldots, D_{96}\}$, in the middle chain $\{\tilde{D}_{\text{non-toric}}, \tilde{E}_1, \tilde{E}_2, E_3\}$, in the right chain $\{D_{101}, D_{100}, D_{99}, D_{98}\}$.

the curves after the blow-up process can be determined in the usual fashion: the -12-curve $\tilde{D}_{97}$ is the proper transform of the -9-curve after the three blowups

$$\tilde{D}_{97} = D_{97} - E_1 - E_2 - E_3, \tag{6.11}$$

where E_1, E_2, E_3 are the exceptional divisors associated with the three blowups. The proper transform of the non-toric curve is

$$\tilde{D}_{\text{non-toric}} = D_{\text{non-toric}} - E_1, \tag{6.12}$$

which is a -1-curve. The three curves, $-2, -2, -1$, connecting $\tilde{D}_{97}$ and $\tilde{D}_{\text{non-toric}}$ are respectively

$$\tilde{E}_1 = E_1 - E_2, \ \ \tilde{E}_2 = E_2 - E_3, \ \ \text{and } E_3. \tag{6.13}$$

Now we figure out the gauge symmetries on these divisors. There was an $\mathfrak{su}(3)$ on the 0-curve, $D_{\text{non-toric}}$, which is now on the -1-curve, $\tilde{D}_{\text{non-toric}}$. This forces an $\mathfrak{su}(2)$ on the -2-curve, $\tilde{E}_1$, connecting to $\tilde{D}_{\text{non-toric}}$. The configuration of the intersecting curves and the symmetry enhancements are drawn in figure 6.

Remarkably, the described configuration gives the correct counting of the shifts in Hodge numbers through the anomaly calculation. The contributions to $h^{1,1}$ and $h^{2,1}$ from the tunings through equations (2.6) and (2.7) are

- $\mathfrak{su}(2)$ on D_{100}: $\Delta h^{1,1} = \Delta r = +1$ and $\Delta h^{2,1} = \Delta V - \Delta H_{\text{charge}} = 3 - 4 \times \mathbf{2} = -5$.

- $\mathfrak{su}(2) \oplus \mathfrak{su}(3)$ on $\{\tilde{E}_1, \tilde{D}_{\text{non-toric}}\}$: $\Delta h^{1,1} = +1 + 2$ and $\Delta h^{2,1} = (3 + 8) - (12 \times \mathbf{3} + 4 \times \mathbf{2} - \mathbf{2} \times \mathbf{3} \text{ (shared)}) = -27$.

The total gives the desired Hodge number shifts $\{\Delta h^{1,1}, \Delta h^{2,1}\} = \{4, -32\}$. Note that the final Hodge numbers correspond to the flat elliptic fibration over the non-toric base, and correctly reflect the associated contribution of three tensor multiplets from the three

blow-ups of the base.[18] The correspondence between the non-flat and the flat models may be considered as that the four irreducible components of the 2-dimensional fiber over the $(4, 6)$ point transform to the three divisors resolving the -9-curve in the base and one divisor in the fiber to resolve the forced $\mathfrak{su}(2)$ on $\tilde{E}_1$.

We now consider the remaining non-standard $\mathbb{P}^{2,3,1}$ fibered "extra" cases at large $h^{1,1}$. The model associated with Hodge numbers $\{245, 57\}$ has a gauge symmetry that is enhanced on the non-toric curve, but there are no $(4, 6)$ singularities involved, which is similar to the example in 6.2.1; we must, however, be careful to properly include the shared matter contribution to the matter multiplets, as a curve intersecting the non-toric curve also carries a gauge symmetry. The models with Hodge numbers $\{261, 51\}$, $\{260, 62\}$, $\{260, 54\}$, $\{259, 55\}$, $\{258, 84\}$, and $\{254, 56\}$ are all similar to that of $\{261, 45\}$ that we have treated in detail here.

We conclude the discussion of these cases by briefly summarizing the details of the model M:82 10 N:351 10 H:254,56, where we need to include one extra tensor multiplet in the Hodge number counting.

- generic model (total 100 toric curves in the base)

$$\{251, 79, \{-12// -11// -12// -12// -12// -12// -12// -12, \qquad (6.14)$$
$$-1, -2, -2, -3, -1, -5, -1, -3, -2, -1, -7, -1, -2, -1, 0\}\}$$

- one $(4, 6)$ point on the -7-curve D_{96}.

- gauge symmetry enhancements

  1. $\mathfrak{su}(2)$ on the -2-curve D_{98}

  2. $\mathfrak{su}(2)$ on the non-toric 0-curve $D_{\text{non-toric}}$ intersecting the 0-curve D_{100} and the -7-curve D_{96} at the $(4, 6)$ point.

The corresponding flat elliptic fibration model has

- base structure:
  The $(4, 6)$ is blown up. D_{96} is resolved into a -8-curve $\tilde{D}_{96} = D_{96} - E_1$ and $D_{\text{non-toric}}$ into $\tilde{D}_{\text{non-toric}} = D_{\text{non-toric}} - E_1$, where E_1 is the exceptional divisor of the blowup.

- enhanced gauge symmetries:

  1. $\mathfrak{su}(2)$ on the -2-curve D_{98}, which shifts $h^{1,1}$ by $r(\mathfrak{su}(2)) = 1$ and $h^{2,1}$ by $V(\mathfrak{su}(2)) - H_{\text{charged}}(\mathfrak{su}(2)$ on -2-curve$) = 3 - 4 \times \mathbf{2} = -5$.

  2. $\mathfrak{su}(2)$ on the -1-curve $\tilde{D}_{\text{non-toric}}$, which shifts $h^{1,1}$ by $r(\mathfrak{su}(2)) = 1$ and $h^{2,1}$ by $V(\mathfrak{su}(2)) - H_{\text{charged}}(\mathfrak{su}(2)$ on -1-curve$) = 3 - 10 \times \mathbf{2} = -17$.

---

[18]The Hodge numbers denoted in a generic model containing a $-9/-10/-11$-curve are understood to be those of the flat elliptic fibration over the base that has been resolved at the (4,6) points.

- Hodge numbers

  1. contributions from the enhanced gauge symmetries $\Delta h^{1,1} = 1 + 1 = 2, \Delta h^{2,1} = -5 - 17 = -22$

  2. contribution from the tensor multiplet associated with the one extra blowup in the base $\Delta h^{1,1} = 1, \Delta h^{2,1} = -29$

  3. compensation of $\Delta h^{2,1} = \frac{1}{2}\mathbf{56} = 28$ due to the fact that there are half-hyper multiplets $\frac{1}{2}\mathbf{56}$ on the NHC -7-curve, but there are no localized matter fields on the NHC -8-curve.

In total we have $h^{1,1} = 251 + 2 + 1 = 254$ and $h^{2,1} = 79 - 22 - 29 + 28 = 56$, which agree with the Hodge numbers of the polytope model.

6.2.3 Example: a model with a tuned genus one curve in the base

In the final part this section we consider an additional non-standard $\mathbb{P}^{2,3,1}$-fibered models that has the further interesting feature that a gauge group is tuned on a non-toric curve that has nonzero genus. While this phenomenon does not occur in the "extra" models at large Hodge numbers that we have focused on here, the fact that this non-toric tuning structure can arise even in the context of toric hypersurface Calabi-Yau constructions seems sufficiently interesting and novel that we provide some details for understanding the structure of models of this type.

We study in particular a model with an $\mathfrak{su}(2)$ tuning on a non-toric curve of genus one in the base: M:223 7 N:10 6 H:3,165. The vertex set of Δ is

$$\{((-1,-1,-2,1),(2,-1,-2,1),(-1,2,-2,1),(-4,-4,1,1),(8,-4,1,1), \\ (-4,8,1,1),(0,0,1,-1))\}, \qquad (6.15)$$

where the first three lattice points contribute to a x^3 term with base dependence. Then ∇ is a non-standard $\mathbb{P}^{2,3,1}$-fibered polytope over $\mathbb{P}^2$. The base rays are

$$\{(1,0),(0,1),(-1,-1)\} \leftrightsquigarrow \{b_1,b_2,b_3\}, \qquad (6.16)$$

which come from the projection of the 4D rays $\{(1,0,1,2),(0,1,1,2),(-1,-1,1,2)\}$ (in fact, these are the only three lattice points in ∇ that do not project to $(0,0)$, so none of the preimages are in the form $((v^{(B)})_{1,2},2,3)$.)

We analyze the Weierstrass model of the non-standard $\mathbb{P}^{2,3,1}$ polytope: treating ∇ again as the Bl$_2$ $\mathbb{P}^{1,1,2}$-fibered polytope (in particular, the fiber coordinates are associated to $\{v_x,v_y,v_z\} = \{(0,0,-1,0),(0,0,0,-1),(0,0,1,2)\}$) we find the associated tuned Weierstrass model. The orders of vanishing of $\{f,g,\Delta\}$ are enhanced to $\{0,0,2\}$ on the curve in the base $D_{\text{non-toric}} \equiv \{I_{\mathfrak{su}(2)} = 0\}$, where

$$I_{\mathfrak{su}(2)} = c_1 b_1^3 + c_{179} b_2 b_3^2 + c_{180} b_2^2 b_3 + c_{181} b_1 b_3^2 + c_{182} b_1 b_2 b_3 \\ + c_{183} b_1 b_2^2 + c_{184} b_1^2 b_3 + c_{185} b_1^2 b_2 + c_2 b_2^3 + c_3 b_3^3. \qquad (6.17)$$

In particular, the result for the discriminant Δ is

$$\Delta = I_{\mathfrak{su}(2)}^2 I_1, \tag{6.18}$$

where the I_1 component of Δ is a degree 30 polynomial in the homogeneous coordinates. Note that $D_{\text{non-toric}}$ is a smooth curve of genus one, which can be calculated by the formula (2.22)

$$3[b_1] \cdot (3[b_1] - ([b_1] + [b_2] + [b_3])) = 0 = 2g - 2 \Rightarrow g = 1. \tag{6.19}$$

We calculate Hodge numbers from the anomaly conditions: the matter representations of $\mathfrak{su}(2)$ on a $g = 1$ curve of self-intersection $D_{\text{non-toric}}^2 = 9$ is $54 \times \mathbf{2} + \mathbf{3}$ [13], but only two components of the adjoint representation $\mathbf{3}$ are charged under the Cartan (see the footnote in section 2.1). Therefore, $H_{\text{charged}} = 108 + 2 = 110$. Then $h^{1,1} = \Delta r = 1$ and $h^{2,1} = \Delta V - H_{\text{charged}} = 3 - 110 = -107$, which agree with $\{3, 165\} - \{2, 272\} = \{+1, -107\}$.

7 Conclusions

7.1 Summary of results

In this paper we have carried out a systematic comparison of elliptic Calabi-Yau threefolds with large Hodge numbers that are realized by tuning Tate-form Weierstrass models over toric bases and those that are realized as hypersurfaces in toric varieties through the Batyrev construction. Specifically, we have considered a class of Tate-tuned models over toric bases that have nonabelian gauge groups tuned over toric divisors. These tunings give a specific class of "standard" $\mathbb{P}^{2,3,1}$-fibered reflexive polytopes, all of which give Calabi-Yau threefolds with Hodge numbers that appear in the Kreuzer-Skarke database.

- Almost all Hodge number pairs of known CY3's in the regime studied come from elliptically fibered Calabi-Yau threefolds associated with polytopes constructed in this fashion that are associated with an explicit Tate/Weierstrass construction of the restricted class that we considered in our initial analysis.

- We have explicitly analyzed the structure of the Calabi-Yau threefolds in the Kreuzer-Skarke database for the 18 Hodge number pairs not found in our initial analysis from Tate constructions. All of these admit elliptic fibrations of slightly more complicated forms.

- Thus, we have found explicit realizations of elliptic Calabi-Yau threefolds that produce all Hodge number pairs with $h^{1,1} \geq 240$ or $h^{2,1} \geq 240$ that are known to be possible for Calabi-Yau threefolds. This matches with the results of a companion paper [20] showing that all polytopes in the KS database giving Calabi-Yau threefolds with $h^{1,1} \geq 150$ or $h^{2,1} \geq 150$ have a genus one fibration, and have an elliptic fibration whenever $h^{1,1} \geq 195$ or $h^{2,1} \geq 228$. These results provide additional evidence that virtually all known Calabi-Yau threefolds with large Hodge numbers are elliptically fibered, building on a variety of other recent work that has led to similar observations [12–19]. Since the number of elliptic Calabi-Yau threefolds is finite, this in turn

suggests that the number of distinct topological classes of Calabi-Yau threefolds is in fact finite.

- In the course of this analysis we have encountered some novel structures in the Tate/Weierstrass tunings needed to reproduce certain CY3's associated with polytopes in the KS database. This has led to new insights into the Tate algorithm as well as in the structure of fibrations that may occur through polytopes.

  - A novel Tate tuning of SU(6) gives rise to exotic 3-index antisymmetric matter, of a form recently studied in [30, 62].

  - Some polytopes in the KS database correspond to tunings of very large gauge algebras with components like $\mathfrak{so}(20)$.

  - Polytopes in the KS database include non-flat elliptic fibrations over toric bases that resolve into flat elliptic fibrations over more complicated non-toric bases including not only blow-ups of $-9, -10, -11$ curves, but also more exotic structure such as an $\mathfrak{e}_8$ over a -8 curve that must be blown up four times, or tunings of $\mathfrak{so}(n), n \geq -13$ on -3 curves that must be blown up to -4 curves to satisfy anomaly conditions. In some of the $\mathfrak{so}(n)$ cases the resolved geometry also gives rise to a nontrivial Mordell-Weil group associated with a U(1) factor in the gauge group.

  - Some polytopes in the KS database have elliptic fibrations over toric bases in which nonabelian gauge algebras are tuned over non-toric curves in the base.

  - We worked out the tops associated with the gauge algebras $\mathfrak{so}(n), 13 \leq n \leq 25$, as well as the tops associated with gauge algebras $\mathfrak{su}(n), 7 \leq n \leq 13$. For $\mathfrak{so}(n)$, these match the tops found in [22] after an appropriate linear transformation; our construction gives explicit realizations of these tops in reflexive polytopes for the range of algebras listed, which is not guaranteed from the construction of [22]. The tops associated with I_n and I_n^* types have the feature that they develop along the fiber direction, and the projection to the fiber plane falls outside the $\mathbb{P}^{2,3,1}$ fiber subpolytope. Another interesting feature of the $\mathfrak{so}(n)$ tops is that there can be multiple distinct tops for certain gauge algebras, corresponding to monodromy conditions on the associated Tate tunings.

7.2 Possible extensions of this work

In the companion paper [20], we carry out a complementary analysis to that of this paper. Here we have started from the Tate tuning picture and matched to data in the Kreuzer-Skarke database. One can instead start with the polytopes in the database and try to derive the elliptic fibration structure. This is essentially the approach taken by Braun in [31], in which the database was scanned for elliptic fibrations over the base $\mathbb{P}^2$. In [20], we take that point of view and analyze the fibration structure of the polytopes in the KS database directly. The approach taken in this paper, however, shows that at large Hodge numbers most Calabi-Yau threefolds have a standard elliptic fibration structure;

the "sieve" approach taken here enables us to identify some of the most interesting cases that present novel features.

There are several closely related analyses that could be carried out that we have not done here or in [20]; each of these represents an opportunity for further work that would give increased understanding of the set of Calabi-Yau threefolds, the role of elliptic fibrations, and the landscape of 6D F-theory models.

First, we have started from the point of view of tuning Tate models and used the output of that analysis to match Hodge numbers in the KS database. In principle, we could have tried to reproduce all the polytopes in the database, i.e. included multiplicity information. For reasons discussed in section 4.7, this would be a more complicated analysis. In many cases there are multiple local Tate tunings that give equivalent gauge groups, and we have in each case systematically taken only the lowest possible choice for NHCs and the lowest order choice with no further monodromy condition required for a given gauge group tuning. For bases with many toric divisors, the number of combinatorial possibilities of local tunings can become quite large. There are also many equivalent models that correspond to carrying out explicitly different subsets of toric blow-ups to partially resolve (4, 6) singularities. We have checked in some cases that the multiplicity of Hodge numbers in the KS database is reproduced by distinct Tate/Weierstrass tunings of elliptic fibrations, but we have not approached this systematically. This would be a natural next step for this kind of analysis, and might reveal additional novel structures for the elliptic fibrations found in the KS database.

Second, we have restricted to large Hodge numbers in part because we have only focused on Tate models associated with the most generic $\mathbb{P}^{2,3,1}$ fiber structure for the polytope. There are 16 distinct possible toric fibers, analyzed in detail in the F-theory context in [23, 31, 57], each leading to a distinct class of Weierstrass tuning types with characteristic nonabelian and abelian gauge structure, and in principle we could systematically analyze all tunings that correspond to each of the different fiber types. This would be necessary to extend the analysis of this paper systematically to smaller Hodge numbers, where the other fiber types become prevalent [20]. We leave such an endeavor for future work. It would also be interesting to see whether the more general class of fibers considered in [64] may give further insights into other Weierstrass tuning types that may be possible with complete intersection fibers.

Acknowledgments

A Standard $\mathbb{P}^{2,3,1}$-fibered polytope tuning

In this appendix, we go through the details of a standard $\mathbb{P}^{2,3,1}$-fibered polytope tuning with an example of polytopes for elliptic fibrations with tuned $\mathfrak{su}_3, \mathfrak{g}_2$ over the curve of self-intersection -2 in the Hirzebruch surface base $\mathbb{F}_2$.

Standard $\mathbb{P}^{2,3,1}$-fibered polytopes naturally correspond to Tate (tuned) models. In principle, as long as the Tate tunings on adjacent curves do not lead to $(4,6)$ singularities,[19] and are not merely further specialization of existing tunings that do not change the gauge algebra,[20] removing the lattice points corresponding to a given tuning gives a different reflexive polytope, associated with the resolved CY of the tuned singular model. The Hodge numbers of the new resolved polytope model can be computed either directly from the polytopes or through F-theory by anomaly cancellation.

As an example, consider tuning a type I_3^s $\mathfrak{su}(3)$ gauge algebra on the -2 curve in the base $\mathbb{F}_2$. The polytope model for the generic CY is M:335 5 N:11 5 H:3,243, of which the set of vertices of ∇ is

$$\{(1,0,2,3),(0,1,2,3),(-1,-2,2,3),(0,0,-1,0),(0,0,0,-1)\}, \tag{A.1}$$

and the set of vertices of Δ is

$$\{(-6,-6,1,1),(0,0,-2,1),(18,-6,1,1),(0,0,1,-1),(-6,6,1,1)\}. \tag{A.2}$$

The projection along the fiber gives the rays in the base $\{v_i^{(B)}\} = \{(1,0), (0,1), (-1,-2), (0,-1)\}$ corresponding to curves of self-intersection $\{0,2,0,-2\}$. We calculate the hypersurface equation (3.7) and take the set of homogeneous coordinates $\{z_j\} = \{x,y,z,b_4\}$ associated respectively to rays v_x, v_y, v_z in the fiber plane and $(v_{B4}^{(1)}, v_{B4}^{(2)}, 2, 3)$ in the base plane to get

$$y^2 + a_1 xyz + a_3 yz^3 = x^3 + a_2 x^2 z^2 + a_4 xz^4 + a_6 z^6, \tag{A.3}$$

where the 5 sections a_i in the coordinates b_4 and some second coordinate ζ in the base have the forms

$$a_1(b_4, \zeta) = a_{1,0}(\zeta) + a_{1,1}(\zeta)b_4 + a_{1,2}(\zeta)b_4^2, \tag{A.4}$$

$$a_2(b_4, \zeta) = a_{2,0}(\zeta) + a_{2,1}(\zeta)b_4 + a_{2,2}(\zeta)b_4^2 + a_{2,3}(\zeta)b_4^3 + a_{2,4}(\zeta)b_4^4, \tag{A.5}$$

$$a_3(b_4, \zeta) = a_{3,0}(\zeta) + a_{3,1}(\zeta)b_4 + \cdots + a_{3,5}(\zeta)b_4^5 + a_{3,6}(\zeta)b_4^6, \tag{A.6}$$

$$a_4(b_4, \zeta) = a_{4,0}(\zeta) + a_{4,1}(\zeta)b_4 + \cdots + a_{4,7}(\zeta)b_4^7 + a_{4,8}(\zeta)b_4^8, \tag{A.7}$$

$$a_6(b_4, \zeta) = a_{6,0}(\zeta) + a_{6,1}(\zeta)b_4 + \cdots + a_{6,11}(\zeta)b_4^{11} + a_{6,12}(\zeta)b_4^{12}. \tag{A.8}$$

The numbers of monomials (lattice points) in the sections a_i are $\{9, 25, 49, 81, 169\}$; together with the two points associated with x^3 and y^2 these compose the total set of 335 lattice points in the M polytope Δ. The number of monomials in each section can be further divided according to the power of the monomials in the b_4 expansion. According to Tate table 4, the vanishing orders have to reach $\{0, 1, 1, 2, 3\}$ in b_4 to tune an I_3^s $\mathfrak{su}(3)$ over D_{B4}, so all lattice points contributing to $a_{2,0}, a_{3,0}, a_{4,0}, a_{4,1}, a_{6,0}, a_{6,1}, a_{6,2}$ should be

---

[19]Although in some cases such $(4,6)$ singularities still lead to reflexive polytopes that can be associated with flat elliptic fibrations over blown-up bases, as encountered in the examples of section 6.1.3.

[20]None of the lattice points corresponding to such further specialization are vertices of Δ, so removing those points does not affect the polytope.

removed. As one can check those are

$$a_{2,0} \leftrightarrow \{(-2,2,-1,1)\}, \tag{A.9}$$

$$a_{3,0} \leftrightarrow \{(-3,3,1,0)\}, \tag{A.10}$$

$$a_{4,0} \leftrightarrow \{(-4,4,0,1)\}, \tag{A.11}$$

$$a_{4,1} \leftrightarrow \{(-4,3,0,1),(-3,3,0,1),(-2,3,0,1)\}, \tag{A.12}$$

$$a_{6,0} \leftrightarrow \{(-6,6,1,1)\}, \tag{A.13}$$

$$a_{6,1} \leftrightarrow \{(-6,5,1,1),(-5,5,1,1),(-4,5,1,1)\}, \tag{A.14}$$

$$a_{6,2} \leftrightarrow \{(-6,4,1,1),(-5,4,1,1),(-4,4,1,1),(-3,4,1,1),(-2,4,1,1)\}. \tag{A.15}$$

After reduction, the vertex set of the new dual polytope Δ' for the tuned model becomes

$$\{(-6,-6,1,1),(0,0,-2,1),(18,-6,1,1),(0,0,1,-1),(-6,3,1,1), \tag{A.16}$$

$$(-3,2,1,0),(-1,1,0,0),(-1,2,1,0),(0,3,1,1)\}. \tag{A.17}$$

This new polytope is again reflexive, and corresponds to the example M:320 9 N:13 7 H:5,233 in the KS database. Comparing the two sets of data (for the generic and tuned models), the difference in the number of lattice points of the monomial polytopes Δ and Δ', $335 - 320 = 15$, is the number of the lattice points being removed. On the other hand, the fan polytope is enlarged $\nabla \to \nabla'$, and the increased number N, $13 - 11 = 2$, comes from lattice points $\{(0, -1, 1, 1), (0, -1, 1, 2)\}$, which together with the affine node $(0, -1, 2, 3)$ form exactly the $\mathfrak{su}(3)$ top. The Hodge shifts $\{5, 233\} - \{3, 243\} = \{2, -10\}$ match exactly with the calculation from anomalies for tuning the algebra $\mathfrak{su}(3)$ on an isolated -2-curve.

There are two polytopes in the KS database with Hodge numbers $\{5, 233\}$. The other polytope M:316 6 N:14 6 H:5,233 is the polytope arising from an enhancement to a $\mathfrak{g}_2$ gauge algebra by further removing from the $\mathfrak{su}(3)$ model

$$a_{1,0} \leftrightarrow \{(-1,1,0,0)\}, \tag{A.18}$$

$$a_{3,1} \leftrightarrow \{(-3,2,1,0),(-1,2,1,0),(-2,2,1,0)\}; \tag{A.19}$$

so that the vanishing orders along the -2-curve becomes $\{1, 1, 2, 2, 3\}$, and the number of lattice points in Δ (M) decreases by 4. Comparing the fan polytope of the $\mathfrak{g}_2$ tuning model to that of the generic model, there are three more lattice points $\{(0, -2, 2, 3), (0, -1, 1, 1), (0, -1, 1, 2)\}$, which together with $(0, -1, 2, 3)$ form the $\mathfrak{g}_2$ top. The Hodge numbers are the same as those of the $\mathfrak{su}(3)$ model, since $\mathfrak{su}(3) \to \mathfrak{g}_2$ is a rank-preserving tuning (section 2.1).

B Elliptic fibrations over the bases $\mathbb{F}_9, \mathbb{F}_{10}$, and $\mathbb{F}_{11}$

The "standard stacking" construction (section 4) of a polytope for a standard $\mathbb{P}^{2,3,1}$-fibered model over a base surface containing $-9, -10, -11$-curves produces a flat toric fibration that leads to a hypersurface that is a non-flat elliptic fibration. There are $(4, 6)$-points in the $-9, -10, -11$-curves where the fiber becomes two-dimensional; the singular fiber is resolved into an irreducible component of the non-generic toric fiber, which is two-dimensional, as

the hypersurface CY equation restricting to the component is trivially satisfied over these points. For a flat elliptic fibration, the $(4,6)$-points in the base must be blown up, which in general leads to a non-toric base. Note that in the Calabi-Yau hypersurface picture, some flops may be necessary before the blow-ups can be done in the toric picture [31]. Nonetheless, this provides a clear correspondence between the non-flat elliptic fibrations associated with polytopes leading to $(4,6)$ points in the base and flat elliptic fibrations over blown up bases, which provide Calabi-Yau threefolds with the same Hodge numbers. In this appendix we go through the details of these constructions for the Hirzebruch surface bases $\mathbb{F}_m, m = 9, 10, 11$.

The flat toric fibration of M:560 6 N:26 6 H:14,404 gives a non-flat elliptic fibration model over the toric base $\mathbb{F}_{m=9}$. The vertices of the ∇ polytope are

$$\{((0, 0, -1, 0), (0, -6, 2, 3), (-1, -m, 2, 3), (1, 0, 2, 3), (0, 1, 2, 3), (0, 0, 0, -1))\}. \tag{B.1}$$

We associate the base coordinates $\{b_1, b_2, b_3, b_4\}$ to the toric curves $\{0, -m, 0, m\}$ whose corresponding rays in the base are $\{(1, 0), (0, -1), (-1, -m), (0, 1)\}$. The set of lattice points in the top over the $-m$-curve is given by the set of lattice points in ∇ of the form $(0, a, x, y)$,

$$\begin{aligned}
\{&(0, -6, 2, 3), (0, -5, 2, 3), (0, -4, 1, 2), (0, -4, 2, 3), (0, -3, 1, 1), (0, -3, 1, 2), \\
&(0, -3, 2, 3), (0, -2, 0, 1), (0, -2, 1, 1), (0, -2, 1, 2), (0, -2, 2, 3), (0, -1, 0, 0), \\
&(0, -1, 0, 1), (0, -1, 1, 1), (0, -1, 1, 2), (0, -1, 2, 3)\}. \tag{B.2}
\end{aligned}$$

Each of these points represents an irreducible component of the 2-dimensional non-generic toric fiber over the $-m$-curve $\{b_2 = 0\}$ and projects to the corresponding base ray $(0, -1)$. Over a generic point on the $-m$ curve, the hypersurface CY, p given by equation (3.7), intersects with only the irreducible components on the boundary of the top giving a $\mathbb{P}^1$ for each, which combine to form the E_8 affine Dynkin diagram. These nine components are

$$\begin{aligned}
\{&((0, -6, 2, 3), (0, -5, 2, 3), (0, -4, 2, 3), (0, -3, 2, 3), (0, -2, 2, 3), (0, -1, 2, 3), \\
&\qquad\qquad (0, -4, 1, 2), (0, -2, 0, 1), (0, -3, 1, 1)\}, \tag{B.3}
\end{aligned}$$

where the set of components in first line forms the longest leg of the diagram, and the sets $\{(0, -6, 2, 3), (0, -4, 1, 2), (0, -2, 0, 1)\}$ and $\{(0, -6, 2, 3), (0, -3, 1, 1)\}$ form the other two legs. $((0, -6, 2, 3)$ is the node where three legs connect, and $(0, -1, 2, 3)$ is the affine node.)

However, p also intersects the full irreducible component $(0, -1, 0, 0)$ over three points in the $-m$-curve, but does not meet the component over the other points: p restricted to the divisor $I = (0, -1, 0, 0)$ is

$$p|_I = b_2^5(c_4 b_1^3 + c_{284} b_1^2 b_3 + c_{285} b_1 b_3^2 + c_3 b_3^3) b_4^7, \tag{B.4}$$

where c_3, c_4, c_{284}, and c_{285} are some complex structure moduli. This vanishes identically over the three points $\{c_4 b_1^3 + c_{284} b_1^2 b_3 + c_{285} b_1 b_3^2 + c_3 b_3^3 = 0\}$ in the $-m$-curve (I projects to the ray of the $-m$-curve), and is otherwise a constant. It is these three points in the toric

base that must be blown up to give the -12-curve and the semi-toric base over which the elliptic fibration model becomes flat and gives a good model for F-theory compactification.

Similarly, the flat toric fibrations of M:600 6 N:26 6 H:13,433 and M:640 6 N:26 6 H:12,462 give non-flat elliptic fibration models over the toric bases $\mathbb{F}_{m=10}$ and $\mathbb{F}_{m=11}$, respectively. Both vertex sets are given by equation (B.1), and the tops over the $-m$-curves are the same as that over the -9 curve in equation (B.2). We know that a -10-curve (resp. a -11-curve) would need two blowups (resp. one blowup) to become a -12-curve, so we expect there are two $(4,6)$ points (resp. one point) in the $-m$-curve over which the resolved fiber is two-dimensional. Indeed, we calculate the CY hypersurface in equation (3.7), and restrict it on each component in (B.2), and we find

$$p|_I = b_2^5(c_4 b_1^2 + c_{305} b_1 b_3 + c_3 b_3^2) b_3 b_4^7 \tag{B.5}$$

in the case of $m = 10$, and

$$p|_I = b_2^5(c_4 b_1 + c_3 b_3) b_4^7 \tag{B.6}$$

in the case of $m = 11$. Over a generic point in the $-m$-curve, $p|_I$ is non-vanishing, and p intersects with the nine components in (B.3), each giving a $\mathbb{P}^1$ that corresponds to a node in the extended E_8 Dynkin diagram.

The correspondence between the non-flat and the flat models may be thought of as encoding the relationship between the irreducible component of the 2-dimensional fiber over a $(4,6)$ point and divisors that resolve the $-m$-curve to a -12-curve in the base.

C An example with a nonabelian tuning that forces a U(1) factor

In this appendix, we work through the details of an example of the missing Hodge pairs in the last part of table 17: M:47 11 N:362 11 H:263,32. This example involves huge tunings, a blow-up from an $\mathfrak{so}(n)$ tuning on a -3 curve, and the further feature of a forced nontrivial Mordell-Weil group giving a U(1) factor. After describing the geometry, we do a detailed calculation of the Hodge numbers through the associated flat elliptic fibration model.

The rational sections of an elliptic fibration form the Mordell-Weil group, which is a finitely generated group of the form $\mathbb{Z}^{\mathrm{rank}} \times$ (torsion subgroup). If an elliptically fibered Calabi-Yau has a non-trivial Mordell-Weil rank, the F-theory compactification on it has an abelian sector $U(1)^{\mathrm{rank}}$ [7]. The Weierstrass model of an elliptically fibered Calabi-Yau automatically comes with a zero section $z = 0$. Additional sections can be produced through constraints in the toric geometry [23]. For instance, an abelian global $\mathfrak{u}(1)$ symmetry is forced when we set all the monomials in the section a_6 to vanish (the condition $a_6 = 0$ in [36].) While this can be simply imposed as a constraint to tune a U(1) factor, this condition can also be imposed when we tune a large enough set of nonabelian gauge algebras on the toric curves. The lack of the monomials in a_6 occurs in this way in the four missing Hodge pairs $\{263, 32\}, \{251, 35\}, \{247, 35\}, \{240, 37\}$ in table 17, which are therefore $\mathrm{Bl}_{[0,0,1]}\mathbb{P}^{2,3,1}$-fibered polytope models (see figure 7).

The ∇ polytope of M:47 11 N:362 11 H:263,32 is $\mathrm{Bl}_{[0,0,1]}\mathbb{P}^{2,3,1}$-fibered over the base

$$\{-4, -1, -3, -1, -4, -1, -4, -1, -4, 0, 2\}. \tag{C.1}$$
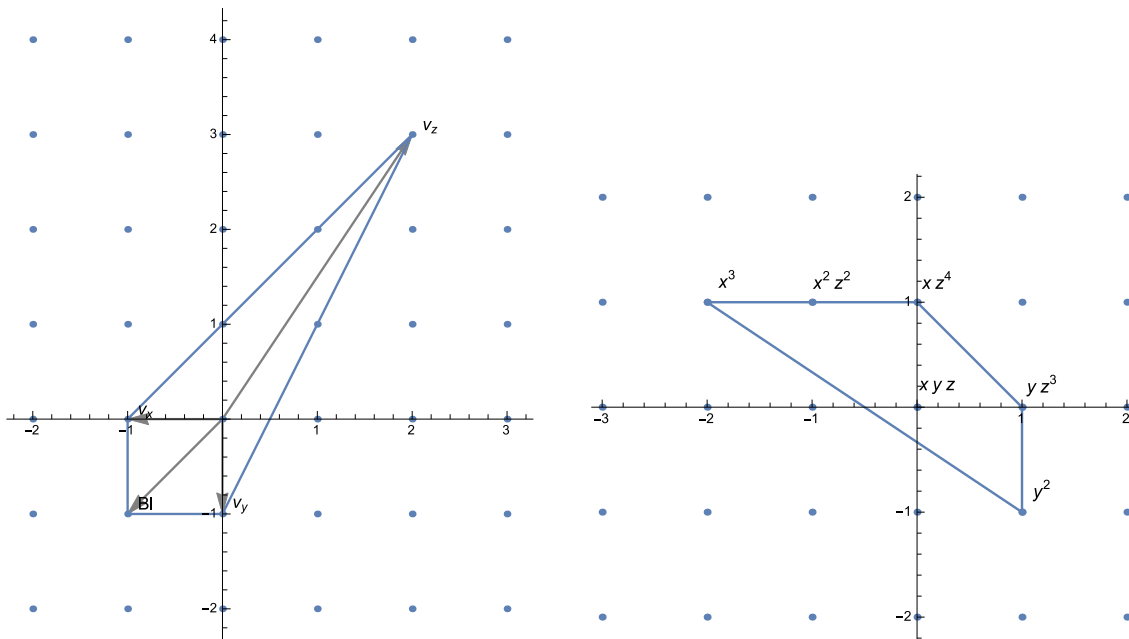
(a) ∇_2: the additional ray blown up from $\mathbb{P}^{2,3,1}$ resolves $\mathfrak{u}(1)$-tuned models.

(b) Δ_2: all monomials in the section a_6 are removed in the tuning, which leads to a global $\mathfrak{u}(1)$ factor in $\mathrm{Bl}_{[0,0,1]}\mathbb{P}^{2,3,1}$-fibered polytopes.

Figure 7. The reflexive polytope pair for the $\mathrm{Bl}_{[0,0,1]}\mathbb{P}^{2,3,1}$ ambient toric fiber.

The generic model over this base has Hodge numbers $\{28, 160\}$. The polytope of interest can be obtained by Tate-tuning a polytope model, for example M:225 6 N:31 6 H:28,160, associated with the generic model over the base (C.1). Indeed, ∇ is a standard $\mathbb{P}^{2,3,1}$-fibered polytope, where the tunings are

$$\{\{-4, \mathfrak{so}(38)\}, \{-1, \mathfrak{sp}(29)\}, \{-3, \mathfrak{so}(92)\}, \{-1, \mathfrak{sp}(36)\}, \{-4, \mathfrak{so}(68)\}, \{-1, \mathfrak{sp}(24)\}, \quad \text{(C.2)}$$
$$\{-4, \mathfrak{so}(44)\}, \{-1, \mathfrak{sp}(12)\}, \{-4, \mathfrak{so}(20)\}, \{0, \cdot\}, \{2, \cdot\}\}.$$

The non-flat fiber results from the $\mathfrak{so}(92)$ on the -3-curve, as it exceeds the upper bound $\mathfrak{so}(12)$ associated with anomaly conditions. As the non-abelian tuning uses all of the monomials in a_6, the dual fiber subpolytope ∇_2 becomes a blowup of $\mathbb{P}^{2,3,1}$, $\mathrm{Bl}_{[0,0,1]}\mathbb{P}^{2,3,1}$ (see figure 7).

Now we compute the Hodge numbers from the associated flat elliptic fibration model over the resolved base

$$-1 \qquad\qquad\qquad\qquad\qquad\qquad\qquad \text{(C.3)}$$
$$-4, -1, \ -4, \ -1, -4, -1, -4, -1, -4, 0, 2,$$

with tuned gauge symmetries

$$\mathfrak{sp}(19) \qquad\qquad\qquad\qquad\qquad\qquad\qquad \text{(C.4)}$$
$$\mathfrak{so}(38), \mathfrak{sp}(29), \ \mathfrak{so}(92), \ \mathfrak{sp}(36), \mathfrak{so}(68), \mathfrak{sp}(24), \mathfrak{so}(44), \mathfrak{sp}(12), \mathfrak{so}(20), \cdot, \cdot.$$

The $\mathfrak{sp}(19)$ on the exceptional -1-curve is forced by the $\mathfrak{so}(92)$ on the intersecting -4-curve. Again, the tuned non-abelian symmetries force a global U(1). The dimensions of the non-abelian gauge group factors in equation (C.5) are

$$741$$
$$703, 1711, 4186 \,\,, 2628, 2278, 1176, 946, 300, 190, 0, 0,$$

which differ from the total dimension of the gauge groups in the NHCs in (C.1) by $\Delta V_{\text{non-abelian}} = 14859 - (4 \times 28 + 8) = 14739$. The representations of the gauge group factors on the individual curves are [13]

$$46 \times \mathbf{38} \tag{C.5}$$
$$30 \times \mathbf{38}, 66 \times \mathbf{58}, 84 \times \mathbf{92}, 80 \times \mathbf{72}, 60 \times \mathbf{68}, 56 \times \mathbf{48}, 36 \times \mathbf{44}, 32 \times \mathbf{24}, 12 \times \mathbf{20}, \cdot, \cdot.$$

But some representations are shared between each pair of intersecting curves. The representations that are charged under both of the two corresponding group factors, $\mathfrak{so}(n) \oplus \mathfrak{sp}(m)$, are:

$$\frac{1}{2} \cdot 92 \cdot 38 \tag{C.6}$$
$$\frac{1}{2} \cdot 38 \cdot 58, \frac{1}{2} \cdot 58 \cdot 92 \,\,, \frac{1}{2} \cdot 92 \cdot 72, \frac{1}{2} \cdot 72 \cdot 68, \frac{1}{2} \cdot 68 \cdot 48, \frac{1}{2} \cdot 48 \cdot 44, \frac{1}{2} \cdot 44 \cdot 24, \frac{1}{2} \cdot 24 \cdot 20, \cdot, \cdot,$$

where the 1/2 factors come from the group theoretic normalization constant of $\mathfrak{so}(n)$. Hence, $\Delta H_{\text{non-abelian charged}} = (\text{sum of all terms in (C.5)} - \text{sum of all terms in (C.6)}) = 14830$. Note that all representations of a forced non-abelian gauge group are shared: $1/2(92) = 46$ on the exceptional -1-curve are shared. All representations on the blown up -4-curve are also shared: $1/2(38 + 58 + 72) = 84$, so the gauge symmetries can not be enhanced further on the three intersecting -1-curves.

The final piece needed is the U(1) charged matter. These fields are not charged under the non-abelian group, and therefore have not yet been taken into account in our computations. These matter fields are localized at codimension two on the I_1 component (away from the non-abelian components) of the discriminant locus (equation (2.10)), and the number of the U(1) charged matter fields corresponds to the number of the nodes, over which the fiber is Kodaira I_2, on the I_1 component [63]. Concretely, as described for example in [32], we calculate the discriminant locus of the I_1 with respect to one of the two local coordinates, which we choose to be b_1 associated with the 2-curve and b_2 associated with the 0-curve; then the I_1 discriminant locus factors into

$$\Delta_{I_1}(b_2) = p_1(b_2)(p_2(b_2))^2(p_3(b_2))^3, \tag{C.7}$$

where p_1 is a polynomial of degree 76 in b_2, p_2 is a polynomial of degree 9 in b_2, and p_3 is a polynomial of degree 63 in b_2. The degrees of the polynomials p_2, and p_3 correspond to the number of nodes and cusps on the I_1, respectively. The hypermultiplets charged only under the U(1) are localized at the nodes, and therefore $\Delta H_{\text{abelian charged}} = 9$ in this example.

Summing up all the pieces, we obtain $\Delta h^{1,1} = \Delta T + \Delta r_{\text{non-abelian}} + \Delta r_{\text{abelian}} = 1 + (251-18)+1 = 235$ and $\Delta h^{2,1} = (\Delta V_{\text{non-abelian}} + \Delta V_{\text{abelian}}) - 29\Delta T - (\Delta H_{\text{non-abelian charged}} + \Delta V_{\text{abelian charged}}) = (14739+1) - 29 - (14830+9) = -128$, which agrees with the differences in Hodge numbers from the polytopes: $\{263, 32\} - \{28, 160\} = \{235, -128\}$.

Open Access. This article is distributed under the terms of the Creative Commons Attribution License (CC-BY 4.0), which permits any use, distribution and reproduction in any medium, provided the original author(s) and source are credited.

References

[1] P. Candelas, G.T. Horowitz, A. Strominger and E. Witten, *Vacuum Configurations for Superstrings*, *Nucl. Phys.* **B 258** (1985) 46 [INSPIRE].

[2] V. Batyrev, *Variations of the mixed Hodge structure of affine hypersurfaces in algebraic tori*, *Duke Math. J.* **69** (1993) 349.

[3] M. Kreuzer and H. Skarke, *Complete classification of reflexive polyhedra in four-dimensions*, *Adv. Theor. Math. Phys.* **4** (2002) 1209 [hep-th/0002240] [INSPIRE].

[4] M. Kreuzer and H. Skarke, *Calabi-Yau data*, http://hep.itp.tuwien.ac.at/~kreuzer/CY.html.

[5] C. Vafa, *Evidence for F-theory*, *Nucl. Phys.* **B 469** (1996) 403 [hep-th/9602022] [INSPIRE].

[6] D.R. Morrison and C. Vafa, *Compactifications of F-theory on Calabi-Yau threefolds. I*, *Nucl. Phys.* **B 473** (1996) 74 [hep-th/9602114] [INSPIRE].

[7] D.R. Morrison and C. Vafa, *Compactifications of F-theory on Calabi-Yau threefolds. II*, *Nucl. Phys.* **B 476** (1996) 437 [hep-th/9603161] [INSPIRE].

[8] D.R. Morrison and W. Taylor, *Classifying bases for 6D F-theory models*, *Central Eur. J. Phys.* **10** (2012) 1072 [arXiv:1201.1943] [INSPIRE].

[9] D.R. Morrison and W. Taylor, *Toric bases for 6D F-theory models*, *Fortsch. Phys.* **60** (2012) 1187 [arXiv:1204.0283] [INSPIRE].

[10] G. Martini and W. Taylor, *6D F-theory models and elliptically fibered Calabi-Yau threefolds over semi-toric base surfaces*, *JHEP* **06** (2015) 061 [arXiv:1404.6300] [INSPIRE].

[11] W. Taylor and Y.-N. Wang, *Non-toric bases for elliptic Calabi-Yau threefolds and 6D F-theory vacua*, *Adv. Theor. Math. Phys.* **21** (2017) 1063 [arXiv:1504.07689] [INSPIRE].

[12] S.B. Johnson and W. Taylor, *Calabi-Yau threefolds with large $h^{2,1}$*, *JHEP* **10** (2014) 23 [arXiv:1406.0514] [INSPIRE].

[13] S.B. Johnson and W. Taylor, *Enhanced gauge symmetry in 6D F-theory models and tuned elliptic Calabi-Yau threefolds*, *Fortsch. Phys.* **64** (2016) 581 [arXiv:1605.08052] [INSPIRE].

[14] P. Candelas, A. Constantin and H. Skarke, *An Abundance of K3 Fibrations from Polyhedra with Interchangeable Parts*, *Commun. Math. Phys.* **324** (2013) 937 [arXiv:1207.4792] [INSPIRE].

[15] J. Gray, A.S. Haupt and A. Lukas, *Topological Invariants and Fibration Structure of Complete Intersection Calabi-Yau Four-Folds*, *JHEP* **09** (2014) 093 [arXiv:1405.2073] [INSPIRE].

[16] L.B. Anderson, F. Apruzzi, X. Gao, J. Gray and S.-J. Lee, *A new construction of Calabi-Yau manifolds: Generalized CICYs*, *Nucl. Phys.* **B 906** (2016) 441 [arXiv:1507.03235] [INSPIRE].

[17] L.B. Anderson, X. Gao, J. Gray and S.-J. Lee, *Tools for CICYs in F-theory*, *JHEP* **11** (2016) 004 [arXiv:1608.07554] [INSPIRE].

[18] L.B. Anderson, X. Gao, J. Gray and S.-J. Lee, *Multiple Fibrations in Calabi-Yau Geometry and String Dualities*, *JHEP* **10** (2016) 105 [arXiv:1608.07555] [INSPIRE].

[19] L.B. Anderson, X. Gao, J. Gray and S.-J. Lee, *Fibrations in CICY Threefolds*, *JHEP* **10** (2017) 077 [arXiv:1708.07907] [INSPIRE].

[20] Y.-C. Huang and W. Taylor, *On the prevalence of elliptic and genus one fibrations among toric hypersurface Calabi-Yau threefolds*, arXiv:1809.05160 [INSPIRE].

[21] P. Candelas and A. Font, *Duality between the webs of heterotic and type-II vacua*, *Nucl. Phys.* **B 511** (1998) 295 [hep-th/9603170] [INSPIRE].

[22] V. Bouchard and H. Skarke, *Affine Kac-Moody algebras, CHL strings and the classification of tops*, *Adv. Theor. Math. Phys.* **7** (2003) 205 [hep-th/0303218] [INSPIRE].

[23] V. Braun, T.W. Grimm and J. Keitel, *Geometric Engineering in Toric F-theory and GUTs with* U(1) *Gauge Factors*, *JHEP* **12** (2013) 069 [arXiv:1306.0577] [INSPIRE].

[24] J. Borchmann, C. Mayrhofer, E. Palti and T. Weigand, *Elliptic fibrations for* SU(5) × U(1) × U(1) *F-theory vacua*, *Phys. Rev.* **D 88** (2013) 046005 [arXiv:1303.5054] [INSPIRE].

[25] J. Borchmann, C. Mayrhofer, E. Palti and T. Weigand, SU(5) *Tops with Multiple* U(1)*s in F-theory*, *Nucl. Phys.* **B 882** (2014) 1 [arXiv:1307.2902] [INSPIRE].

[26] D.R. Morrison, *TASI lectures on compactification and duality*, in *Strings, branes and gravity. Proceedings, Theoretical Advanced Study Institute, TASI'99*, Boulder, U.S.A., May 31–June 25, 1999, pp. 653–719 (1999) [hep-th/0411120] [INSPIRE].

[27] W. Taylor, *TASI Lectures on Supergravity and String Vacua in Various Dimensions*, arXiv:1104.2051 [INSPIRE].

[28] S.H. Katz and C. Vafa, *Matter from geometry*, *Nucl. Phys.* **B 497** (1997) 146 [hep-th/9606086] [INSPIRE].

[29] M. Bershadsky, K.A. Intriligator, S. Kachru, D.R. Morrison, V. Sadov and C. Vafa, *Geometric singularities and enhanced gauge symmetries*, *Nucl. Phys.* **B 481** (1996) 215 [hep-th/9605200] [INSPIRE].

[30] D.R. Morrison and W. Taylor, *Matter and singularities*, *JHEP* **01** (2012) 022 [arXiv:1106.3563] [INSPIRE].

[31] V. Braun, *Toric Elliptic Fibrations and F-theory Compactifications*, *JHEP* **01** (2013) 016 [arXiv:1110.4883] [INSPIRE].

[32] V. Braun and D.R. Morrison, *F-theory on Genus-One Fibrations*, *JHEP* **08** (2014) 132 [arXiv:1401.7844] [INSPIRE].

[33] D.R. Morrison and W. Taylor, *Sections, multisections and* U(1) *fields in F-theory*, arXiv:1404.1527 [INSPIRE].

[34] M.-X. Huang, A. Klemm and M. Poretschkin, *Refined stable pair invariants for E-, M- and [p, q]-strings*, *JHEP* **11** (2013) 112 [arXiv:1308.0619] [INSPIRE].

[35] L.B. Anderson, I. García-Etxebarria, T.W. Grimm and J. Keitel, *Physics of F-theory compactifications without section*, *JHEP* **12** (2014) 156 [arXiv:1406.5180] [INSPIRE].

[36] C. Mayrhofer, D.R. Morrison, O. Till and T. Weigand, *Mordell-Weil Torsion and the Global Structure of Gauge Groups in F-theory*, *JHEP* **10** (2014) 16 [arXiv:1405.3656] [INSPIRE].

[37] M. Cvetič, R. Donagi, D. Klevers, H. Piragua and M. Poretschkin, *F-theory vacua with $\mathbb{Z}_3$ gauge symmetry*, *Nucl. Phys.* **B 898** (2015) 736 [arXiv:1502.06953] [INSPIRE].

[38] F. Bonetti and T.W. Grimm, *Six-dimensional $(1,0)$ effective action of F-theory via M-theory on Calabi-Yau threefolds*, *JHEP* **05** (2012) 019 [arXiv:1112.1082] [INSPIRE].

[39] W. Taylor, *On the Hodge structure of elliptically fibered Calabi-Yau threefolds*, *JHEP* **08** (2012) 032 [arXiv:1205.0952] [INSPIRE].

[40] W. Buchmüller, M. Dierigl, P.-K. Oehlmann and F. Ruehle, *The Toric* SO(10) *F-theory Landscape*, *JHEP* **12** (2017) 035 [arXiv:1709.06609] [INSPIRE].

[41] M. Dierigl, P.-K. Oehlmann and F. Ruehle, *Global Tensor-Matter Transitions in F-Theory*, *Fortsch. Phys.* **66** (2018) 1800037 [arXiv:1804.07386] [INSPIRE].

[42] L. Bhardwaj and P. Jefferson, *Classifying* 5d *SCFTs via* 6d *SCFTs: Arbitrary rank*, arXiv:1811.10616 [INSPIRE].

[43] F. Apruzzi, L. Lin and C. Mayrhofer, *Phases of* 5d *SCFTs from M-/F-theory on Non-Flat Fibrations*, arXiv:1811.12400 [INSPIRE].

[44] S. Katz, D.R. Morrison, S. Schäfer-Nameki and J. Sully, *Tate's algorithm and F-theory*, *JHEP* **08** (2011) 094 [arXiv:1106.3854] [INSPIRE].

[45] A. Grassi and D.R. Morrison, *Anomalies and the Euler characteristic of elliptic Calabi-Yau threefolds*, *Commun. Num. Theor. Phys.* **6** (2012) 51 [arXiv:1109.0042] [INSPIRE].

[46] V. Kumar, D.R. Morrison and W. Taylor, *Global aspects of the space of* 6D $N = 1$ *supergravities*, *JHEP* **11** (2010) 118 [arXiv:1008.1062] [INSPIRE].

[47] M. Bertolini, P.R. Merkx and D.R. Morrison, *On the global symmetries of* 6D *superconformal field theories*, *JHEP* **07** (2016) 005 [arXiv:1510.08056] [INSPIRE].

[48] J.J. Heckman, D.R. Morrison and C. Vafa, *On the Classification of 6D SCFTs and Generalized ADE Orbifolds*, *JHEP* **05** (2014) 028 [*Erratum ibid.* **06** (2015) 017] [arXiv:1312.5746] [INSPIRE].

[49] A. Grassi, *On minimal models of elliptic threefolds*, *Math. Ann.* **290** (1991) 287.

[50] W. Fulton, *Introduction to Toric Varieties*, Annals of Mathematics Study 131, Princeton University Press, Princeton (1993).

[51] K. Hori et al., *Mirror Symmetry*, American Mathematical Society (2003).

[52] V.V. Batyrev, *Dual polyhedra and mirror symmetry for Calabi-Yau hypersurfaces in toric varieties*, *J. Alg. Geom.* **3** (1994) 493 [alg-geom/9310003] [INSPIRE].

[53] M. Kreuzer and H. Skarke, *PALP: a Package for Analyzing Lattice Polytopes*, http://hep.itp.tuwien.ac.at/~kreuzer/CY/CYpalp.html.

[54] A.C. Avram, M. Kreuzer, M. Mandelberg and H. Skarke, *Searching for K3 fibrations*, *Nucl. Phys.* **B 494** (1997) 567 [hep-th/9610154] [INSPIRE].

[55] M. Kreuzer and H. Skarke, *Calabi-Yau four folds and toric fibrations*, *J. Geom. Phys.* **26** (1998) 272 [hep-th/9701175] [INSPIRE].

[56] H. Skarke, *String dualities and toric geometry: An Introduction*, *Chaos Solitons Fractals* **10** (1999) 543 [`hep-th/9806059`] [ɪɴSPIRE].

[57] D. Klevers, D.K. Mayorga Pena, P.-K. Oehlmann, H. Piragua and J. Reuter, *F-Theory on all Toric Hypersurface Fibrations and its Higgs Branches*, *JHEP* **01** (2015) 142 [`arXiv:1408.4808`] [ɪɴSPIRE].

[58] P. Candelas, E. Perevalov and G. Rajesh, *Toric geometry and enhanced gauge symmetry of F-theory/heterotic vacua*, *Nucl. Phys.* **B 507** (1997) 445 [`hep-th/9704097`] [ɪɴSPIRE].

[59] E. Perevalov and H. Skarke, *Enhanced gauged symmetry in type-II and F theory compactifications: Dynkin diagrams from polyhedra*, *Nucl. Phys.* **B 505** (1997) 679 [`hep-th/9704129`] [ɪɴSPIRE].

[60] *SageMath, the Sage Mathematics Software System*, version 7.1, The Sage Developers (2016) [http://sagemath.org/doc/reference/schemes/sage/schemes/toric/weierstrass.html].

[61] R. Slansky, *Group Theory for Unified Model Building*, *Phys. Rept.* **79** (1981) 1 [ɪɴSPIRE].

[62] L.B. Anderson, J. Gray, N. Raghuram and W. Taylor, *Matter in transition*, *JHEP* **04** (2016) 080 [`arXiv:1512.05791`] [ɪɴSPIRE].

[63] D.R. Morrison and D.S. Park, *F-Theory and the Mordell-Weil Group of Elliptically-Fibered Calabi-Yau Threefolds*, *JHEP* **10** (2012) 128 [`arXiv:1208.2695`] [ɪɴSPIRE].

[64] V. Braun, T.W. Grimm and J. Keitel, *Complete Intersection Fibers in F-theory*, *JHEP* **03** (2015) 125 [`arXiv:1411.2615`] [ɪɴSPIRE].